UNIVERSITÀ DEGLI STUDI DI SALERNO

Department of Chemistry and Biology "A. Zambelli"

Ph.D. in Chemical, Biological and Environmental Sciences

Curriculum in Biological and Environmental Sciences

XXXV cycle

Biological effects of synthetic compounds and bioactive molecules in human cell models

Ph.D. Tutor:

Professor Ivana Caputo

Ph.D. student:

Dr. Antonio Massimiliano Romanelli

Matr. 880180000

Ph.D. Coordinator:

Professor Claudio Pellecchia

Academic Year 2021/2022

ABSTRACT

During the course of my Ph.D., I focused my studies on two main topics: the cytotoxic effects induced by 4-nonylphenol (4-NP) and 4-octylphenol (4-OP) and the anti-cancer properties of natural cardenolides extracted from the aerial parts of the plant *Pergularia tomentosa*. For both topics, human cell cultures were used as a suitable study model.

4-NP and 4-OP are widely distributed environmental pollutants in different compartments such as water, soils and sediments. They are mainly derived from the degradation of polyethoxylated alkylphenols, which due to their chemical characteristics are widely used in many industrial applications. Humans are continuously exposed to these substances mainly through ingestion of contaminated water and food, but also through inhalation and dermal absorption. After their introduction into the human body, they accumulate in various organs and biological fluids, particularly in the liver and intestine. They can act as endocrine disrupting chemicals and exert toxic and harmful effects on many organs and tissues. Therefore, my aim was to understand the molecular and biochemical mechanisms by which they induce cytotoxicity in human cell lines. The results of my research revealed that alkylphenols (APs) profoundly alter human cell physiology by inducing viability reduction linked to a cell cycle arrest and to the triggering of apoptosis. Moreover, they are responsible for inducing organelles stress conditions and damage, such as ER-stress, altered calcium homeostasis, mitochondrial dysfunction, oxidative stress and induction of autophagic flux.

The natural compounds, investigated in my research, have been extracted, from the first time, from the leaves of *P. tomentosa*, a member of the Asclepiadaceae family. They belong to the group of cardiac glycosides. Structurally, they have a steroid nucleus, a glycosidic portion and a lactone ring. However, cardenolides extracted from *P. tomentosa* have peculiar structural features, i.e. transfused A/B rings and sugar moiety linked by a double bond, generating the dioxanoid attachment. Precisely, the compounds under investigation are calactin, calotropin and their derivatives. Over time, it has been shown that cardiac glycosides, in addition to their classic cardiotonic action, are able to exert effects that counteract cancer cells. Therefore, my aim, here, was to understand the molecular mechanisms by which these compounds exerted their anti-cancer action. I realized, firstly, that the compounds are not selective for tumour cells, however, calactin strongly reduces the viability of HepG2 tumour cells on which, consequently, I decided to focus my attention. I showed that *P. tomentosa* compounds reduced the viability, proliferation and migration of cancer cells. Furthermore, they were able to trigger autophagy and apoptosis in the same cell line. In light of these results, they represent good candidates for developing anti-cancer drugs or adjuvants to current therapies.

In conclusion, by using the same *in vitro* models represented by human cell cultures, and similar methodological approaches, I obtained findings useful to elucidate the biochemical and molecular mechanisms by which APs induced cytotoxicity and those underlying the anti-tumour properties of *P. tomentosa* compounds.

INTRODUCTION

One of the problems plaguing modern society is certainly pollution. Humans, for a long time, have focused their attention on developing industrial processes that bring profit and make life more comfortable without thinking about their environmental impact. Even today, people use substances and materials with high industrial performance and low cost without giving any thought to the damage these compounds can cause when they are released into the environment. We never think that the environment around us is our true home and therefore we should respect and preserve it. Compounds that are released into the environment have, over time, led to radical changes, such as climate change, or have been responsible for hydrogeological disasters that we are currently seeing. Furthermore, the substances released into the environment not only disrupt its balance but, by contaminating water and various environmental matrices, they enter in the food chain undergoing biomagnification phenomena. Thus, man is constantly exposed to these pollutants that represent a serious risk to his state of health. One of the projects I participated in my PhD course concerns the study of the molecular mechanisms by which alkylphenols, widespread environmental pollutants, exert their cytotoxicity on human cells. In the first chapter of the introduction, I will focus on how alkylphenols are produced, how they are accumulated in environmental matrices, what the exposure pathways are and the main toxic effects.

Another serious problem that worries humanity is the increase in cancer cases. We are constantly searching for new drugs to fight cancer in an efficient and targeted manner. Throughout history, a great source of drugs has been natural substances extracted mainly from plants. These compounds were initially used in traditional medicine in various countries, showing anti-inflammatory, lenitive, analgesic action. Very often, man has everything he needs to cure and protect his health in nature; he just has to observe and research carefully. Today, many researchers are focusing their attention on the anti-cancer activity of cardiac glycosides, compounds extracted from a large number of plant species. Therefore, another research project I got interested in during my PhD course concerns understanding the biological effects of cardenolides extracted from the aerial parts of *Pergularia tomentosa* on human cells. Thus, in the second chapter of the introduction, I will present the structural characteristics of cardiac glycosides, their biological activities, and focus the attention on the mechanisms by which they exert their anti-carcinogenic action.

On the whole, in the following chapters, I will review the state of the art concerning both alkylphenols and cardiac glycosides.

CHAPTER 1. Alkylphenol ethoxylates (APEOs)

The alkylphenol ethoxylates (APEOs) belong to the class of non-ionic-surfactants. They present two portions: the alkylphenol (AP) and the ethoxylate moiety (Ying et al, 2002). This structure, with a polar (hydrophilic) and a hydrophobic part, gives them the ability to concentrate on different surfaces forming micelles in solution. The hydrophilic character is due to the ethoxyl chain. The hydrophobic property is provided by AP with hydrocarbon chains (Acir and Guenther, 2018).

APEOs are used in several industrial applications: in paper production, in the textile industry, in the formulation of pesticides, cosmetics and detergents. The most important members of this compounds' class are nonylphenol ethoxylate and octylphenol ethoxylate, which represent approximately 80% and 20% of the APEOs produced (Chokwe et al, 2017).

Due to their toxicity and spread, they have been heavily restricted by some European countries (Directive 2003/53/EC 2003; Directive 2000/60/EC 2000) but are still used in other countries, such as India and China, and in South America (Campbell et al, 2002).

1.1 4-Nonylphenol (4-NP) and 4-octylphenol (4-OP): source, structure and physico-chemical characteristics

APEOs' release into the environment can occur during their synthesis, incorporation into finished products or during the disposal phase (Chokwe et al, 2017). Most of these compounds are manipulated in the aqueous phase, which means that they are discharged into wastewater and then transported to wastewater treatment plants where they undergo biodegradation processes by microorganisms (Acir and Guenther, 2018). Thanks to a kinetic study (Jonkers et al, 2001), it has been demonstrated that the APs in the environment undergo a gradual shortening process of the ethoxyl chain. The biodegradation leads to short-chain APEOs containing one or two ethoxylate units. Then, the transformation involves the oxidation of the ethoxylated chain producing mainly alkylphenoxy-ethoxy-acetic acid and alkylphenoxy-acetic acid.

This process is schematized in figure 1.
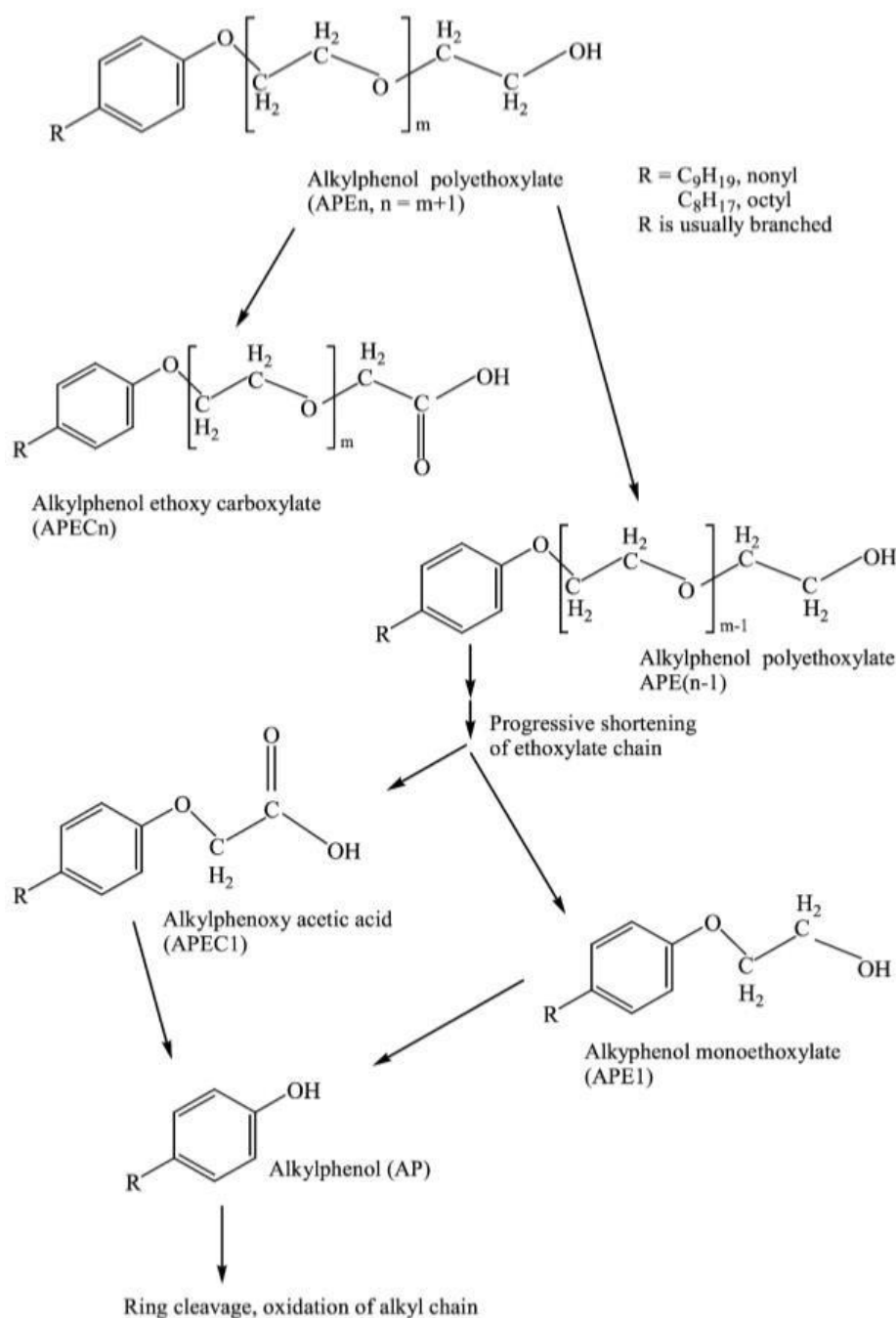
Figure 1. The degradation process of alkylphenol polyethoxylates. (Ying et al, 2002).

Among the degradation products there are APs, in particular, 4-nonylphenol (4-NP) and 4-tert-octylphenol (4-tOP).

4-NP is more abundant in the environment than 4-tOP (Acir and Guenther, 2018). Specifically, NP is produced by alkylation of phenol with mixed isomeric nonenes under acidic conditions. The

product is a mixture containing mainly para substituted (4-NP) and occasionally ortho substituted (2-NP) with various isomeric and branched chains. Theoretically, there can be 211 isomers in the NP mixture because of the different branching and substitution patterns (Thiele et al, 2004).

The structure of 4-NP consists of a phenolic ring and an alkyl branched or linear chain with nine carbon atoms in the para position (Figure 2).
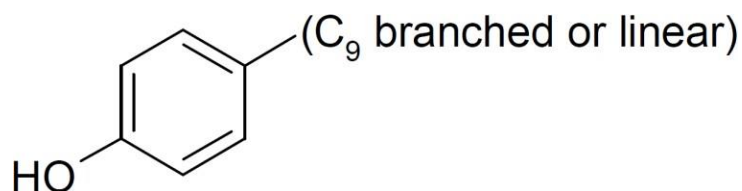
Figure 2. Typical structure of 4-NP. (Soares et al, 2008, modified)

4-tOP also contains a phenolic head and an alkyl tail (Figure 3) which gives it hydrophobicity. (Olaniyan et al, 2018).
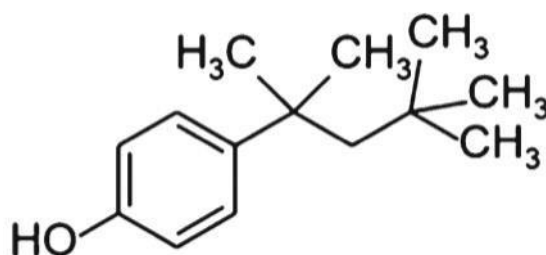
Figure 3. Structure of 4-tOP (CAS 140-66-9)

4-NP and 4-tOP are hydrophobic compounds. This chemical property is responsible for the accumulation of APs in sediments and in organisms' tissues. Furthermore, it confers the ability to interact with biological membranes (Diao et al, 2017).

The structures of 4-NP and 4-tOP are also closely linked to their toxic action. In fact, some isomers mimic the structure of the hormone 17 β-estradiol thus competing for the binding to the receptor (Figure 4).

Therefore, these compounds can be considered as endocrine chemical destroyers (EDCs) (Jambor et al, 2016).
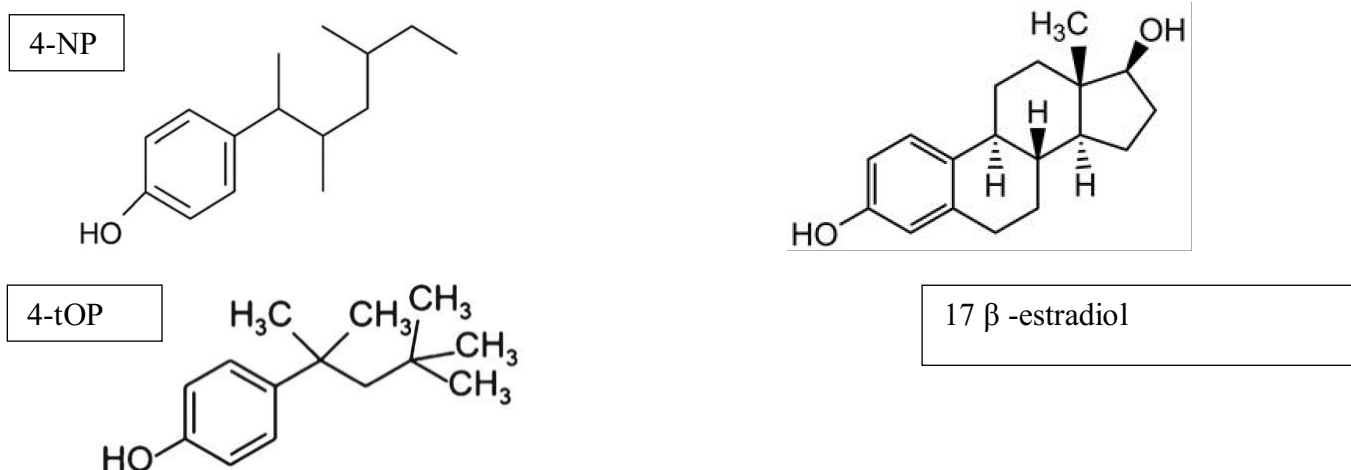
Figure 4. Comparison between the structures of 4-NP, 4-tOP and hormone 17 β-estradiol.

I will discuss their toxicity in detail in the appropriate section.

1.2 4-NP and 4-OP: environmental occurrence and exposition routes

In this paragraph I'll analyze the presence of 4-NP and 4-OP in different environmental compartments and possible pathways of exposure. Given the chemical-physical characteristics of these compounds, of which I talked about previously, they are found in different environmental matrices such as groundwater, sediments, surface waters, soils and air (Acir and Guenther, 2018). Graca et al. (2015) analyzed the concentrations of 4-NP and 4-OP in the Baltic Sea, which represents a good model of study as there is a stable sedimentation in it, and sediments reflect the trends of natural and anthropogenic terrestrial runoff. The authors observed that 4-NP concentrations in sediments of the surface layer varied between 15.80 and 239.88 ng / g dry weight (d. w.) and those of 4-OP between 5.61 and 13.01 ng / g d. w. However, it should be noted that the concentrations recorded in the Baltic Sea were much lower than those found in the sediments of the Tokyo coast or China (Graca et al, 2015). In fact, the concentration of these APs was higher in Countries where their use has not been restricted. An interesting study by Vikelesoe et al. (2002) showed the difference in concentration of 4-NP in non-fertilized and fertilized fields. Precisely, in non-cultivated fields the concentration of 4-NP was between 0.01 and 0.98 µg / kg d. w.; in those fertilized with manure and sewage sludge the concentration was 34 µg / kg. This study demonstrated how the concentration of APs present in the environment was closely linked to anthropic activity. In addition, APs are found in wastewaters in highly variable concentrations depending on the industrialization of the area and the efficiency of the wastewater treatment system (Chokwe et al, 2017). From their solubility, we expect these compounds to be less concentrated in surface water and in the air. Indeed, the concentration of 4-NP, for example,

in surface water was between 0,0004-24,3 μg / L (Yie et al, 2017). Few studies concern the measurement of the concentrations of these pollutants in the air. However, for both compounds, it has been recorded that their concentration was higher in indoor air than in the outdoor one. (Chokwe et al, 2017; Olaniyan et al, 2018). It is interesting to note that in 120 houses analyzed, among 89 organic compounds found in the air, the most abundant was 4-NP. From this, we understand how the presence of 4-NP is also becoming important in the atmosphere (Soares et al, 2008). Given the high presence in different environmental matrices, humans can be exposed to APs through different routes that include ingestion of water and contaminated food, inhalation, dermal absorption (Ying et al, 2002). A study by Guenther et al. (2002) on 60 food products marketed in Germany showed that 4-NP was almost ubiquitous. The presence of 4-NP and 4-OP was found in shrimp, clams and fish. Furthermore, the percentage found in organisms represented the large percentage of the aquatic ecosystem (Diao et al, 2017). 4-NP and 4-OP are also detected in bottled water in a mean concentration range of 18.5 ng / L (Acir and Guenther, 2018). In Italy, the APs concentrations in bottled water and fountain water oscillated between 7.7 ng / L and 84 ng / L (Maggioni et al, 2013). Vegetables and fruit are also polluted by 4-NP and 4-OP (Dodgen et al, 2013). Other sources of exposure to APs consist of beauty products and detergents, which contain concentrations of APs, and inhalation of contaminated air (Soares et al, 2008; Olaniyan et al, 2018). From these studies, it is clear how man introduces these pollutants into his body every day. For example, according to Ademollo et al. (2008), in Italy there was a maximum 4-NP intake of 3.94 μg / kg / day. For 4-OP it was thought that ingestion is six orders of magnitude lower (Ademollo et al. 2008).

1.3 Presence of 4-NP and 4-OP in human tissues and biological matrices

Given the high presence of APs in multiple environmental compartments, from aquatic to terrestrial, we can think that there is a transfer of these pollutants into the trophic chain. Particularly infested with these compounds are aquatic environments close to areas with prevalent anthropogenic activity. Indeed, in urban Moon Lake (Wuhan, China), it was demonstrated that 4-NP and 4-OP were present in water and accumulated in submerged macrophytes, particularly in *Myriophyllum verticillatum* and *Elodea nuttallii*, aquatic plants (Zhang et al, 2008). Considering the presence of these pollutants also in soils and that they are often irrigated with contaminated water, there is also a translocation to terrestrial plant species. A study by Jiang et al (2019) showed that NP accumulated in tomato (*Solanum lycopersicum*), one of the most important plants in agriculture worldwide. Precisely, the pollutant in this plant species caused serious toxic damages: reduced growth and chlorophyll production, intensified lipid peroxidation in the tissues, alteration of the antioxidant system with upregulation of Cu/Zn-SOD (Superoxide dismutase) expression (Jiang et al, 2019). From these

studies, it is evident that APs accumulate already at the level of the first link in the trophic chain, that of the producers, thus transferring to animal species up to humans with possible biomagnification phenomena. This also explains the presence in different mammalian biological matrices on which we will focus our attention.

A study by Espinosa et al. (2009) showed that out of 20 Spanish women, 100% of them accumulated 4-NP in the adipose tissue, with an average level of 57 ng / g, while 23.5% of them accumulated 4-OP with an average level of 4,5 ng / g. Furthermore, the accumulation of APs was linked to the diet, as obese women had higher concentrations of 4-NP in their adipose tissue (Espinosa et al, 2009). 4-NP and 4-OP have been found in maternal blood plasma and amniotic fluid. Indeed, there was a close correlation between the maternal blood concentration and the quantity of these compounds in the amniotic fluid. From this, we understand that there is a pre-natal exposure to these pollutants that can profoundly alter the development of the fetus (Shekar et al, 2016). In addition, it has been shown in an *ex vivo* model of placental perfusion that 4-NP was able to cross the placenta. Therefore, the placental barrier did not protect the fetus from these dangerous pollutant (Balakrishnan et al, 2008). Ademollo et al. (2008) investigated the presence of 4-NP and 4-OP also in breast milk of Italian women. Precisely, the level of 4-NP (13-56 μg / L) was higher than the recorded one in other Countries, while the level of 4-OP was lower by at least an order of magnitude (Ademollo et al, 2008). Several studies have verified the presence of these APs in the urine. For example, in urine samples from the Korean population, 4-NP and 4-OP were found respectively at levels of 3.70 ng / L and 0.60 ng / L like those recorded in China and Taiwan (Park et al, 2017). Furthermore, the amount of APs in the urine is dependent on the place where one lives and on certain lifestyle habits, such as smoking (Park et al, 2017). From these studies, it appears clear that the exposure to these environmental pollutants leads to a significant bioaccumulation in different tissues and biological fluids that could cause serious problems both to adult organs and to the development of the fetus.

1.4 Toxic effects of 4-NP and 4-OP

The first historical toxic action to be discovered has been the ability of these compounds to act as EDCs, interfering with the hormonal system. Indeed, Soto et al. in 1991 accidentally observed that 4-NP used to manufacture the experimental tubes could induce the proliferation of breast cells, a typical effect induced by estrogen (Soto et al, 1991). Also, for 4-OP, many of the toxic effects were due to its interaction with the estrogen receptor (Olaniyan et al, 2018). The reason is that both these pollutants, in particular some branched isomers, mimic the structure of 17 β-estradiol, competing with it for binding to the estrogen receptor (Figure 5) (Soares et al, 2008; Acir et al, 2018).
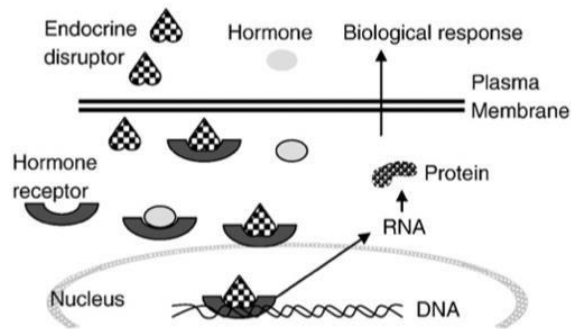
Figure 5. Competition between EDCs and the hormone for binding to the natural receptor (Soares et al, 2008).

In the following paragraphs I will analyze the toxicity exerted by these compounds on different *in vivo* and *in vitro* models.

1.4.1 Effects on the reproductive system

A study by Ko et al. (2019) investigated the effects of APs on the decidualization of human endometrial stromal cells, a very important phenomenon for female reproductive biology and for the establishment of pregnancy. Precisely, in this work, it has been shown that treatments with different doses of OP and NP reduced the expression of essential genes (PRL, IGFBP1, LEFTY2) for the decidualization process. Moreover, this reduction occurred in the first 3 days of exposure, therefore in the early stages of the decidualization phenomenon. This phenomenon can lead to embryo implantation failure, spontaneous abortion, and preeclampsia (Ko et al, 2019). Another study (Albaladejo et al, 2017) showed that 4-OP and 4-NP induced severe damages to JEG-3 placental cells. In particular, they induced a dose-dependent increase in the level of reactive oxygen species (ROS), and exhibited a strong cytotoxicity even at low concentrations. The increase in ROS levels has often been associated with malformation of the reproductive organs and reduced fertility (Albaladejo et al, 2017). Oxidative stress associated with cytotoxicity also strongly influences male reproductive biology. Indeed, Sertoli testicular cells treated with micromolar concentrations of 4-NP showed increased ROS levels, lipid peroxidation, loss of mitochondrial membrane potential and reduction of cell viability (Gong et al, 2006). 4-OP also exerts cytotoxic action on the male reproductive system. Specifically, male rats treated with different doses of 4-OP showed severe alterations in the reproductive system. First, they showed variations in the weight of the testicles, prostate and epididymis. By histological analysis it has been shown that the seminiferous tubules had reduced size and altered cellular organization in rats exposed to 4-OP. In addition, testicular cells exposed to 4-OP exhibited intracellular vacuoles, abnormal heterochromatin distribution and endoplasmic reticulum expansion (Bian et al, 2006).

1.4.2 Effects on the nervous system

As above described, APs often induced damage to cells and tissues by increasing the production of ROS. Nervous system toxicity is also partly explained by oxidative stress. It has been observed that rats exposed for 45 days to oral administration to 4-OP and 4-NP had high levels of malondialdehyde (MDA) and low levels of reduced glutathione (GSH), inducing the production of ROS in the brain. In addition, the histological analysis confirmed the oxidative stress damage in the cortical portion of the brain, which appeared spongiform and rich in hyperchromatic cells (Aydogan et al, 2008).

This damage could be induced not only by exposure to APs but by their accumulation in the brain too. Indeed, the study by Bianco et al. (2011) showed that there was an accumulation of 4-OP in different brain areas of the treated rats, in particular at the level of the cortical area (Bianco et al, 2011). This finding suggests that lipophilic endocrine disruptors, such as 4-OP and 4-NP, can cross the blood-brain barrier. As previously said, 4-OP and 4-NP mimic the structure of estradiol, a hormone also responsible for the growth of Purkinje cells. An interesting study showed that these environmental pollutants induced the dendritic growth of Purkinje cells, demonstrating strong estrogenic action (Shikimi et al, 2004). Furthermore, APs can profoundly alter cognitive abilities. By means of special tests, it has been shown that rats exposed for 35 days to 4-NP had important problems related to memory and anxiety. Precisely, these rats had difficulty in spatial learning as well as in remembering the escape route (Kazemi et al, 2018). In addition, 4-NP accumulated in the hippocampus and amygdala, brain areas involved in the processes of memorization and the genesis of anxiety. Major cognitive problems were related to increased accumulation of 4-NP; so, there was a linear correlation between accumulation of pollutant and brain problem (Kazemi et al, 2018).

1.4.3 Effects on the immune system

The modern lifestyle leads us to consume a lot of detergents, synthetic clothes and to eat foods that can contain APs. Since they are lipophilic, they can accumulate in our body and therefore we are subjected to chronic exposure. Furthermore, allergic diseases are increasing in contemporary society. Therefore, in this section, I'll analyze the relationship between the exposure to these environmental pollutants and the genesis or aggravation of the immune system diseases. An *in vivo* study by Sadakane et al. (2013) showed that exposure to 4-NP and 4-OP could aggravate the symptoms of atopic dermatitis. These compounds were injected intraperitoneally into mouse models of atopic dermatitis. The exposure to these APs led, first of all, to a worsening of mice dermal lesion. The serum level of allergen specific immunoglobulins (IgG1) was increased after treatments with 4-NP and 4-OP. In addition, there was a reduction of T-helper-1 (Th1) cytokines, such as interferon gamma

(IFN-γ), and an increase of T-helper-2 (Th2) cytokines, such as interleukin-4 (IL-4). There was also an increase in thymic stromal lymphopoietin (TSLP), a factor closely linked to the aggravation of inflammation. The strongest effect was given by the 4-NP (Sadakane et al, 2013). Thus, in this study it has been shown that APs induced a Th2-mediated immune response, which aggravated the symptoms of atopic dermatitis. This work was in agreement with one by Iwata et al. (2004). Specifically, T cells undergoing differentiation with specific cytokines for development into Th1 and Th2 were cultured in the presence of AP. After 5 days, the levels of IL-4 increased and those of IFN-γ decreased, favouring the development of Th2. Furthermore, scientists have shown that only OP and NP induced this effect compared to other APs (dodecylphenol) or other compounds (octylbenzene). This finding suggests that the length and branching of the alkyl chain plays a fundamental role in the biological activity (Iwata et al, 2004). Another allergic disease is asthma in which T lymphocytes play a fundamental role. This pathology is characterized by chronic inflammation of the airways and bronchial tubes. Recent studies have shown that 4-NP could induce severe damages to the bronchial epithelium by activating apoptosis. It could also induce an increase in interleukin 6 and 8 (IL-6 and IL-8), factors involved in the migration and proliferation of bronchial smooth muscle cells. (Suen et al, 2012). In the light of these studies, we understand that chronic exposure to these pollutants can profoundly alter the development and activity of the human immune system, inducing or aggravating various diseases.

1.4.4 Effects on the gastrointestinal system

I mentioned earlier that the main route of introduction of APs into the human body is through the ingestion of contaminated water and food. Therefore, in this section I will analyze the effects of these environmental pollutants on the intestine, an organ mainly involved in digestion, and on the liver, an organ involved in detoxification processes. A study by Lepretti et al. (2015) showed that exposure to 4-NP could induce severe damage to human intestinal epithelial cells (Caco-2). In detail, authors performed a TUNEL assay and found that 4-NP induced apoptosis. They also observed that caspase-3 activity increased in the presence of this pollutant. In addition, by western blot and PCR respectively they showed that 4-NP led to increased expression of glucose-regulating protein 78 (GRP78) and splicing of X-box binding protein 1 (XBP1), both markers of ER-stress. Thus, 4-NP can alter intestinal cell physiology by inducing cell death and ER-stress (Lepretti et al, 2015). 4-OP can also disrupt the physiology of intestinal cells. In fact, pregnant mice treated with 4-OP showed reduced serum calcium levels. Furthermore, the expression of transient receptor potential cation channel subfamily 6 (TRPV6) and calbidin-D9K (CaBP-9K), both intestinal factors involved in calcium absorption, was severely reduced following 4-OP treatment (Kim et al, 2013). Altered intestinal

calcium absorption resulting in reduced serum calcium levels during pregnancy can lead to serious damage not only to maternal bones but also to fetal development. In fact, in order to develop properly, the fetus requires an amount of calcium that is removed from the mother's bones (Kim et al, 2013). The liver is the organ involved in the detoxification of substances and is also a target tissue for estrogens, which are considered primary liver mitogens (Zumbado et al, 2002). Precisely, APs induced high mitotic activity with the formation of mitotic hepatocytes presenting alterations in spindle formation, especially in the lobular zone. Excessive proliferation may underlie the onset of carcinogenesis (Zumbado et al, 2002). Hepatotoxicity can also be triggered through induction of oxidative stress mediated by APs. Indeed, rats treated with 4-NP showed an alteration of the oxidant/antioxidant system balance. In particular, 4-NP led to an increase in ROS and a reduction in antioxidant enzymes superoxide dismutase, reduced glutathione, catalase (SOD, GSH-Px, CAT). Furthermore, histological analysis revealed lobular inflammation, fat accumulation and liver ballooning, characteristic signs of hepatic steatosis (Kourouma et al, 2015). 4-OP can also cause liver damage through induction of oxidative stress. Indeed, 4-OP-treated mice showed reduced levels of antioxidant enzymes (GSH, SOD and CAT), increased levels of aspartate aminotransferase (AST), alanine transaminase (ALT) and alkaline phosphatase (ALP). This condition is typical of liver failure. In addition, histological analysis of liver sections confirmed that there was a cirrhotic condition, fibrotic tissue accumulation, hepatocellular vacuolization, dilatation and necrosis in different area (Saggu et al, 2014). These works were in agreement with an *in vitro* study by Magnifico et al (2018) performed on human hepatocarcinoma cells (HepG2), which elucidated the mechanism of action by which 4-NP and 4-OP induced oxidative stress and liver damage. Specifically, these investigators showed that exposure to 4-OP led to an increase of endothelial nitric oxide synthase (eNOS) while, in contrast, 4-NP induced increased expression of unspeakable NOS (iNOS). In addition, 4-NP decreased phosphorylation of eNOS at serine 1177 (P-Ser 1177) and increased phosphorylation at threonine 495 (P-Thr 495). This phenomenon showed that 4-NP was able to uncoupling of eNOS. Comparing the action of the two pollutants with that of estradiol, it could be seen that 4-OP acted similarly to the hormone instead 4-NP acted in a different way by activating iNOS and uncoupling eNOS. However, both compounds led to increased ROS levels by interfering with the NO pathway (Magnifico et al, 2018). On the whole, it is evident how these environmental pollutants in the gastrointestinal system, as well as in other systems, can cause severe damage by establishing a condition of chronic inflammation through the alteration of the cellular oxidative balance.

CHAPTER 2. Cardiac Glycosides (CGs): structure and characteristics

CGs are a large class of secondary compounds with an enough similar structure, found in plants and animals. They have a steroidal core to which an unsaturated lactone is bound in position 17 and, in most cases, a sugar is bound in position 3 (Botelho et al, 2019). The steroid portion is the most important part of the structure as it represents the active pharmacophore fraction (Ayogu et al, 2020). CGs are structurally different from other sterols such as sex hormones, mineralocorticoids or glucocorticoids, which have all rings connected in *trans* conformation. Indeed, CGs have a different stereochemical conformation: B/C rings are fused in *trans* conformation; A/B and C/D rings in *cis* conformation (Ayogu et al, 2020). The lactone ring bound to the steroid nucleus can be of two types, characterising two subfamilies of CGs:

- cardenolides with an unsaturated five-carbon-atom butyrolactone ring
- bufadienolides with six-carbon-atom α-pyrone ring (Mijatovic et al, 2007).

The structure of the CGs is shown in figure 6.
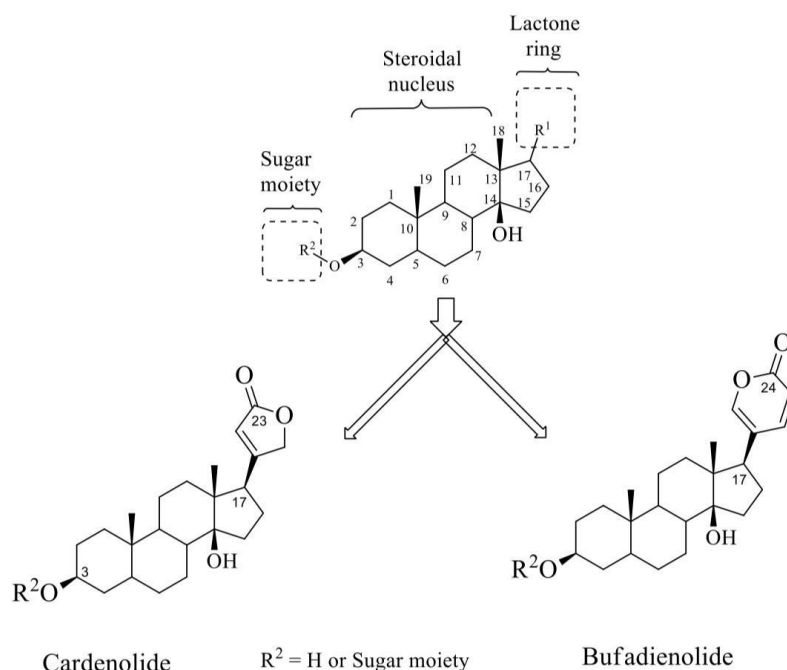
Figure 6. Structural classification of cardiac glycosides (Ayogu et al, 2020).

Although the sugar moiety does not determine the activity of these compounds, it is responsible for determining the pharmacodynamic and pharmacokinetic characteristics (Prassas and Diamandis, 2008). Different sugars can be bound to the steroid nucleus via 3 β-OH: L-rhamnose, D-glucose, D-digitose, D-digitalose, D-fructose (Mijatovic et al, 2007). Free aglycones are usually metabolized more easily than related glycosylated compounds (Prassas and Diamandis, 2008). Even Langenhan

et al. have developed a tool called "neoglycorandomization", which is able to predict the pharmacological potency of a CG compared to another based on the sugar that is bound to the steroid nucleus. For example, the addition of rhamnose can increase the potency of a cardiotonic steroid from 6- to 35-fold; instead, the addition of mannose has no effect (Langenhan et al, 2005; Prassas and Diamandis, 2008)

Usually, cardenolides are mostly found in angiosperm plants such as Asclepiadaceae, Apocynaceae and Moraceae; instead bufadienolides are present in animals such as toads of the genus *Bufo* (Ayogu et al, 2020). The best known CGs are ouabain isolated from plants of the genus *Acokanthera* and *Strophanthus*; digoxin from the genus *Digitalis*; oleandrin from *Nerium oleander*; bufalin in the toxins of toads of the genus *Bufo* (Botelho et al, 2019). Chemical characteristics of these compounds are reported in table 1.

Table 1. Chemical formula and characteristics of main cardiac glycosides (Botelho et al, 2019).

Cardiac glycosides	Chemical formula	Molecular weight (g/mol)	Sugar moiety
Bufalin	$C_{24}H_{34}O_4$	386.532	Absent
Digoxin	$C_{41}H_{64}O_{14}$	780.949	Hexopyranosyl polysaccharides
Oleandrin	$C_{32}H_{48}O_9$	576.727	Hexopyranosyl monosaccharide and acetoxyl
Ouabain	$C_{29}H_{44}O_{12}$	584.659	Mannopyranosyl monosaccharide

However, mass spectrometry studies have identified endogenous CGs in mammals: ouabain in human plasma and hypothalamus, digoxin in urine, marinobufagenin in human urine after a heart attack (Prassas and Diamandis, 2008). A work by Lichtstein et al. (1998) proposed a biosynthetic pathway of CGs in mammals. In this study, the biosynthesis of digitalis-like compounds was investigated in rat and bovine adrenal homogenates. Adrenocortical cells have been shown to metabolize hydroxycholesterol and pregnenolone. Furthermore, the metabolite co-migrated with digitalis in chromatographic systems. In addition, scientists demonstrated that aminoglutethimide and cyanoketone inhibited the production of these compounds. This meant that cytochrome P450 was involved in the first step of cleavage of the cholesterol side chain with subsequent conversion to pregnenolone and progesterone. Therefore, the first biosynthesis steps of digitalis-like compounds are like those of steroids (Lichtstein et al, 1998). Regulation of this process is under the control of

hormones: ranin-angiotensin, endothelin, adrenaline (Prassas and Diamandis, 2008). The functions performed by endogenous CGs are numerous. Certainly, the balance of their levels is important in regulating salt homeostasis. Furthermore, they participate in cell signaling, blood pressure regulation, natriuresis and cell proliferation (Mijatovic et al, 2007).

2.1 Mechanism of action and biological effects of CGs

The medical application of CGs is very ancient: Romans and Greeks already used the juice of *Digitalis* to treat bruises and sprains (Mijatovic et al, 2007). In traditional Chinese medicine, bufalin-based Ch'an Su tea is used in phytotherapy (Botelho et al, 2019). The pharmacological effect to which *Digitalis* compounds is still associated, today, is in the treatment of heart failure. Historically, their use began after the English physicist William Wethering observed that a patient with a congestive heart failure improved after administration of an extract of *Digitalis purpurea* (Newman et al, 2008). To understand different pharmacological and biological effects in which CGs are involved, we need to analyze the main target and the mechanism of action of these compounds. Their main target is the sodium potassium pump (Na^+/K^+-ATPase), a transmembrane protein composed of the catalytic α-subunit, containing the binding sites for Na^+, K^+, ATP and CGs, and the regulatory β-subunit (Mijatovic et al, 2007). These subunits are often associated with a single-transmembrane-spanning protein FXYD involved in the regulation of catalytic activity (Newman et al, 2008). The biological function of this protein complex is to use the energy derived from the hydrolysis of ATP to transport potassium ions inside and sodium ions outside the cell in a 2:3 ratio (Ayogu et al, 2020). It has been shown that CGs inhibited Na^+/K^+-ATPase, leading to an increase in intracellular Na^+ ions. Thus, the activity of the Na^+/Ca^{2+} pump was reduced and the concentration of Ca^{2+} increased within the cell (Škubník, 2021). In addition to the function of ion transporter, the Na^+/K^+-ATPase pump can interact with nearby membrane proteins and trigger an intracellular signaling cascade to send various messages to the organelles (Mijatovic et al, 2007). Thus, CGs can act as ligands that are able to trigger signal transduction and regulate many biological processes such as cell growth, mobility and apoptosis (Prassas and Diamandis, 2008). Two important reviews (Prassas and Diamandis, 2008; Newman et al, 2008) described the two most accredited pathways by which signal transduction can occur after a CG is bound to the sodium-potassium pump (Figure 7).

Immediately after binding of a CG to the Na^+/K^+-ATPase, its catalytic subunit changes conformation and activates the tyrosine kinase Src, which, in turn, activates the epidermal growth-factor receptor (EGFR). This activated receptor recruits the SHC adaptor protein, i.e. the growth factor receptor-bound protein 2 (GRB2), and SOS to allow the activation of mitogen-activated protein kinases (Ras-

Raf-MAPK). Activation of the MAPK pathway can lead to the opening of mitochondrial K^+ channels, thus generating ROS production, which interfere with NF-kB factor activation (Prassas and Diamandis, 2008). Another parallel pathway involves the formation of a microdomain in which phospholipase C (PLC) and inositol 1,4,5-triphosphate (IP_3), which are in contact with the cytosolic portion of the Na^+/K^+-ATPase, associate with the IP_3 receptor of the endoplasmic reticulum. In this way, there is a signaling based on fluctuations in intracellular calcium levels, which can lead to a decrease in the expression of the transcription factor activating protein-1 (AP-1) (Newman et al, 2008; Prassas and Diamandis, 2008). The signaling pathways are summarized in Figure 7.
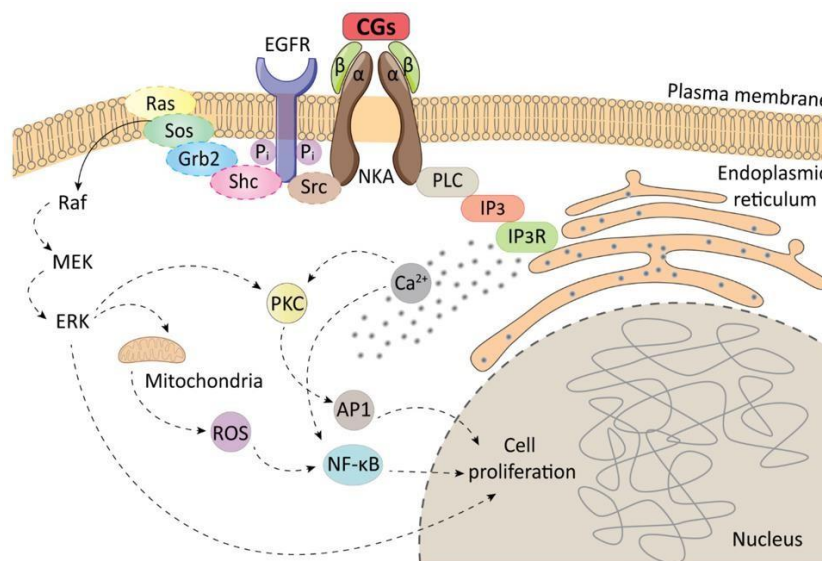
Figure 7. Scheme of possible signaling pathways of CGs (Škubník et al, 2021).

Since ligands of the Na^+/K^+-ATPase can mediate numerous effects, it is reasonable that they can be used in the treatment of various diseases. As previously mentioned, the historical application of CGs is the treatment of heart failure. Rahimtoola's (2004) work showed the effect of digoxin on patients affected by cardiac anomalies. First, digoxin reduced endodiastolic pressure and left ventricular (LV) endosystolic volumes but they increased LV ejection fraction (LVEF). This compound slowed down the ventricular rate in sinus rhythm leading to an improvement in heart failure. In addition, it had effects on the peripheral circulatory system by causing vasodilation, reduction of vascular vessel resistance and venous pressure. Consequently, it can be used to prevent and manage vasoconstriction in cases of myocardial ischaemia (Rahimtoola, 2004).

Another study performed on 4843 patients with chronic heart failure showed that the group receiving low-dose digoxin, after 42 months of follow-up, had a reduced mortality compared to the group receiving placebo (Ahmed et al, 2008). Thus, digoxin can be used in low doses in the treatment of heart failure when ACE inhibitors, beta-blockers and angiotensin receptor blockers are not tolerated

or have no effect (Ahmed et al, 2008). Indeed, although cardiotonic steroids are dangerous when used close to the toxic dose, they remain the most effective treatment for cardiac damage caused by hypertension and arteriosclerosis. About 17 million people in the USA have received *Digitalis* compounds to treat atrial fibrillation and heart failure (Mijatovic et al, 2008). Currently, digoxin is approved by the Food and Drug Administration (FDA), and it is sold in capsules, pills and elixirs. Its biotransformation is mainly hepatic and the average excretion half-life in subjects with physiological renal activity is between 36 and 48 h (Botelho et al, 2019).

Another application of CGs is in the treatment of cystic fibrosis. An *in vitro* study on a model of cystic fibrosis represented by IB-3 lung cells showed that different CGs can block the hypersecretion of IL-8, characteristic of this genetic disease. The most potent of tested compounds to mediate this effect was digitoxin. The mechanism by which it acted was by blocking the phosphorylation of the NF-kB inhibitor (IkBα). As a consequence, NF-kB cannot migrate to the nucleus and trigger the IL-8 production. Furthermore, the treatment appeared to have the same effects as gene therapy on the expression in IB-3 cells of genes relevant for disease progression (Srivastava et al, 2004).

Another *in vitro* study highlighted that CGs can potentially be used in the treatment of neurodegenerative pathologies such as spinobulbar muscular atrophy. This pathology is caused by an expansion of the CAG triplet in the first exon encoding the androgen receptor. This expansion leads to cell apoptosis by activating caspase 3. Of 1040 drugs tested, four were effective, including three CGs (nerifolin, peruvoside, digitotoxin). They were able to decrease the cytotoxicity induced by CAG expansion by blocking the release of the pro-apoptotic factor Bax, which induces caspase activation (Piccioni et al, 2004). In addition, CGs can also be applied in the treatment of inflammatory diseases involving the immune system. In particular, digoxin inhibited the transcriptional activity of the retinoic acid receptor-related orphan receptor γ thymus (RORγt), present only in T helper cells expressing IL-17 (Th17). So, digoxin blocked the differentiation of Th17 and the production of IL-17 and IL-22, involved in many inflammatory and autoimmune diseases such as colitis, rheumatoid arthritis, and abdominal aortic aneurysm (Škubník et al, 2021).

On the whole, CGs show a wide range of potential therapeutic applications. Today, research has focused especially on their use in oncology as reported in the following paragraph.

2.1.1 CGs anti-cancer activity

There are numerous reports in the scientific literature demonstrating the anti-tumour activity of CGs, triggered by various biological mechanisms. Certainly, one of the mechanisms most utilized by CGs is the activation of apoptosis in cancer cells. McConkey et al. (2000) showed that oleandrin, digoxin and ouabain were able to trigger apoptosis in prostate cancer cells, both with low metastasis potential

(PC-3 M-Pro4 cells) and with high metastasis potential (PC-3 M-LN4 cells). Researchers observed that CGs led to the activation of caspase-8 and -3 and to the cleavage of Poly (ADP-ribose) polymerase (PARP), all characteristic signs of the apoptotic program. However, the response of the two cell lines to treatments was different: in the Pro4 cell line there was a more rapid caspase activation than in the LN4 cell line, which was more refractory to apoptosis activation. Furthermore, apoptosis was strongly correlated with an increase in intracellular calcium levels that induced the release of cytochrome c (McConkey et al, 2000). This study was in agreement with another by Yeh et al. (2003) showing that bufalin and cinobufagin (other CGs) blocked proliferation and triggered apoptosis in androgen-independent (PC-3 and DU-145) and androgen-dependent (LNCaP) prostate cancer cells. Specifically, it was observed that there was activation of caspase-3 in DU-145 cell line and caspase-9 in LNCaP cell line. In addition, the two compounds induced an increase in intracellular calcium levels that was linked to apoptosis. In fact, using a specific inhibitor of L-type calcium channels (nifedipine), researchers observed a reduced percentage of apoptotic cells after treatment with bufalin (Yeh et al, 2003). Work by Daniel et al (2003) also showed that bufadienolides could activate apoptosis in cancer cells, specifically in malignant T lymphoblast cells (Jurkat). In this study, six compounds were tested: one natural (hellebrin) and five chemically modified to make them non-cardioactive. Three of the modified compounds and hellebrin showed the ability to trigger apoptosis by activating upstream caspase-8 and -9 and downstream caspase-3. Apoptosis and cytotoxicity were mediated by these cysteine proteases. Indeed, in the presence of inhibitors for caspases-3, -8 and -9, there were no characteristic signs of the apoptotic process such as phosphatidylserine externalization and internucleosomal DNA fragmentation. Researchers also noted that the effects of the compounds were selective for Jurkat tumour cells and not for normal peripheral mononuclear blood cells (Daniel et al, 2003). The selectivity for human cancer cells could be due to a different expression of Na^+/K^+-ATPase in cancer cells than in normal cells (Winnicka et al, 2006).

Certainly, one of the biological processes to be targeted in the search for new anti-cancer drugs is autophagy. Autophagy in the cancer process has a dual role: it acts both as a tumour suppressor, by preventing organelle damage, and as a survival mechanism by which cancer cells defend themselves against stress and obtain energy (Yang et al, 2011). Today, there is evidence that autophagy can be an alternative cell death mechanism to apoptosis and that there is a close interplay between autophagy and apoptosis (Yang et al, 2011). For example, P62, an autophagic marker, can bind caspase-8 and thus lead to the activation of apoptosis (Jiin et al 2009). CGs can also exert their anti-cancer activity by acting on the autophagic process. Meng et al (2016) showed that ouabain was able to induce apoptosis and autophagy in Burkitt's lymphoma Roji cells. Precisely, they observed by flow cytometry numerous cells in apoptosis and by western blot the increase of pro-apoptotic markers

caspase-3 and Bax and the decrease of anti-apoptotic protein Bcl-2 after ouabain treatment. Furthermore, by transmission electron microscopy (TEM) they noted the accumulation of double-membrane vacuoles, a hallmark feature of autophagy. In addition, western blot analysis showed that there was an increase in autophagy markers such as microtubule-associated proteins 1A/1B light chain 3B (LC3-II) and beclin-1 after ouabain treatment (Meng et al, 2016). Newman et al (2007), on the other hand, found that oleandrin could trigger cell death through autophagy without apoptosis in pancreatic cancer cells (PANC-1). Oleandrin blocked cell cycle progression in the G2/M phase, induced the formation of autophagosomes observed by TEM and increased LC3-II observed by western blot and by fluorescence in PANC-1 cells transfected with a plasmid containing green fluorescent protein (GFP)-LC3 (Newman et al, 2007). The study by Trenti et al (2014) agreed with Newman et al. (2007). Indeed, Trenti and her team observed that ouabain induced an increase in the LC3-II / LC3-I ratio and a reduction in P62 expression, a peculiar condition of autophagy induction. P62 (also called sequestome, SQSTM1) is a ubiquitin-binding scaffold protein that binds LC3 and is degraded in the autophagic process. Thus, the increase in LC3-II and decrease in P62 indicated that ouabain induced autophagy in non-small cell lung cancer cells (Trenti et al, 2014). Another mechanism by which CGs can exhibit an anti-cancer action involves DNA synthesis. The research of Bielawski et al (2006) showed that proscillaridin A, digoxin and ouabain led to the reduction of DNA synthesis by inhibiting topoisomerase II activity. In addition, proscillaridin A was the only one that also inhibited topoisomerase I (Bielawski et al 2006). Not only CGs are important for the development of new cancer drugs but they can also be used as adjuvants in traditional therapies. The report by Verheye -Dua and Böhm highlighted that several tumour cell lines were more sensitive to radiotherapy when treated with ouabain for one hour before and three hours after irradiation than cells treated with CGs or radiation alone. Precisely, combined treatment led to alteration of the cell cycle with prolongation of G2 phase and an increase in the percentage of apoptotic cells. Moreover, this effect was much more marked in tumour cells than in normal cells (Verheye -Dua and Böhm, 1998 and 2000). Furthermore, Lawrence in 1988 observed that ouabain made lung adenocarcinoma cells (A549) more sensitive to radiotherapy when treated with 10^{-6} M of cardenolides without having any influence on normal lung fibroblasts (CCL-210) (Lawrence, 1988). In line with these studies, Nasu et al. (2002) showed that oleandrin enhanced the effect of radiotherapy in PC-3 prostate cancer cells. They observed that the cytotoxic effect of the combined treatment occurred one hour after the cells were exposed to oleandrin and became maximal after 24 hours of exposure to cardenolides. In addition, researchers pointed out that cytotoxicity was linked to the triggering of apoptosis through the activation of caspase 3, which was not activated by radiotherapy alone (Nasu et al, 2002).

On the whole, anti-cancer activities of CGs in *in vitro* models are numerous. However, there are only few studies in *in vivo* models because these compounds either displayed an anti-cancer activity at concentrations toxic to organisms or had no effect at tolerated doses (Mijatovic et al, 2007). Furthermore, rodents such as mice resulted not a good model for studying the effects of CGs because these compounds were 100 times more toxic to human and monkey cells than rodent cells. In fact, CGs inhibited the rodent Na^+/K^+-ATPase at much higher concentrations. This difference seemed to be related to the different localization and expression of the Na^+/K^+-ATPase in rodents, especially α-subunit (Calderon-Montano et al, 2014). Han et al. tested the anti-tumour activity of bufalin in mice xenografted with human liver carcinoma cells (BEL-7402). Groups of mice treated with 1 mg/kg and 1.5 mg/kg bufalin (BF 1-2 groups) showed a reduction in tumour volume and increased survival compared to control mice treated with saline (NS group) and adriamycin (ADM group). Furthermore, in the BF 1-2 groups it was observed by electron microscopy that there were characteristic signs of apoptosis in the tumour cells: cell shrinkage, condensation of chromatin on the medial side of the nuclear membrane, presence of apoptotic bodies. By immunohistochemistry, researchers revealed that bufalin upregulated pro-apoptotic factors such as Bax at the transplantation site. No toxicity was induced to other organs such as heart, brain, lungs and kidneys (Han et al, 2007). Afaq et al. (2004) observed that oleandrin could have beneficial effects against induced skin cancer in mice treated with 12-O-tetradecanoylphorbol-13-acetate (TPA). Mice receiving topical application (2 mg) of oleandrin, 30 min prior to TPA treatment, showed inhibition of oedema, hyperplasia, expression of epidermal ornithine decarboxylase (ODC) and cyclooxygenase-2 (COX-2), which are characteristic for skin cancer (Afaq et al, 2004). In view of the numerous anti-tumour effects of CGs, the Food and Drug Administration (FDA) approved the first phase I clinical trial involving the treatment of patients with Anvirzel^TM, an aqueous extract of *Nerium oleander* containing mainly oleandrin and its aglycone form, oleandrigenin. Although well tolerated by patients, it did not show good effects on tumour regression. However, it must be considered that the patients had refractory solid tumours (Mekhail et al, 2006). Another preclinical phase II study recruited patients to test treatment with digoxin and EGFR-targeting antibodies. Specifically, the protocol involved daily administration of Tarceva with digoxin in patients with non-small cell lung cancer (NSCLC). Only one of the 26 patients recruited showed real improvement (ClinicalTrials.gov Identifier: NCT00281021). In summary, CGs can induce cytotoxicity in cancer cells through various biological mechanisms such as autophagy and apoptosis. The specific mechanism of action depends on the cell type. Furthermore, CGs can be good adjuvants in traditional therapies such as radiotherapy. Unfortunately, *in vivo* studies are few and clinical trials show that so far known CGs, at safe doses tolerated by organisms, have little effect on

tumour regression. Therefore, future research should focus on discovering new CGs or on their chemical modifications to make them less toxic and more efficacious against cancer.

2.2 Cardenolides from *Pergularia tomentosa*: structural characteristics and biological effects

Pergularia tomentosa belongs to the subfamily of Asclepiadaceae and it is a semi-erect perennial climbing herb used in traditional medicine to treat fungal infections, skin diseases, bronchitis and constipation (Hassan et al, 2007). This plant is a rich source of CGs: uzarigenin, ghalakinoside and its derivatives, calactin and its derivatives were found in the roots; desglucouzarin, coroglauceginin and uzarigenin in the leaves (Hamed et al, 2006; Hosseini et al, 2019). CGs extracted from the Asclepiadaceae exhibit peculiar structural characteristics. Unlike other cardiotonic steroids such as digitalis, which have *cis*-fused A/B steroid core rings and *trans*-fused B/C rings, they have *trans*-fused A/B rings. This conformation makes the structure flatter (Figure 8) (Mijatovic et al, 2007).

cis-trans-cis   Configuration of CGs such as digitalis

trans-trans-cis   Configuration of Asclepiadacae CGs

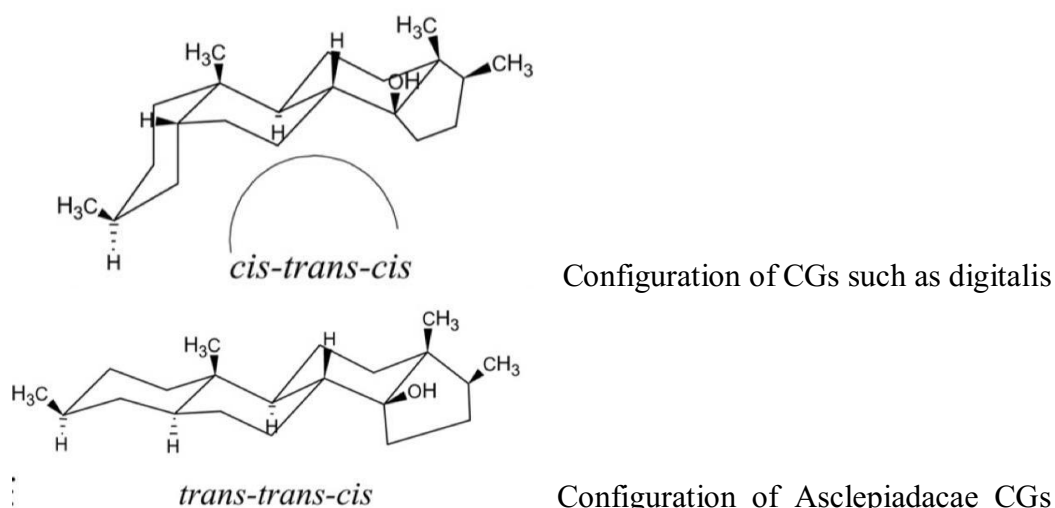**Figure 8**. Comparison between CGs configurations (Mijatovic et al, 2007; modified)

The glucidic portion in *P. tomentosa* CGs is generally represented by a single sugar (4,6-dideoxyhexosulose or its modified form 4-deoxyhexosulose) which is bound to the steroid core at position 2α and 3β with haemiacetalic and acetalic functions respectively, generating the dioxanoid attachment (Figure 9) (Piacente et al, 2009).
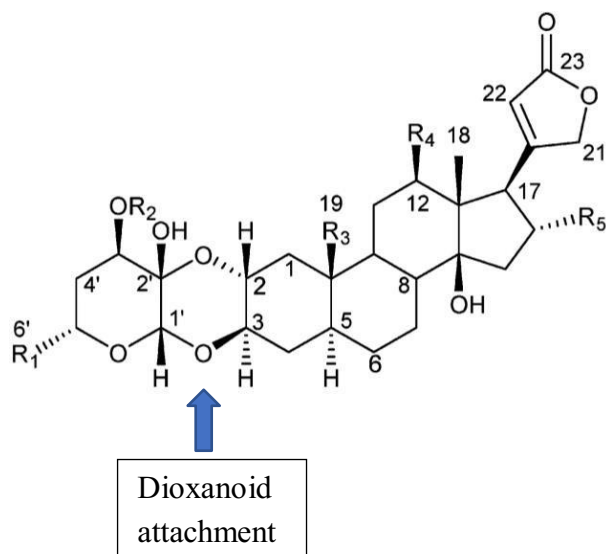
Figure 9. Typical structure of *P. tomentosa* CGs (Piacente et al, 2009; modified)

These peculiar structural features give these compounds the ability to bind the Na^+/K^+-ATPase more powerfully (Piacente et al, 2009). Given the interest (as outlined in the previous paragraph) in studying the anti-tumour effects of CGs, activity against cancer cells has also been tested for those isolated from *P. tomentosa*. A first study by Hamed et al. (2006) showed that compounds extracted from *P. tomentosa* roots (ghalakinoside and its derivatives, calactin and its derivatives) had cytotoxic action against Kaposi's sarcoma cells (KS cells). Using flow cytometry, researchers demonstrated that cytotoxicity was linked to the triggering of apoptosis. Indeed, using a specific DEVD-AFC assay, they observed that there was an increase in caspase activity in cells treated with cardenolides extracted from *P. tomentosa* roots (Hamed et al, 2006). Piacente et al. (2009) also tested the cytotoxic activity of cardenolides extracted from *P. tomentosa* roots on six cancer cell lines (U373, BxPC-3, PC-3, LoVo, A549, MCF-7). Precisely, the scientists found that:

1) all eight compounds had cytotoxic action; 2) the most potent compound was calactin; 3) there was a cell type-dependent response (e.g. the compounds were 10 times more toxic on the A549 cell line than on the others).

Furthermore, using a specific colorimetric assay based on the presence of Na^+/K^+-ATPase from porcine cerebral cortex, they measured the concentration at which 50% of the Na^+/K^+-ATPase was inhibited (IC_{50}) in the presence of *P. tomentosa* compounds. In this way, they showed that there was a good correlation between anti-proliferative activity and inhibition of this multiprotein complex (Piacente et al, 2009). In 2019, Hosseini et al. isolated 18 cardenolides from *P. tomentosa* leaves, belonging to two categories: calotropin derivatives and calactin derivatives. Authors showed that all compounds had cytotoxic activity on five different human cancer cell lines: PC-3 (prostate carcinoma

cells), Hela (cervical carcinoma cells), Calu-1 (epithelial lung cancer cells), MCF-7 (breast cancer cells) and U251MG (human glioma cells). Like Piacente et al., they found that cytotoxicity was cell type-dependent and that the most sensitive cells were PC-3 cells. In a more recent research, Hosseini et al. (2020) tested the effect of *P. tomentosa* extracts on angiogenesis. They found that extracts inhibited the growth of intersegmental vessels (ISVs) in a transgenic zebrafish *Tg(flil:EGFP)* model at 48h post fertilization. They also found that the aqueous fraction of these extracts (PtR2), containing mainly ghalakinoside, calactin and calotropin derivatives, exhibited the greatest anti-angiogenic effect with minor consequences on viability. Furthermore, by performing wound-healing assay and the assay of tube formation on matrigel, they showed that PtR2 reduced migration and vessel formation of HUVECs cells (human umbilical vein endothelial cells). Immunocytochemistry and western blot also showed that PtR2 reduced the expression of VE-cadherin and β-catenin, important factors for proper angiogenesis. Thus, *P. tomentosa* extracts displayed anti-angiogenic action by targeting the migration of endothelial cells (Hosseini et al, 2020). The search for new CGs from this plant is still continuing. Indeed, Shatat et al. (2022) recently isolated two new compounds, pergularol and 3-O-acetyl-28-hydroxytaraxasterol, from the aerial parts of *P. tomentosa*. Moreover, for the first time, the already known apigenin 7-(6"-crotonoyl) glucoside has been isolated from the genus *Pergularia* (Shatat et al, 2022).

CHAPTER 3. Aims

In the light of the studies presented in the introduction, during my PhD course, my primary aim was to study biological effects induced by APs (4-NP and 4-OP) and cardenolides extracted from *P. tomentosa* by using human cell models.

For APs, I intended to investigate cytotoxic effects on different cell lines representing possible target organs. The goal was to understand biochemical and molecular mechanisms underlying the APs cytotoxicity. In particular, I evaluated whether these substances affected the cell cycle progression, whether they were responsible for triggering cell death and related cellular stress conditions such as ER-stress, mitochondrial dysfunction, oxidative stress and altered calcium homeostasis. In addition, with studies still in progress, I was interested to understand whether these pollutants could affect the balance of autophagic flux, another cellular process closely related to apoptosis. For my investigations I mainly used 2D models but I also set a 3D model consisting of spheroids of hepatic human cells, with the aim to study metabolic changes induced by APs through a metabolomic approach.

Then, considering the interest in the scientific literature around the anti-cancer activity of CGs, another aim of my investigations was to understand the potential anti-cancer effect of cardenolides extracted for the first time from the aerial parts of *P. tomentosa*. Also in this case, I was interested to investigate biochemical and molecular mechanisms by which these compounds acted on human cells. Since some important characteristics of cancer cells are the ability to migrate and the resistance to the induction of apoptosis, I evaluated whether cardenolides from *P. tomentosa* could trigger cell death and also how they modulate cell migration. In addition, given that a favourable property of an anti-cancer drug, today, is the modulation of autophagy, I studied whether these compounds could affect this biological process.

In summary, salient aims of my research, conducted on human cell lines as a model, were, on the one hand, to understand the molecular mechanisms underlying APs-induced cytotoxicity and, on the other hand, to characterize anti-tumour properties of cardenolides extracted from *P. tomentosa*.

CHAPTER 4. Materials and Methods

4.1 Cell cultures

Studies reported in this thesis were performed on different cell models:

- HepG2 (human hepatocellular carcinoma cells)
- Caco-2 (human intestinal adenocarcinoma cells)
- MRC5 (human lung fibroblasts cells)
- HUVECs (human umbilical vein endothelial cells)
- HEK293 (human embryonic kidney cells)

All cell lines were obtained from Interlab Cell Line Collection, National Institute for Cancer Research, (Genoa, Italy) whereas HUVECs from Lonza (Milan, Italy). HepG2 and Caco-2 cell lines were cultured in Eagle's Minimum Essential medium (MEM, Gibco, Stanley Rd., Grand Island, NY, USA) supplemented with 1% (v/v) non-essential amino acids (Gibco), 0.2 mM L-glutamine, 50 units/mL penicillin and 50 µg/mL streptomycin (Euroclone, Milan, Italy) and 10% (v/v) or 20% (v/v) fetal bovine serum (FBS, Gibco) for HepG2 or Caco-2, respectively; MRC5 was cultured in Dulbecco's Modified Eagle medium (DMEM, Gibco) supplemented with 10% (v/v) fetal bovine serum, 0.2 mM L-glutamine, 50 units/mL penicillin and 50 µg/mL streptomycin; HUVEC cells were cultured in Endothelial Growth medium-2, supplemented with FBS (2%), VEGF (0.1%), rH FGF-B (0.4%), rH EGF (0.1%), GA-1000 (0.1%), hydrocortisone (0.04%), R3-IGF-1 (0.1%), heparin (0.1%) and ascorbic acid (0.1%). Cells were maintained at 37 °C in a 5% CO_2 atmosphere and passaged twice a week.

4.2 Reagents employed to test the biological activity

Regarding experiments with environmental pollutants, we used 4-NP and 4-tOP (Sigma-Aldrich, St. Louis, MO, USA) solubilized in dimethyl sulfoxide (DMSO) to generate starting solutions of 200 mM stored at room temperature in the dark. Cardenolides from the aerial parts of *P. tomentosa* were isolated and characterized by the team of Professor Sonia Piacente of the Department of Pharmacy of the University of Salerno. They were dissolved in DMSO to obtain stock solutions at 20 mM concentration, then stored at -20°C in small aliquots. Subsequent dilutions were made in MEM. For all treatments, the final concentration of DMSO in culture medium was less than 0.05%.

Other reagents used such as staurosporine (STS, an apoptosis inducer), thapsigargin (TAP, an ER-stress inducer) and salubrinal (an ER-stress inhibitor) (all from Sigma-Aldrich) were also solubilized in DMSO to obtain stock solutions, then stored at -20°C in small aliquots.

4.3 Cell viability assay

To investigate the effects of compounds on cell viability we realized a MTT colorimetric assay. It exploits the ability of the enzyme succinate dehydrogenase, which is active only in live cells, to cut the tetrazolium ring of the yellow-coloured 3-(4,5-dimethylthiazol-2-yl)-2,5-diphenyltetrazolium bromide (MTT) (Sigma-Aldrich) leading to the formation of purple-coloured formazan crystals. So, the number of live cells will be directly proportional to the amount of crystals formed. Specifically, 7500 cells were seeded in each well of a 96-wells microplate and, after 48 h, were treated with the desired concentration of APs or *P. tomentosa* compounds for 24 h (sometimes for 48 h). As a control, cells were treated with the equal concentrations of DMSO to verify that this substance had no effect on viability. As a positive control of cytotoxicity, instead, the cells were treated with 0.2% H_2O_2 for 30 min after which the complete medium was restored. After the treatments, 0.5 mg/mL MTT was added to the culture medium in the wells and incubated for 90 min at 37 °C. Once the crystals were obtained, the multiwell was centrifuged at 2000 rpm for 1 min using the Universal 320R centrifuge so that crystals deposited on the bottom. Then, the culture medium was aspirated and crystals dissolved in 100 μL of DMSO. To obtain a uniform solution after the addition of DMSO, the plate was shaken for 10 min at 70 oscillations per minute.

Finally, measurements were done by using a Microplate Reader (Bio-Rad) at a wavelength of 595 nm, to evaluate the absorbance of formazan, and at 655 nm, to evaluate that of background. The absorbance at 655 nm was subtracted from that recorded at 595 nm. For each experiment, biological triplicates were averaged to obtain the data, and the absorbance of the blank was subtracted from each value. The cell viability was expressed as: OD compound tested / OD DMSO; in some cases, it was reported as percentage of viability measured in vehicle-treated cells.

4.4 IC$_{50}$ calculation

Data obtained from MTT assays were employed to calculate the IC$_{50}$, i.e., the concentration of each compound that is required to reduce cell viability *in vitro* by 50%. IC$_{50}$ was calculated as reported in the work of Piacente et al. (2009), on the base of the following formula:

$$IC_{50} = (X2 - X1) \times (50 - Y1) / (Y2 - Y1)) + X1$$

where X1 is the highest concentration that reduced cell growth by 50%; X2 is the lowest concentration that reduced growth by 50%; Y1 is the percentage of viable cells at X1 stimulus concentration and Y2 is the percentage of viable cells at X2 stimulus concentration (Piacente et al, 2009).

4.5 Cell proliferation assay

To analyze whether compounds affect cell cycle progression we performed the bromodeoxyuridine (BrdU) incorporation assay. BrdU is a thymidine analogue that is incorporated into the neosynthesized DNA of cells that are proliferating and thus are in S phase. Initially, cells were seeded on round glass coverslips (12 mm diameter) and cultured for 24 h; then they were treated with the appropriate concentrations of compounds. In some cases, cells were starved i.e., cultured in medium containing 0.1 % FBS instead of 10 % for 24 h and then stimulated to proliferate by the addition of 20 mM EGF in the presence or absence of APs for 18 h. After the desired treatment time (generally 18-24 h), in the same culture medium, BrdU (Sigma-Aldrich) was added so that it reaches the final concentration of 100 µM and incubated for 90 min. Then cells were washed twice with phosphate buffered saline (PBS, Euroclone), then fixed with 4% paraformaldehyde (PFA, Sigma-Aldrich) for 10 min, washed, twice more, with PBS and permeabilized with 0.2% Triton X-100 (Sigma-Aldrich) for 5 min. To decondense chromatin and allow the primary antibody to bind to the incorporated BrdU, we performed treatment with 1.5 N HCl for 8 min at 37 ˚C. Then we washed three times with PBS and incubated the cells with anti-BrdU antibody diluted 1:100 (clone BU33, Sigma-Aldrich) in PBS-1% BSA (bovine serum albumin) for 1 h and 30 min in a humid chamber. After 3 washes with PBS, coverslips were incubated with a TRITC fluorophore-conjugated secondary antibody (Thermo Scientifics, Milan, Italy) diluted 1:100 in PBS-0.1% BSA for 1 h at room temperature in a humid chamber. To detect all proliferating and non-proliferating cells, coverslips were treated with a Hoechst 33258 solution (1 mg/mL) in PBS and finally mounted with mowiol (Sigma-Aldrich). Stained cells were observed under a Axioskop 40 fluorescence microscope (Carl Zeiss MicroImaging, Inc, Jena, Germany). Images were acquired with Axiocam MRc5 and processed with Axiovision 4.2 software (Carl Zeiss MicroImaging). The number of proliferating cells was counted with ImageJ software and expressed as the ratio of BrdU-incorporating cells to the total number of cells.

4.6 Protein expression analysis and western blot

To analyze whether the expression of specific proteins changed in the presence of the compounds under investigation, we performed western blot analyses. This approach can be divided into steps: cell lysis and protein extraction, protein concentration determination, electrophoresis, western blot, slab acquisition and densitometry.

4.6.1 Cell lysis and protein extraction

After treatments, cells were mechanically harvested and lysed in RIPA buffer containing: 20 mM Tris-HCl, pH 7.5, 150 mM NaCl, 1 mM EDTA, 1 mM dithiothreitol, 0.1% sodium dodecyl sulphate, 1% Triton X-100, 1 mM orthovanadate, and an inhibitors cocktail (all from Sigma-Aldrich).

RIPA buffer was kept in incubation for 30 min in oscillation at 70 osc/min. All passages were performed on ice to minimize protein degradation.

4.6.2 Protein concentration determination

To quantify the protein concentration, we used Bradford's method. It is based on the principle that Coomassie Brilliant Blue G-250 dye can bind proteins in solution and varies its absorption properties with the appearance of a peak at 595 nm (Bradford M, 1976). Specifically, we used Bio-Rad reagent protein containing this dye diluted 1:5 in distilled water. Generally, 1μL of sample was added to 1 mL of dye-containing solution. Finally, we performed absorbance measurement by using the spectrophotometer (VWRUV-3100PC) at 595 nm. A duplicate measurement was made for each sample and the values were averaged. To know the concentration of the sample, we compared its absorbance with those of a standard curve obtained with known concentrations of BSA.

4.6.3 Polyacrylamide gel electrophoresis

Proteins were separated on the base of their molecular weight by SDS-PAGE (Sodium Dodecyl Sulphate-PolyAcrylamide Gel Electrophoresis).

This technique takes advantage of the principle that proteins in the presence of SDS take on a negative charge and, thus, in an electric field, can migrate starting from the positive pole. In this way, proteins are separated according to their molecular weight. To denature samples, they were mixed with Laemmli sample buffer and heated at 100 °C for 10 min. The 4x sample buffer contains 200 mM Tris-HCl pH 6.8, 20% glycerol, 8% SDS, 400 mM dithiothreitol (DTT, GE Healthcare, Milan, Italy) and 0.04 % bromophenol blue. We used a discontinuous gel, i.e. a gel with two portions at different composition and pH: upper gel (or stacking gel) useful for flattening the proteins before separating them and the lower gel (or separating gel) whose acrylamide concentration varies according to the molecular weight of the proteins we need to separate. Along with the samples, the molecular weight markers (Thermo-Fischer, Milan, Italy) were loaded onto the gel. Electrophoresis was performed in Running buffer 1x containing 25 mM Tris, 192 mM glycine and 0.1% SDS.

4.6.4 Blotting (western blot)

After electrophoresis, the separated proteins were transferred to a polyvinylidene difluoride (PVDF) membrane (EMD Millipore Corporation, Billerica, Massachusetts, USA). The membrane was first activated for one minute in methanol, washed in water and then rehydrated in transfer buffer. The 1x transfer buffer contained Tris (25 mM), glycine (192 mM) and methanol (20%). The blotting was performed using the Trans-Blot Turbo Transfer System (Bio-Rad). After protein blotting, the membrane was incubated for 30 min at 70 osc/min in a blocking solution containing 5% skimmed milk in Tris-Buffered Saline (TBS). The TBS consisted of 50 mM Tris pH 7.5 and 150 mM NaCl. The antibody solution was prepared in TBS-0,1% Tween-20 (T-TBS)

To detect specific proteins membranes were incubated with the following primary antibody (Ab):

- Ab mouse anti P53 (Santa Cruz, Santa Cruz, California, USA) diluted 1:1000 in T-TBS-1% milk
- Ab mouse anti GRP78 (Invitrogen, Milan, Italy) diluted 1:1000 in T-TBS -1% milk
- Ab rabbit anti LC3 (Invitrogen) diluted 1:1000 in T-TBS -1% milk
- Ab mouse anti caspase-3 (Invitrogen) diluted 1:1000 in T-TBS -1% milk
- Ab mouse anti P62 (Invitrogen) diluted 1:1000 in T-TBS -1% milk
- Ab rabbit anti SOD (Elabscience, Houston, Texas, USA) diluted 1:600 in T-TBS -1% milk
- Ab rabbit anti DRP1 (Santa Cruz) diluted 1:1000 in T-TBS -1% milk
- Ab rabbit anti CHOP (Invitrogen) diluted 1:1000 in T-TBS -1% milk
- Ab mouse anti GAPDH (Santa Cruz) diluted 1:4000 in T-TBS -1% milk
- Ab mouse anti Tubulin (Santa Cruz) diluted 1:1000 in T-TBS -1% milk
- Ab rabbit anti MFN2 (Santa Cruz) diluted 1:1000 in T-TBS-1% milk
- Ab goat anti Lamin B (Santa Cruz) diluted 1:2000 in T-TBS-1% milk
- Ab mouse anti ERK (Santa Cruz) diluted 1:1000 in T-TBS-1% milk
- Ab mouse anti p-ERK (Santa Cruz) diluted 1:1000 in T-TBS-1% milk

After incubation with the primary antibody, 4 or 6 washes with T-TBS each of 5 minutes at 70 osc/min were performed. Then, the membrane was incubated with the appropriate secondary Ab conjugated to horseradish peroxidase (HRP) for 1 h at room temperature.

The secondary antibodies that were used are:

Ab anti mouse (Bio-Rad) diluted 1:10000 in T-TBS

Ab anti rabbit (Bio-Rad) diluted 1:10000 in T-TBS

After several washes with T-TBS-Tween, the membrane was incubated with ECL (GE Healthcare) when we expect more intense signals or with ECL (Immobilon Millipore) when we expect less intense signals for 5 min. Signal detection was carried out by autoradiography by impressing a slab (FujiFilm, Tokyo, Japan). The slab was developed by automatic developer (Cawomat 2000 IR).

4.6.5 Densitometric analyses

The impressed slabs were acquired and analyzed using the GS-800 densitometer (Bio-Rad) and Quantity One software (Bio-Rad). Using the excel software, ODs, optical densities, obtained from the product of band area and density per unit area, were calculated. The ODs of the samples were normalized against those of housekeeping proteins such as GAPDH or tubulin.

4.7 Caspase-3 assay

To find out whether the compounds under investigation were exerting cytotoxicity through the induction of apoptosis, we performed the assay of caspase-3 activity, a cysteine protease executor in the process of programmed cell death. This assay is a colorimetric one in which a caspase substrate, p-nitroanilide-labeled acetyl-Asp-Glu-Val-Asp (Sigma-Aldrich) is converted to p-nitroaniline (pNA), which is yellow. The absorbance can be registered at 405 nm; a higher absorbance value corresponds to a higher enzyme activity. HepG2 cells were seeded in 60-mm diameter plates and, after 24 h, treated with the compounds under investigation. Cells were detached in PBS and collected by centrifugation at 60 g for 5 min at 4 °C and lysed in buffer containing 50 mM HEPES, 0.1% CHAPS, 10 mM dithiothreitol, 100 mM NaCl, 1 mM EDTA and 10% sucrose. Lysates were then clarified by centrifuging at 16000 g at 4 °C., and supernatants were collected.

Protein concentration was determined by Bradford's method (section 3.6.2). The assay is set up in a 96-well plate in which proteins (30 μg) are incubated in a reaction mix in which the caspase substrate (0.2 mM) was added and the plate was incubated for 2 h at 37 °C.

Caspase-3 activity was expressed as the ratio of absorbance of treated cells and of cells treated with vehicle.

4.8 TUNEL Assay

The TUNEL (Terminal deoxynucleotidyl transferase dUTP Nick End Labeling) assay is a useful technique to identify apoptotic cells. It is based on the principle that cells in apoptosis undergo DNA double-strand breaks by making free 3-OH groups to which deoxy-UTP can be added by the enzyme terminal deoxynucleotidyl transferase (TdT). Precisely, we used the commercial Fragment End Labelling (FragEL[TM], Jena, Germany) DNA fragmentation Detection Kit (Sigma-Aldrich). We

seeded the cells on round glass coverslips in 24-well plates and after 48 h we treated them with the desired concentrations of compounds for 24 h. Then we fixed cells with 3% PFA, permeabilized with 0.2% Triton X-100 for 5 min and treated with 1.5 N HCl for 8 min. The coverslips were then maintained for 10 min in equilibration buffer and incubated in a mix containing TdT enzyme for 1 h at 37 °C. The coverslips were then mounted with specific mounting medium. Finally, we observed coverslips with an Axioskop-40 fluorescent microscope and acquired images with the Axiocam MRc5 (Carl Zeiss MicroImaging).

4.9 Scratch-Wound-Healing Assay

To investigate whether *P. tomentosa* compounds influenced cell migration, we performed a scratch-wound-healing assay. This method requires that a scratch is done on a uniform layer of cells; then the ability of cells to "heal" the "wound" is evaluated in the presence of compounds under investigation. Specifically, we seeded 500000 HepG2 cells in wells of a 24-well plates and incubated them until they reached confluence. At this stage we performed a pre-treatment with mitomycin C (10 μg/mL) useful to inhibit cell proliferation. This step is very important to exclude that the eventual wound closure will be given by proliferation and not by cell migration. Then, we made a furrow with a sterile tip in the cell layer, washed with PBS to remove detached cells and added medium containing *P. tomentosa* compounds or vehicle. We incubated cells for times ranging from 0 to 72 h. After the incubation times, cells were visualized under an Olympus CKX41 microscope (Olympus, Segrate, Italy) and photographed using cellSens Dimension software.

Analysis was performed using ImageJ software. For each scratch, wound width was measured as the distance between two edges of 4 different sites, and width reductions at times 24, 48, and 72 h were expressed as % width compared with time zero. The degree of closure was calculated using the formula reported in a paper by Grada et al. (2017):

Migration rate= (Initial Width-Final width) / (Migration duration).

4.10 Transwell migration assay

To evaluate cell migration in the presence of *P. tomentosa* compounds, we also performed a migration assay with Transwell chambers with PET membrane (BD biosciences, Milan, Italy). Transwell filters are placed in 24-well plates and coated with a collagen I solution for 3 h at 37 °C. HepG2 cells were seeded in the upper chamber at the density of 75×10^3 in MEM-0.1% BSA and treated with 1 μM of *P. tomentosa* compounds. MEM -0.1% BSA supplemented with 10% FBS was added to the lower chamber as a chemoattractant. As a control, we used wells without 10% FBS to evaluate any random migration. After incubation at 37 °C in 5% CO_2 atmosphere for 18 h, migrated cells were fixed with

4% PFA for 5 min, permeabilized with methanol for 20 min, stained with 0.5% crystal violet (Sigma-Aldrich) for 15 min at room temperature. Non-migrated cells were removed with cotton swabs. Before counting the migrated cells, we dried the filters. Then for each migration chamber we acquired 8 images by Olympus CKX41 Image Analyzer. For each treatment, we performed the migrated cell count, averaged and compared with the control. The result was expressed as % of migrated cells compared with the control.

4.11 Catalase activity assay

To assess whether environmental pollutants caused oxidative stress, we used the commercial Catalase (CAT) Activity Assay Kit (Elabscience). CAT is an enzyme that protects cells from overproduction of ROS. Precisely, CAT catalyses the decomposition of hydrogen peroxide into water and oxygen. The kit is based on the principle that the CAT reaction can be stopped by ammonium molybdate. Residual hydrogen peroxide reacts with ammonium molybdate to generate a yellow complex. CAT activity can be calculated from the production of this yellow complex at 405 nm.

HepG2 cells were seeded in 6-well plates. After 24 or 48 h of incubation, they were treated with desired concentrations of APs for 24 h or 48h. As control we used vehicle (DMSO)-treated cells, instead, as positive control cells treated with 600 μM H_2O_2 for 45 min and then cultured in complete medium. After treatment, cells were collected by scraper, washed twice with PBS, and centrifuged at 1000 g for 10 min to obtain the cell pellet. We added lysis medium (0.01 M PBS including 1 mM EDTA) to each sample.

We promoted lysis by passing each sample through the needle of a syringe. Then we centrifuged at 1500 g for 10 min and stored the supernatant. Protein concentration was determined by Bradford's method. Then we prepared a mix in which to 20 μL of sample we added 200 μL of Kit reagent 1 and incubated at 37 ˚C for 1 min. Then we added 20 μL of reagent 2 and incubated for 1 min. Finally, we added 200 μL of reagent 3 and 20 μL of reagent 4. After mixing by vortex and incubating for 10 min, we took 200 μL of each mix and put it in a well of a 96-well plate to measure absorbance at 405 nm with the microplate reader. The absorbance was proportional to the CAT activity.

4.12 RT-PCR to evaluate markers of ER-stress

To analyze the effect that APs and *P. tomentosa* compounds have on the expression of specific genes indicating the occurrence of ER-stress, RT-PCR analyses were performed. After treatments, RNA was extracted and retrotranscripted; finally, PCR amplification (both real time and conventional) was performed, as described in detail in the following sections.

4.12.1 Cell treatments

To investigate the expression of GRP78 and CHOP, cells were cultured in six-well plates for 24 h and afterwards were treated with different concentrations of the test compounds for 7 h or with TAP (used as a positive control to induce ER-stress). In contrast, to analyze XBP1, treatments were performed for 4 h.

4.12.2 RNA Extraction

After treatments, we added 600 μL of Trizol (Invitrogen) to each plate, then scraped and harvested cells into 1.5 mL tubes. After 15 min of incubation at room temperature, we added 100 μL of chloroform and mixed. Then, we centrifuged at 12350 g for 15 min at 4 °C. We collected the aqueous phase containing RNA, which was subsequently precipitated by addition of isopropanol. After 10 min of incubation, samples were centrifuged at 12350 g for 10 min at 4 °C and the supernatant was removed. Pellets were washed with 75% ethanol, samples centrifuged at 9300 g for 5 min and the ethanol allowed to evaporate. Finally, RNA was resuspended in water and heated to 55 °C.

4.12.3 RNA quantization

RNA concentration was determined by measuring the absorbance of a 1 μL sample drop using nanodrop 2000 (Thermofisher) at a wavelength of 260 nm. The ratio of absorbance at 260 nm to that at 280 nm, indicating possible protein contamination (ideal range between 1.7 and 2.0) and the ratio of absorbance recorded at 260 nm to that at 230 nm (ideal range between 2.0 and 2.2), indicating contamination by phenols, chloroform, guanidinium isothiocyanate (contained in Trizol) were also measured.

4.12.4 Retrotrascription

To obtain the cDNA, we used the QuantiTect Reverse Transcription Kit (Qiagen, Milan, Italy). For each sample, we retro-transcribed 1 μg of RNA. To each RNA sample, 2 μL of gDNA WipeOut Buffer and H_2O RNAse-free were added to reach the final volume of 14 μL. This mix was incubated at 42 °C for 2 min in a thermocycler (Applied Biosystem PCR System 2720). Then, we added the retrotranscription mix containing: 1μL of reverse transcriptase, 4 μL of Quantiscript RT buffer and 1μL of RT primer mix. Finally, we applied the following protocol: incubation for 25 min at 42 °C to make the reaction take place, incubation at 95 °C for 5 min to inactivate reverse transcriptase.

4.13 Real Time PCR

To amplify the transcripts of GRP78 and CHOP genes, we performed Real Time PCR using the iQ™ SYBR Green Supermix (Bio-Rad Laboratories) and the iQ™ 5 Multicolor Real Time PCR Detection System (Bio-Rad Laboratories). The respective primer pairs for GRP78 and CHOP were used for the reaction: 5′-CTGG GTACATTTGATCTGACTGG-3′ and 5′-GCATCCTGGTGGCTTTCCAGC CATTC-3′; 5′-CTTGGCTGACTGAGGAG-3′, and 5′-TCACCATTCG GTCAATCAGA-3′.

The thermocycling protocol included an incubation at 95 ℃ for 3 min followed by 40 cycles of the following steps:

1. 15 seconds at 95 ℃
2. 15 seconds at 60 ℃ for annealing
3. 20 seconds at 72 ℃ for polymerization.

The mRNA concentration was normalized to the concentration of the GAPDH transcript amplified with the following primers: 5′-TTCAACAGCGACACCCACTG-3′ and 5′-CACCCTGTTGCTGTAGC CA-3′.

4.14 PCR

To amplify the cDNA of XBP1 involved in the ER-stress process and study its alternative splicing, we performed a conventional PCR from obtained cDNA. The sequence of the primers used to amplify the cDNA of XBP1 were as follows: 5′CCTGGTTGCTGAAGAGGAGG-3′ and 5′-CCATGGGGAGATGTTCT GGAG-3′. The reaction mix containing reaction buffer, magnesium chloride, reverse and forward primers, Taq polymerase (Invitrogen) and diluted cDNA was prepared for each sample. The thermocycling protocol employed with the PCR System 2720 (Applied Biosystem) includes a first step of Taq polymerase activation at 95 ℃ for 5 min and was followed by 35 cycles of the following steps:

1) DNA denaturation step at 94 ℃ for 35 seconds

2) annealing phase at 58 ℃ for 45 seconds

3) extension phase at 72 ℃ for 1 min

The last phase at 72 ℃ for 7 min allowed completion of all cDNA synthesis.

To visualize amplified cDNA, samples were prepared by adding Blue Juice Loading buffer 6x (Invitrogen) and run on a 2.5 % agarose gel containing ethidium bromide. Bands were visualized by a transilluminator and photographed.

4.15 TG2 activity

To assess whether APs could alter intracellular calcium levels, we evaluated the activity of the calcium-dependent enzyme type 2 transglutaminase (TG2). TG2 enzymatic assay is based on the ability of TG2, after Ca^{2+} mobilization, to covalently link an aminic substrate (pentylamine-biotin) to intracellular proteins. The formation of covalent complexes is quantified by the binding of streptavidin, able to recognize biotin in the complex, conjugated to horseradish peroxidase. Caco-2 cells expressing TG2 were seeded in 6-well plates and incubated for 48 h. After incubation, Caco-2 cells were treated with 0,5 mM of pentylamine-biotin for 5- or 10-min e subsequently treated for 1 h with desired concentrations of APs. After treatments, cells were washed twice with PBS, mechanically harvested and lysed in RIPA lysis buffer for 30 min. Samples were then centrifuged at 13000 g for 10 min to remove cell debris. Then, proteins were coated in 96-well microplate with Tris-HCL/EDTA 50 mM / 2 mM in PBS, treated with a blocking solution consisting of 10% BSA in Borate-Buffered Saline (BBS) for 3 h, washed with BBS and BBS containing 0.01% Tween 20 (T-BBS) and, finally, incubated with streptavidin conjugated to horseradish peroxidase (Thermo Fischer) diluted 1:3000 in T-BBS with 5% BSA for 1 h. Finally, to each well, 100 µL of 3,3',5,5'-tetramethylbenzidine solution (TMB, Sigma-Aldrich), which is the substrate of horseradish peroxidase, were added. The reaction was stopped by the addition of sulfuric acid (H_2SO_4). Absorbances, proportional to TG2 activity, were measured by the Microplate Reader at a wavelength of 450 nm.

4.16 Separation of nuclear and cytoplasmatic proteins

500000 HepG2 cells were plated in the wells of a 6-well plate. After 48 h of incubation, they were treated with 5 µM of *P. tomentosa* compounds. To extract and separate nuclear and cytosolic proteins, we used the commercial kit NE-PER (Nuclear and Cytoplasmatic Extraction Reagents, Thermo Scientificts). We obtained a pellet by trypsinizing the cells and centrifuging at 500 g for 5 min. Subsequently, two washes of PBS were performed. 80 µL of CER 1 (Cytoplasmatic Extraction Reagent I) was added to each cell pellet. Each sample was, then, vortexed and incubated on ice for 10 min. Next, we added 4.4 µL of CER II (Cytoplasmatic Extraction Reagent II), were vortexed and incubated on ice for 1 min. By centrifugation at 16000 g for 10 min at 4 °C, we obtained the cytoplasmic fraction in the supernatant. The pellets, on the other hand, were treated with 40 µL of NER (Nuclear Extraction Reagent), vortexed and incubated on ice for 10 min. By centrifugation at 16000 g we then obtained the supernatant containing the nuclear proteins.

4.17 Production of HepG2 spheroids

To generate a 3D model of HepG2, i.e. spheroids, we used the liquid-overlay technique (Stampar at al, 2019). First, we prepared a substrate dissolving 1% of agarose in PBS. We coated the wells of a 96-well plate with 50 μL. This volume is adequate to cover the entire surface area of the well. Once cooled, the agarose forms a gel. To form the spheroids, we used a suspension of HepG2 cells containing 3000 cells for each 20 μL. We made drops of the cell suspension on the plate cap and filled the wells with 100 μL of PBS. After 48 h of incubation, we removed the PBS from the wells and transferred the drops into them by adding 100 μL of fresh culture medium. After 2 days of incubation part of the medium is removed and replaced with new medium. We have, thus, incubated up to 12 days. To assess that spheroids were well formed, after 5 and 12 days from the initial preparation we evaluated by Real time PCR the expression of liver differentiation genes, albumin and CYP1A2 (Snykers et al, 2009), by comparing it with that of genes expressed at time zero. Specific primers for albumin were: forward primer TGCTTGAATGTGCTGATGACAGGA; reverse primer AAGGCAAGTCAGCAGGCATCTCATC); specific primers for CYP1A2 were: forward primer CTCCTCCTTCTTGCCCTTCA; reverse primer GTAGAAGCCATTCAGCGTTGTG.

Thermocycling conditions were as follows: initial denaturation at 95 °C for 15 min followed by 40 cycles consisting of:

1. denaturation phase at 95 °C for 15 seconds
2. a combined annealing and elongation at 60 °C for 1 min
3. terminal elongation at 60 °C for 15 min

4.18 Samples for metabolomic analyses

In collaboration with Theoreo srl and its CEO Dr. Jacopo Troisi, we are initiating metabolomics studies on 2D and 3D cell models of HepG2 treated with APs. For now, those on two-dimensional cultures of HepG2 are already underway. Precisely we plated 750000 HepG2 cells in 6-well plates After growth for 48 h the HepG2 cells were treated for 14 h with vehicle (DMSO), 4-OP 25 and 50 μM and with 4-NP 25 and 50 μM. The final number of cells after growth should be between 1×10^6 and 5×10^6 for 1 ml of cell suspension.

Each sample was produced in biological triplicate so we will have a total of 15 cell and 15 medium samples. The concentrations of the APs treatments were chosen based on their IC_{50} calculated at 24 h by considering those that did not show particular cytotoxicity.

4.19 Statistical analysis

All data were expressed as means ± standard error (SE) of three independent experiments conducted in triplicate. Statistical analysis was performed by Student's t test. In all experiments, differences were considered statistically significant at values of $p < 0.01$ and $p < 0.05$.

CHAPTER 5. Results

In this chapter, I will present results of my PhD project divided into three sections.

The first section will be dedicated to the characterization of 4-NP biological effects in a hepatic human cell model (HepG2 cells); indeed, liver is the main organ responsible for detoxification and represents a site where 4-NP may potentially accumulate, as demonstrated in livers of rats fed on diet supplied with 4-NP (Yu et al, 2017).

The second section will deal of results regarding the mechanism of action of 4-OP on several cell lines representing cells of potential target organ in humans. These results have been obtained more recently with respect to those regarding 4-NP and include experiments that compare 4-NP and 4-OP effects and also evaluate the effect of their combination.

The third and last section will focus on the characterization of anti-cancer properties of cardenolides from *P. tomentosa*.

5.1 Mechanisms of 4-NP cytotoxicity on HepG2 cells

5.1.1 4-NP reduces cell viability in HepG2 cells

First, to understand whether 4-NP had toxic effects on human hepatic cells, we performed a MTT assay on HepG2 cell line, a useful model to study hepatic physiology (Gomez-Lechon et al, 2014). Specifically, we treated cells with increasing concentrations of 4-NP for 24 h and observed that 4-NP significantly reduced the viability of HepG2 at the highest concentrations (Figure 10 A). The most potent effect was seen when cells were treated with 100 μM of 4-NP. In this case, cell viability was reduced by 50%. H_2O_2 (0.05% in medium) was used as a positive control, which reduced cell viability by about 90% (Figure 10 A). We also investigated the effect of this pollutant on cells already subjected to a stress condition. Precisely, we cultured HepG2 in medium containing only 1% FBS (normally HepG2 are cultured in 10% FBS) for 24 h and then treated them with various concentrations of 4-NP for 24 h. We found that the cytotoxic effect was very pronounced already in cells treated with 25 μM of 4-NP leading to 80% reduction in viability (Figure 10 B).
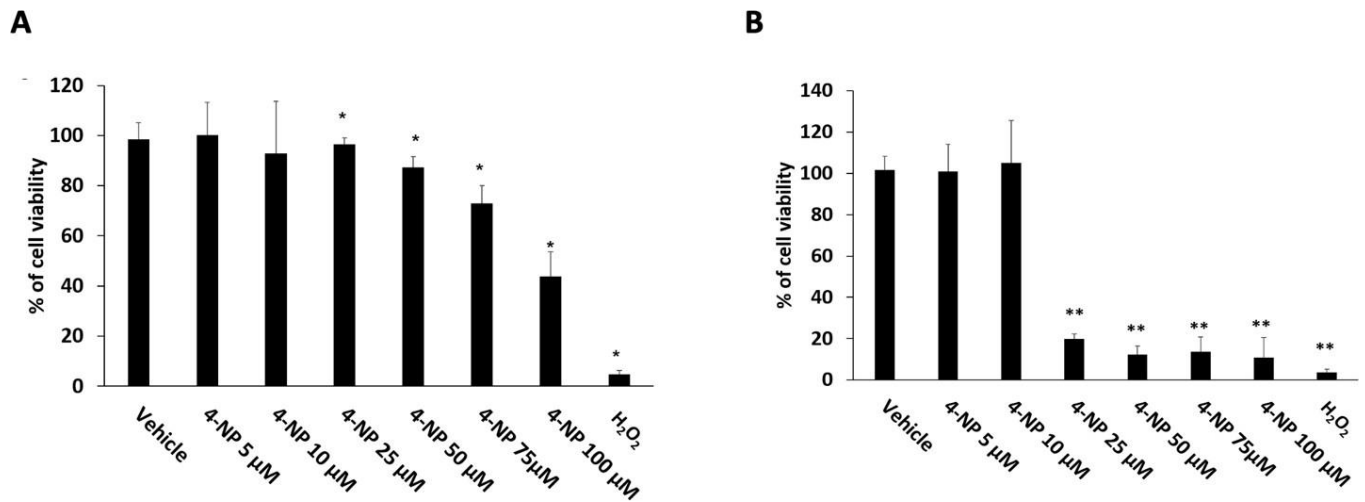
Figure 10. 4-NP reduces cell viability. (A) MTT assay performed on HepG2 cells treated with different concentrations of 4-NP for 24 h. (B) MTT assay on HepG2 cells cultured in 1% FBS for 24 h and subsequently treated with different concentrations of 4-NP. H_2O_2 (0.05 % in medium) was used as a positive control; vehicle is DMSO 0.05%. Results were expressed as means ± standard error (SE) of three independent experiments performed in triplicate. Statistical analysis was performed using Student's t-test. * $p < 0.05$ and ** $p < 0.01$ vs. cells treated with the vehicle (DMSO).

5.1.2 4-NP affects cell cycle progression in HepG2 cells

Given the reduction of cell viability, we investigated whether 4-NP could affect cell cycle progression. We performed the BrdU incorporation assay on HepG2 cells treated with increasing concentrations of 4-NP. As observed in Figure 11 A, treatments with 4-NP at the concentration of 100 μM induced a significant reduction of nuclei entering in the S phase. Next, we performed an experiment to understand whether 4-NP could counteract a pro-proliferative stimulus. Specifically, we starved cells, then added epidermal growth factor (EGF) 20 nM and in the presence or not of different concentrations of 4-NP. In this case, 4-NP reduced cell cycle progression already at low doses (4-NP 10 μM) and completely abrogated pro-proliferative effect of EGF at the 50 μM concentration (Figure 11 B).
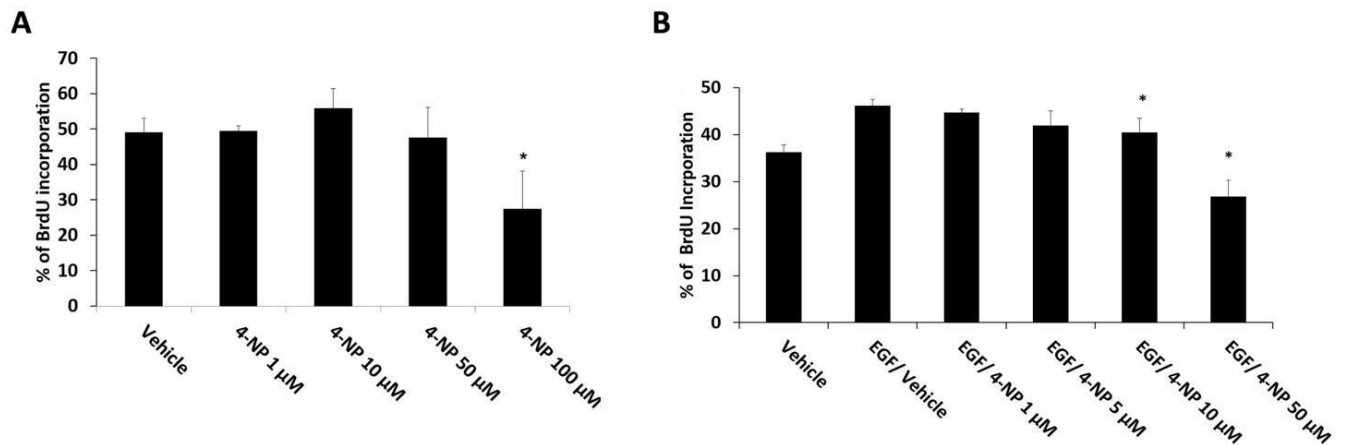
Figure 11. Effects of 4-NP on cell cycle progression. (A) BrdU incorporation assay on HepG2 cells treated with increasing concentrations of 4-NP for 24 h. (B) BrdU incorporation assay on starved HepG2 cells treated with EGF 20 nM and in the presence or the absence of 4-NP. Results were expressed as means ± SE of three independent experiments. Statistical analysis was performed using Student's t-test. * $p < 0.05$ vs. cells treated with EGF/vehicle

In addition, we evaluated the effect of 4-NP on the expression of ERK protein and its phosphorylated form pERK. Indeed, cell proliferation requires several phosphorylation events and subsequent translocation into the nucleus of pERK (Shevzov et al, 2015). Specifically, we treated HepG2 with the pro-proliferative stimulus EGF in the presence and absence of 4-NP. As shown in the western blot, EGF induced increase in pERK, whereas, in the presence of 4-NP at the concentration of 25 μM, the effect of EGF was reduced and the level of pERK decreased (Figure 12).
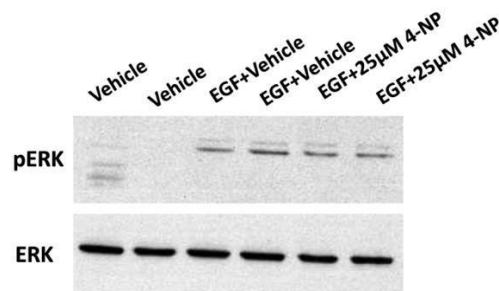

Figure 12. 4-NP reduced EGF-induced ERK phosphorylation. (A) Western blot on HepG2 cells treated with EGF in the presence or absence of 4-NP.

5.1.3 4-NP triggers apoptosis in HepG2 cells

We investigated whether 4-NP-induced cytotoxicity observed with the MTT assay was also related to the process of programmed cell death. First, we evaluated the activity of caspase 3, a cysteine protease that plays a crucial role in the apoptotic process (Porter and Janicke, 1999). We observed that caspase 3 activity increased significantly in the presence of 50 and 100 μM of 4-NP after 8 h of treatment (Figure 13).
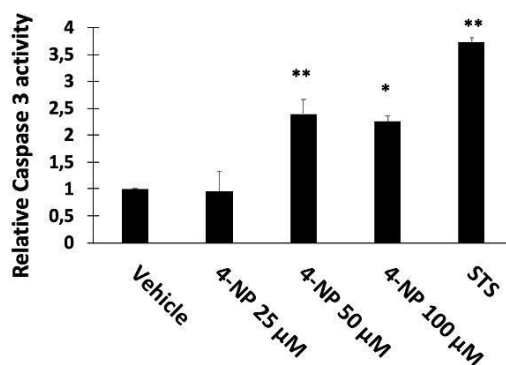

Figure 13. Caspase 3 activity in HepG2 cells treated for 8 h with different concentrations of 4-NP. Results were expressed as means ± SE of three independent experiments and as relative activity respect to vehicle treated cells. STS was used as a positive control of apoptosis. * $p < 0.05$ and ** $p < 0.01$ vs. cells treated with the vehicle.

Subsequently, by western blot, we also evaluated the level of cleaved caspase 3 in HepG2 cells in the presence of 4-NP. We observed the appearance of active caspase 3 in HepG2 after 8 h of treatments with 4-NP at the concentration of 50 and 100 μM (Figure 14 A and B)
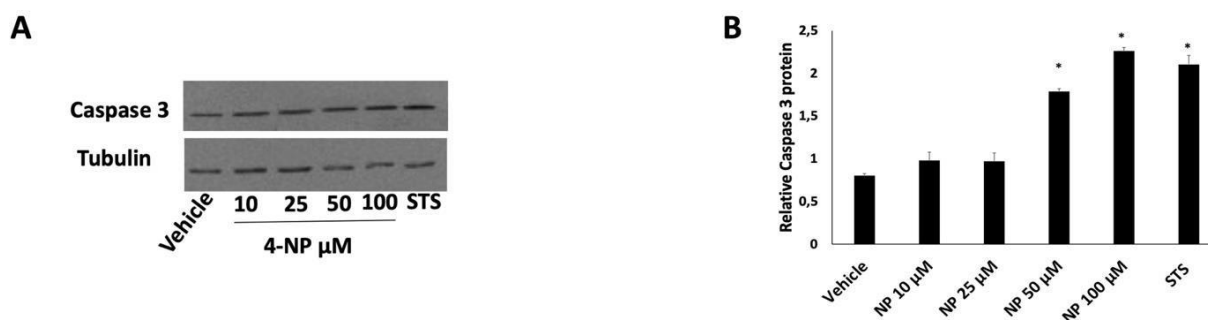

Figure 14. Caspase 3 levels. (A) Representative western blot of caspase 3 level in HepG2 cells in the presence of increasing 4-NP concentrations. (B) Densitometric analysis relative to three independent experiments. Protein levels are normalized with respect to tubulin expression. Data are expressed as means ± SE of three experiment. Statistical analysis was performed using Student's t-test. * $p < 0.05$ vs. vehicle treated-cells. STS, an inductor of apoptosis, was used as positive control.

Since p53 is an important protein in controlling cell proliferation and triggering programmed cell death through caspase activation (Shen and White, 2001), we evaluated its expression. By western blot, we observed that p53 levels increased in HepG2 cells after they had been treated with 25 and 50 μM of 4-NP, whereas with treatment of 100 μM of 4-NP, p53 expression returned to the basal expression (Figure 15 A and B).

Figure 15. p53 expression in HepG2 cells after treatments with increasing concentrations of 4-NP for 24 h. (A) Representative western blot of p53. (B) Densitometric analysis of three independent experiments. Protein levels are normalized with respect to tubulin expression. Data are expressed as means ± SE of three experiment. Statistical analysis was performed using Student's t-test. * $p < 0.05$ vs. vehicle treated-cells. STS, an inductor of apoptosis, was used as positive control.

Finally, by microscopic observation, we evaluated the possible presence of apoptotic nuclei. Specifically, we detected them in cells cultured for 18 h in the presence of 50 and 100 μM of 4-NP (Figure 16)
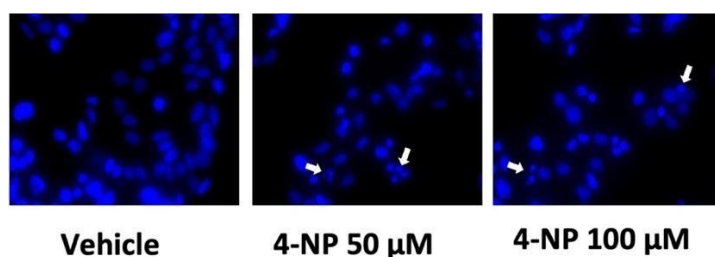

Figure 16. Hoechst staining of HepG2 nuclei treated with 4-NP and vehicle. Arrows indicate apoptotic nuclei presenting condensed chromatin.

5.1.4 4-NP induces ER-stress in HepG2 cells

As mentioned earlier in the introduction, APs can cause ER-stress-related cell death (Lepretti et al, 2015). The cellular organelle responsible for proper protein folding is the ER, however, under certain pathological conditions or cellular stress the unfolding protein response (UPR) can be generated. One of the main molecules involved in the UPR is the chaperone Glucose-regulated protein 78 (GRP78).

When the cell fails to restore its homeostasis, ER-stress can trigger apoptosis involving the C/EBP homologous protein (CHOP) expression, also called gene 153 (GADD153), inducible by growth arrest and DNA damage (Oyadomari and Mori, 2004). Another key modulator in the UPR is XBP1 (X-box-binding-protein 1). Precisely, the mRNA encoding the spliced active form of XBP1 is generated during the UPR (Wang et al, 2011). Therefore, to understand whether 4-NP induced ER-stress, we analysed these three specific markers. By performing western blot, we observed increased expression of GRP78 in HepG2 cells treated with 50 and 100 μM of 4-NP, instead, CHOP protein appears only in treatments with 4-NP at the concentration of 100 μM. TAP, a known inducer of ER-stress, was used as a positive control (Figure 17 A and B).
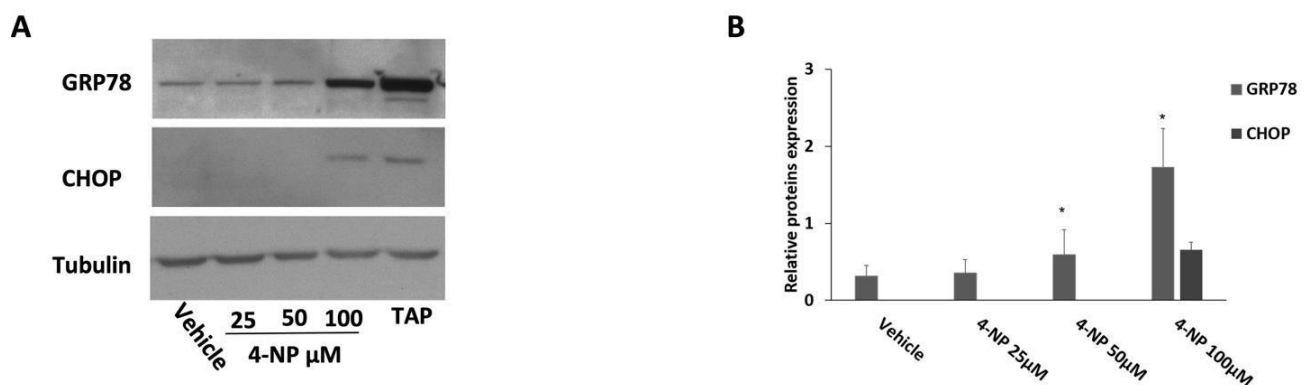

Figure 17. ER-stress markers expression. (A) Representative western blot of GRP78 and CHOP in HepG2 treated for 24 h with increasing concentrations of 4-NP. (B) Densitometric analysis relative to three independent experiments. Protein levels are normalized with respect to tubulin expression. Data are expressed as means ± SE of three experiment. Statistical analysis was performed using Student's t-test. * $p < 0.05$ vs. vehicle treated-cells.

In addition, by Real-Time PCR we evaluated the mRNA levels of GRP78 and CHOP. As shown in Figure 18, the mRNA level of GRP78 increased significantly already with 4-NP treatments of 7 h at 25 μM, while CHOP transcript increased only with treatments at 100 μM of 4-NP (Figure 18).
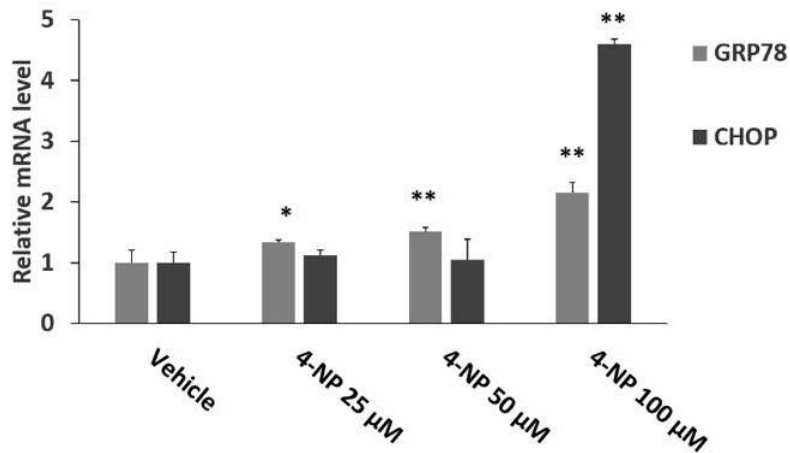
Figure 18. mRNA relative level of ER stress markers GRP78 and CHOP measured by Real Time PCR. Data are expressed as means ± SE of three experiment. Statistical analysis was performed using Student's t-test. * $p < 0.05$ and ** $p < 0.01$ vs. vehicle treated-cells.

Finally, by conventional PCR we evaluated the alternative splicing of XBP1. HepG2 cells were cultured with increasing doses of 4-NP, and we found that a slight spliced form was present after the treatment with 50 μM of 4-NP but became markedly evident with 100 μM of 4-NP (Figure 19).
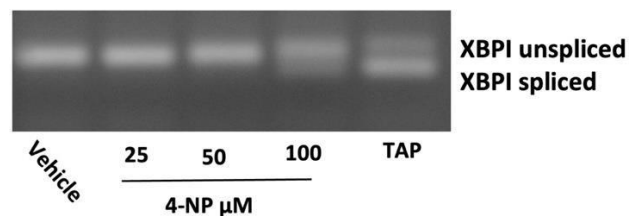

Figure 19. Visualization on a 2.5% agarose gel of XBP1 splicing in HepG2 cells treated with different concentrations of 4-NP for 4 h. TAP was used as a positive control.

5.1.5 4-NP affects mitochondrial dynamics in HepG2 cells

ER-stress affects mitochondria function and vice versa, as ER and mitochondria communicate through mitochondria-associated ER membranes (MAMs), which are implicated in the regulation of various processes such as apoptosis (Giamogante et al, 2021). Therefore, we evaluated the expression of mitofusin 2 (MFN2) and dynamin-related protein 1 (DRP1), proteins responsible for mitochondrial fusion and fission, respectively (Yapa et al, 2021). By western blot we found that 4-NP induced a significant increase in expression of MFN2 at all concentrations tested (Figure 20 A and B) and of DRP1 only at 100 μM (Figure 20 C and D) in HepG2 cells treated for 24 h.
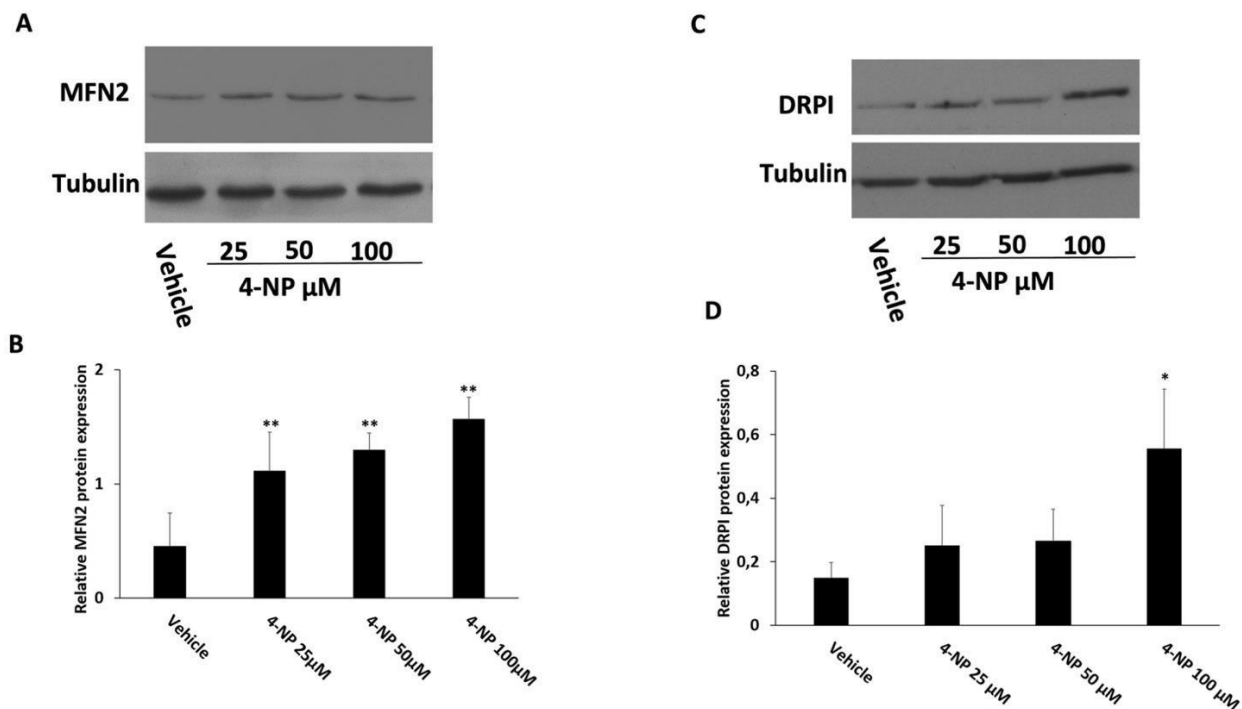
Figure 20. 4-NP affects mitochondrial dynamics. (A and B) Representative western blot and densitometric analysis of MFN2 expression in HepG2 cultured in the presence of 4-NP for 24 h. (C and D) Representative western blot and densitometric analysis of DRP1expression in HepG2 cultured in the presence of 4-NP for 24 h. All proteins expression was normalized respect the housekeeping protein tubulin. Data are relative to three independent experiments and expressed as means ± SE. * $p < 0.05$ and ** $p < 0.01$ vs. vehicle treated-cells.

5.1.6 4-NP-induced ER-stress is responsible for apoptosis and mitochondrial dysfunction in HepG2 cells

To understand whether 4-NP could trigger programmed cell death due to an unresolved ER-stress, we performed experiments in which HepG2 cells were treated with 4-NP in the presence of salubrinal, a specific ER-stress inhibitor (Boyce et al, 2005). By western blot, we evaluated the expression of GRP78 in HepG2 cells pre-treated with salubrinal 50 and 100 μM and then cultured in the presence of 4-NP. As shown in Figure 21 A, salubrinal at 100 μM significantly abrogated the effect of 4-NP on GRP78 expression. Then, by Real Time PCR we also observed that salubrinal 100 μM significantly reduced the mRNA level of GRP78 in HepG2 treated with 4-NP (Figure 21 B).
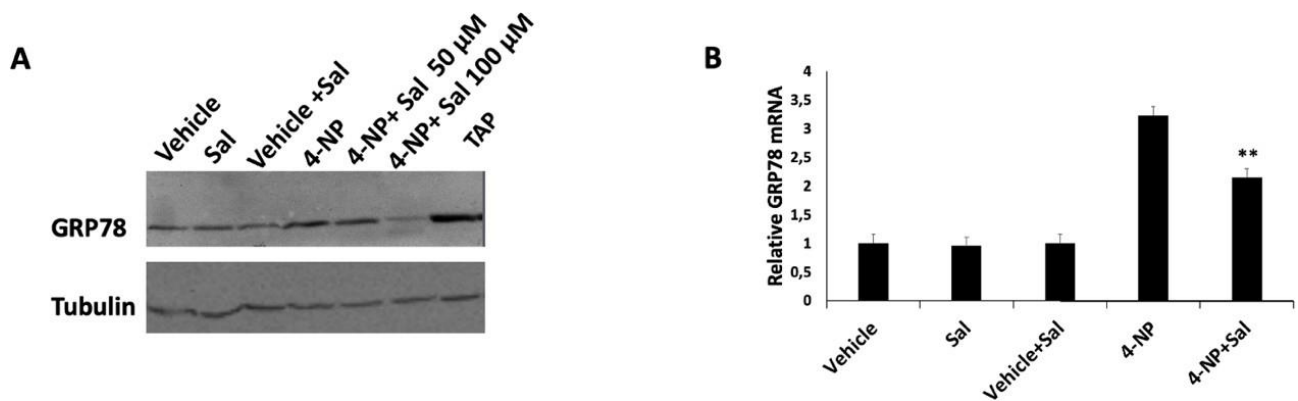
Figure 21. (A) Western blot of GRP78 in HepG2 treated with 4-NP in the presence and absence of salubrinal (Sal). (B) Relative GRP78 mRNA in HepG2 treated with 4-NP in the presence and absence of salubrinal analysed by Real Time PCR. Data are expressed as means ± SE of three experiment. Statistical analysis was performed using Student's t-test. ** $p < 0.01$ vs. vehicle treated-cells.

Next, we investigated whether salubrinal could influence the caspase 3 activity. The caspase 3 activity assay highlighted that in HepG2, treated with 4-NP and salubrinal 100 μM, caspase 3 activity was lower than activity in cells treated with 4-NP alone (Figure 22 B). By western blot, we evaluated the expression of caspase 3 in the presence of salubrinal. As shown in Figure 22 A, salubrinal at the concentration of 100 μM reverted the effect of 4-NP on caspase-3 cleavage. On the whole, results of the activity assay and western blot for caspase agreed.

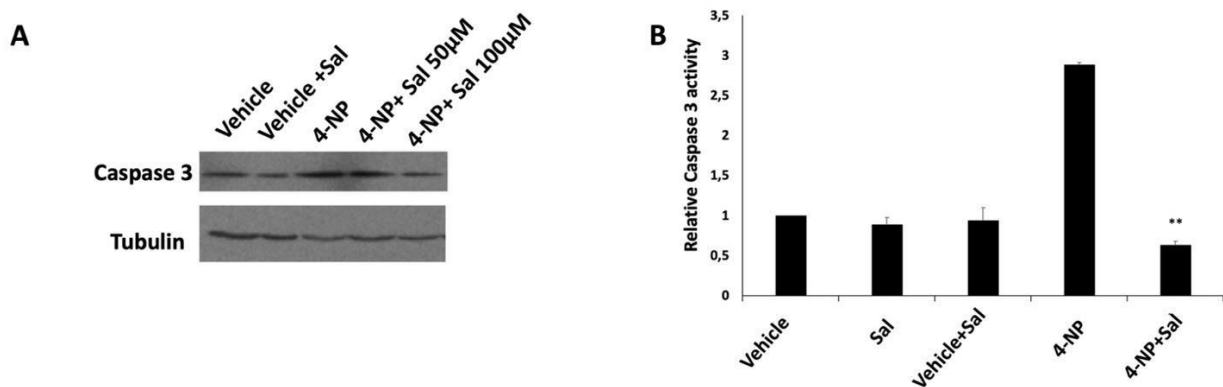**Figure 22**. (A) Representative western blot of caspase 3 in HepG2 cells treated with 100 μM of 4-NP in presence or absence of 50 and 100 μM of salubrinal. (B) Caspase-3 activity assay performed in HepG2 cells treated with 100 μM of 4-NP in presence or absence of salubrinal 100 μM. Data are expressed as means ± SE of three experiment. Statistical analysis was performed using Student's t-test. ** $p < 0.01$ vs. vehicle treated-cells.

Finally, we evaluated whether mitochondrial dysfunction caused by 4-NP could also depend on ER-stress. We found that salubrinal reduced the 4-NP-induced increase in MFN2 and DRP1 protein expression (Figure 23).

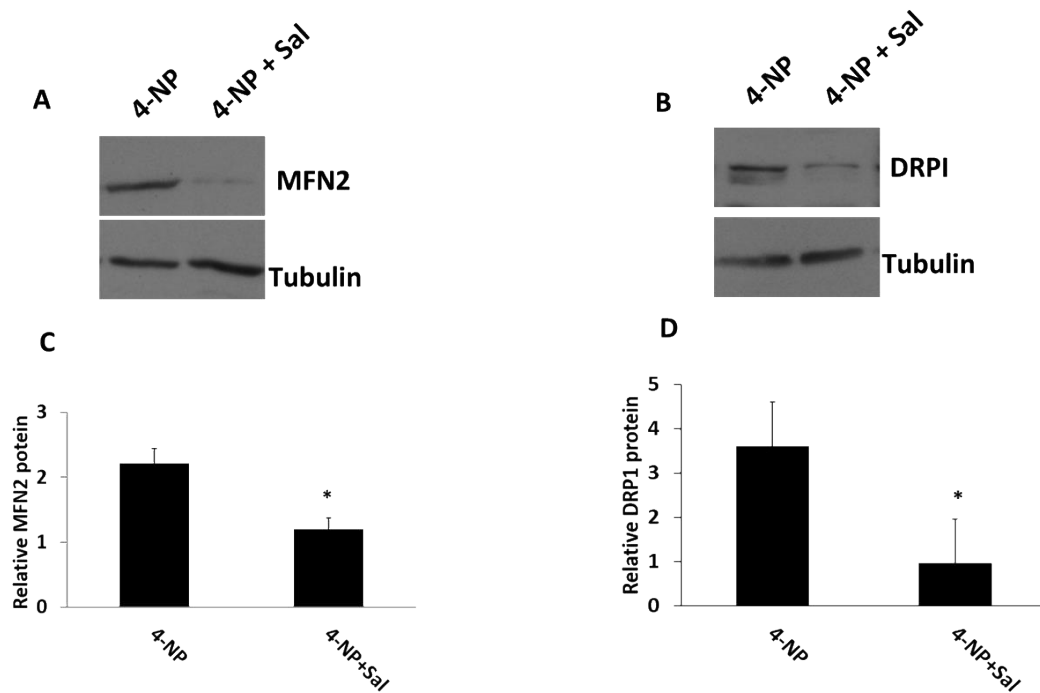**Figure 23**. Correlation between ER stress and mitochondrial dysfunction induced by 4-NP. (A and B) Representative western blot of MFN2 and DRP1 in HepG2 cells treated with 100 µM of 4-NP in the presence or absence of salubrinal 100 µM. (C and D) Densitometric analysis of MFN2 and DRP1 performed on three independent experiments. Statistical analysis was performed using Student's t-test. * p < 0.05 vs. vehicle treated-cells.

5.2 Mechanisms of 4-OP cytotoxicity

5.2.1 4-OP reduces cell viability of human cell lines

In the work of Lepretti et al. (2015) it has been observed that 4-NP reduced cell viability of Caco-2 cells; in the present work, we also found that 4-NP induced cytotoxic effects on HepG2. In the light of these results, we decided to investigate whether another similar AP, i.e. 4-OP, could have cytotoxic effects on these and other human cell lines representing possible target organs. Initially, we used the linear form of 4-OP to carry out the experiments, as we previously used the linear form of 4-NP (the most diffused in the environment). By MTT assays, we observed that this form of 4-OP had effects on HepG2 cell viability but not in a dose-dependent manner (Figure 24). With good probability, this behaviour was related with a problem of solubility, maybe due to a commercial compound not sufficiently pure. We also tried to change the vehicle in which it was dissolved, using ethanol instead of DMSO and we heated the solutions to ameliorate solubilization. In all these cases, we had the same results, too (data not shown).
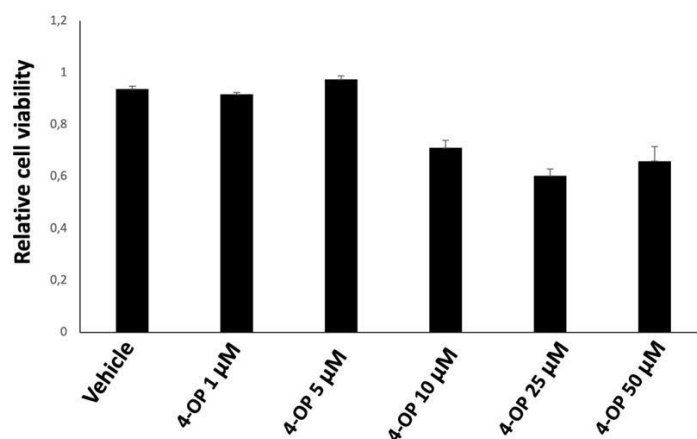
Figure 24. Effect of the linear form of 4-OP on HepG2 cell viability. MTT assay on HepG2 cells treated with different concentrations of 4-OP for 24 h. Values were expressed as means ± SE of three independent experiments.

Therefore, we subsequently decided to use the branched form that is 4-tOP with specific certification for purity (TraceCERT®). Along the thesis, it will be called 4-OP for simplicity of exposition and all the experiments that will be discussed have been performed with this form of 4-OP.

We performed MTT assay on HepG2 and on Caco-2 in the presence of different concentrations of 4-OP for 24 h. We observed that this substance significantly reduced the viability of HepG2 as early as

the concentration of 25 μM, having more evident effect at 75 and 100 μM (Figure 25 A). On Caco-2 the reduction in viability was recorded as soon as at OP 12.5 μM. Thus, at low doses 4-OP had a more pronounced effect on Caco-2 (Figure 25 B), however, HepG2 were more sensitive to the cytotoxic action of the compound at higher doses. By comparing the results, we could assert that 4-OP after 24 h of treatments exerted a dose-dependent cytotoxic action on both cell lines with a trend that is cell type specific (Figures 25 A and B)

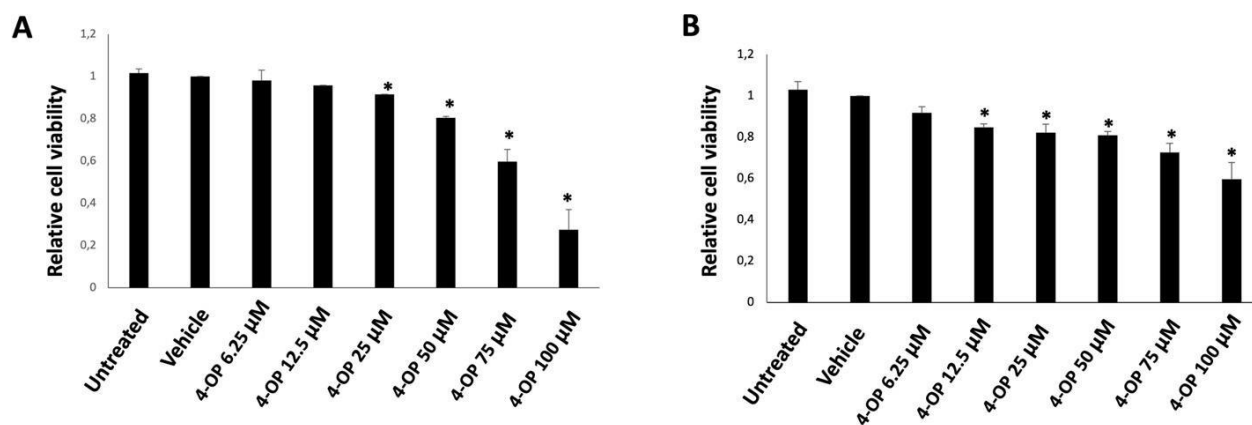**Figure 25.** 4-OP reduces cell viability in HepG2 and Caco-2 cells. (A) MTT assay on HepG2 cells treated with increasing concentrations of 4-OP for 24 h. (B) MTT assay on Caco-2 cells treated with increasing concentrations of 4-OP for 24 h. All results were expressed as means ± SE of three independent experiments performed in triplicate. Statistical analysis was performed using Student's t-test. * $p < 0.05$ vs. cells treated with the vehicle (DMSO).

Next, we compared the effect of 4-OP and 4-NP in each cell line and also focused on the cytotoxic effect of their combination. MTT assays showed that 4-NP and 4-OP had similar effects with no significant differences between them on HepG2 treated for 24 h. Moreover, the combination of the two APs produced only additive but not synergic effects (Figure 26 A). Calculated IC_{50} confirmed this observation, in fact, its values for HepG2 were very similar to each other (Figure 26 C). On Caco-2 cells, 4-NP and 4-OP exerted similar effects without significant differences between them. Only at the concentration of 100 μM, we observed a slight difference in effect on cell viability, being 4-NP more toxic (Figure 26 B). In line with this observation, calculated IC_{50} highlighted that Caco-2 cells were more sensitive to 4-NP compared to 4-OP (Figure 26 C). Interestingly, by combining the pollutants at 25 and 50 μM, we observed significant synergic effects compared with the individual treatments in Caco-2 cells. However, the combination at 100 μM produced no other significant reduction in viability (Figure 26 B). IC_{50} confirmed this synergic effect of combined compounds, as value of the mixture was lower than the value of the single treatments (Figure 26 C).
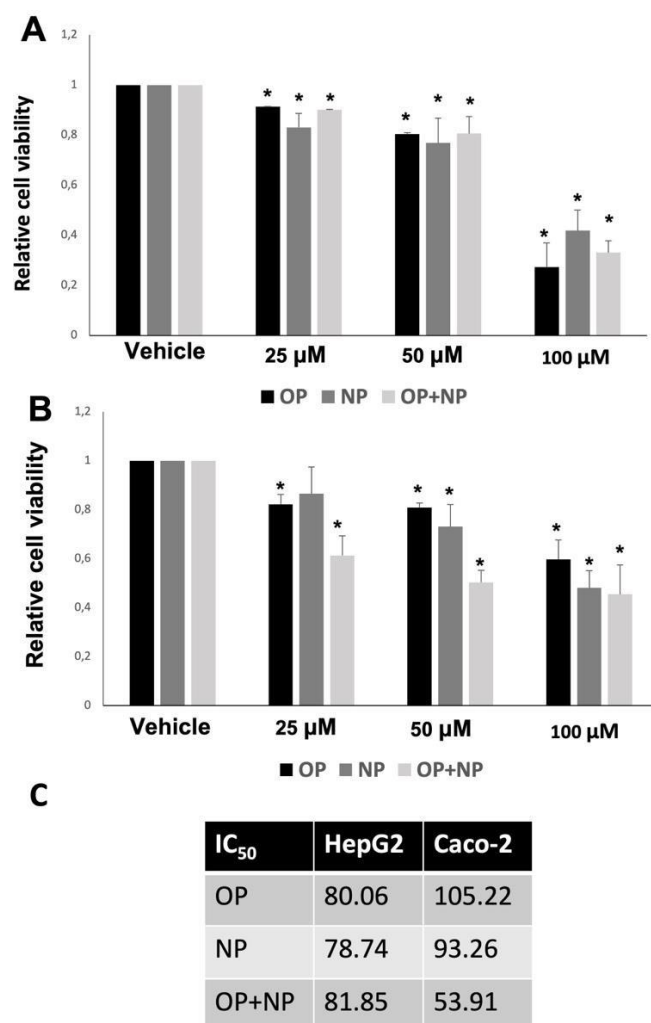
Figure 26. Comparison of cytotoxic effects of 4-OP and 4-NP in single and combined treatments. (A) MTT assay performed on HepG2 cells in the presence of 4-OP and 4-NP and their combination for 24 h. (B) MTT assay performed on Caco-2 cells in the presence of 4-OP and 4-NP and their combination for 24 h. All results were expressed as means ± SE of three independent experiments performed three times. Statistical analysis was performed using Student's t-test. * $p < 0.05$ vs. cells treated with the vehicle (DMSO). (C) Values of IC_{50} (μM) for HepG2 and Caco-2 with 4-NP and 4-OP and their combination (OP+NP) for 24 h; values were expressed as means of three independent experiments each in triplicate; for each value, SE is less than 8 μM.

We also evaluated the cytotoxicity of 4-OP and 4-NP and of their combination on HepG2 and Caco-2 cells after 48 h of treatment. We found that single compounds had greater effects than those obtained with 24 h of treatment, both for HepG2 and Caco-2 cells (Figure 27 A and B). The combination of compounds gave similar results in HepG2, but we observed a strange increase of viability in the combined treatment with the respect to single ones. In Caco-2, the synergic effect of 4-NP and 4-OP we observed at 24 h, still persisted but appeared less evident at 48 h of treatment (Figure 27 B)
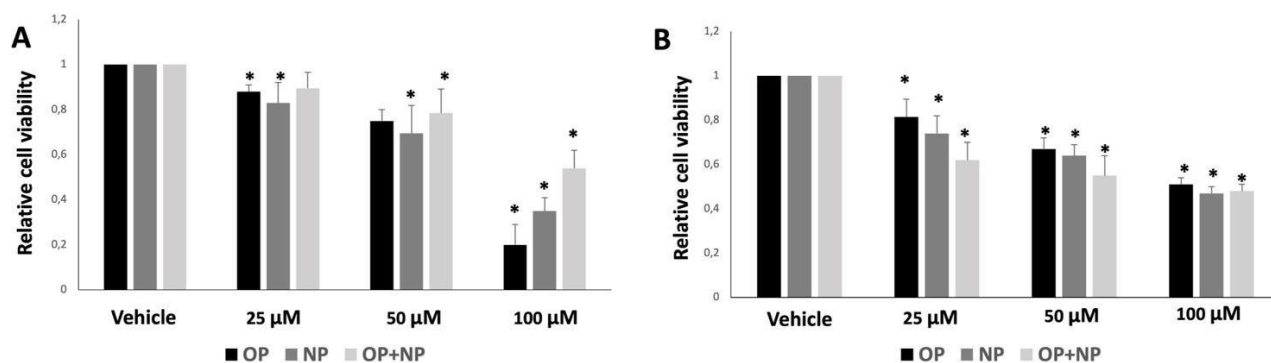
51

Figure 27. Comparison of cytotoxic effects of 4-OP and 4-NP in single and combined treatments for 48 h. MTT assay performed on HepG2 cells in the presence of 4-OP and 4-NP and their combination for 48 h. (B) MTT assay performed on Caco-2 cells in the presence of 4-OP and 4-NP and their combination for 48 h. All results were expressed as means ± SE of three independent experiments performed three times. Statistical analysis was performed using Student's t-test * $p < 0.05$ vs. cells treated with the vehicle (DMSO).

We next investigated cytotoxic effects of both APs on a cell line of lung origin, being lung one possible target of pollutants occurring in the air. To this aim, we employed the MRC5 cell line, an immortalized line of lung fibroblasts. We recorded, by the MTT assay, a reduction in viability at 12.5 μM of 4-OP and 4-NP; the effects became very pronounced with treatments at concentrations of 75 and 100 μM. On the whole, 4-OP and 4-NP similarly reduced the viability of MRC5 with no significant differences (Figures 28 A and B). On MRC5 we also tested the combination of APs for 24 h. We found that the combination treatment significantly reduced cell viability at only the concentration of 25 μM compared to the single treatments; this slight synergic effect was not yet evident with combination at 50 and 100 μM (Figure 28 C). Calculation of IC_{50} confirmed that 4-OP and 4-NP exhibited similar cytotoxicity on MRC5 and that these immortalized non-cancer cells were particularly sensitive to the combination of the two pollutants (Figure 28 D)
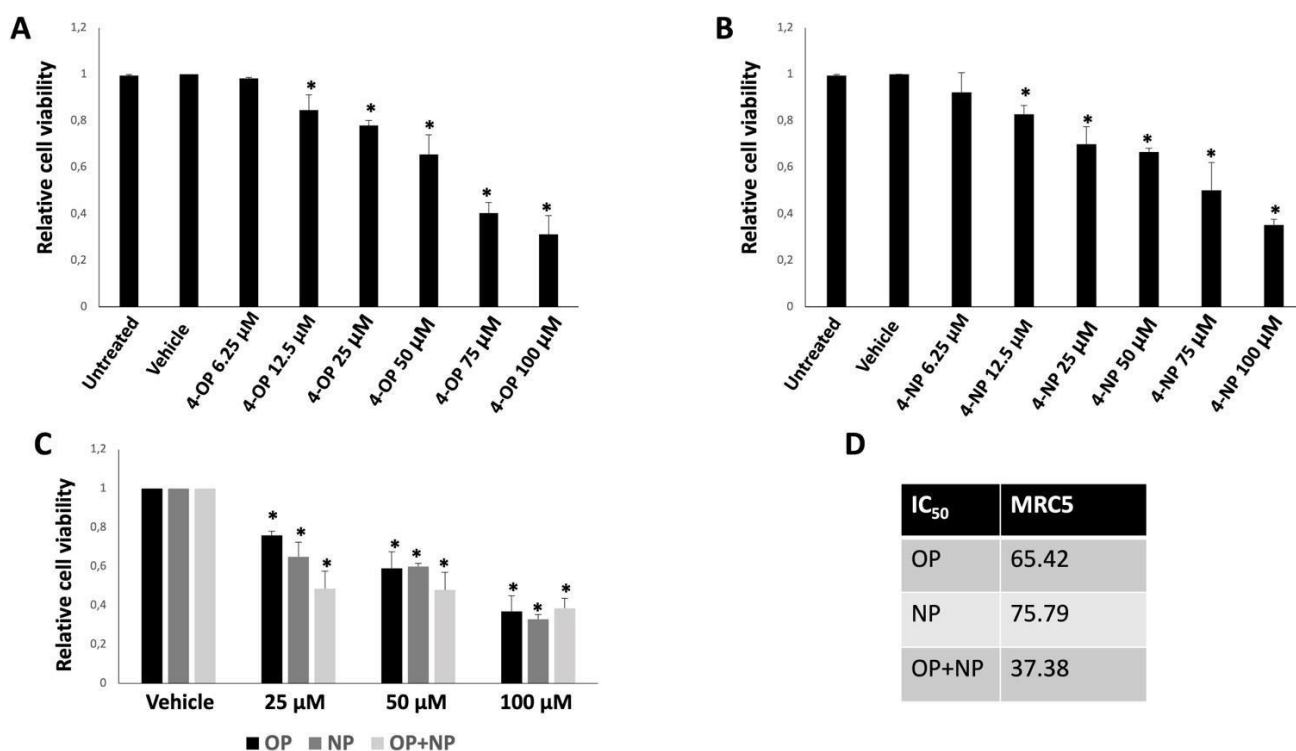
Figure 28. 4-OP and 4-NP reduces cell viability on MRC5. (A) MTT assay performed on MRC5 cells treated with increasing concentrations of 4-OP for 24 h. (B) MTT assay performed on MRC5 cells treated with increasing concentrations of 4-NP for 24 h. (C) Comparison of cytotoxic effects of 4-OP and 4-NP in single and combined treatments for 24 h. All results were expressed as means ± SE of three independent experiments performed three times. Statistical analysis was performed using Student's t-test. * $p < 0.05$ vs. cells treated with the vehicle (DMSO). (D) Values of IC_{50} (μM) for MRC5 cells in the presence of 4-NP and 4-OP, and their combination for 24 h. Values were expressed as means of three independent experiments each in triplicate; for each value, SE is less than 8 μM.

Finally, we investigated the cytotoxicity of both APs on a kidney cell line representing another potential target organ, i.e. HEK293 cells (human embryonic kidney). By the MTT assay, we observed that 4-NP and 4-OP exhibited similar cytotoxicity on this cell line. Precisely, APs significantly reduced cell viability as early as 25 μM concentration; the effect became very pronounced at 75 and 100 μM (Figure 29 A and B). Very similar calculated IC_{50} for 4-NP and 4-OP confirmed this observation (Figure 29 D). The combination of APs produced a slight synergic effect at 25 and 50 μM, but not at 100 μM (Figure 29 C); as a consequence, calculated IC_{50} were all very similar (Figure 29 D).
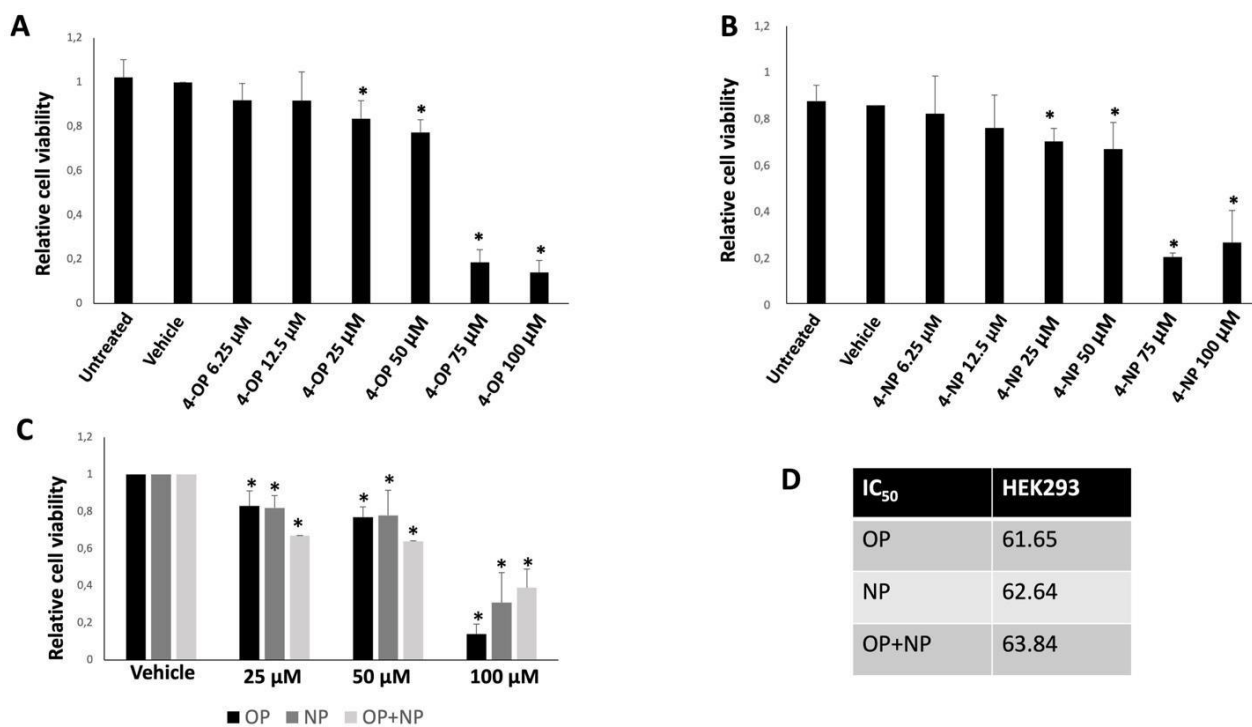
Figure 29. 4-OP and 4-NP reduces cell viability on HEK293. (A) MTT assay performed on HEK293 cells treated with increasing concentrations of 4-OP for 24 h. (B) MTT assay performed on HEK293 cells treated with increasing concentrations of 4-NP for 24 h. (C) Comparison of cytotoxic effects of 4-OP and 4-NP in single and combined treatments for 24 h. All results were expressed as means ± SE of three independent experiments performed three times. Statistical analysis was performed using Student's t-test. * $p < 0.05$ vs. cells treated with the vehicle (DMSO). (D) Values of IC_{50} (μM) for HEK293 in the presence of 4-NP, 4-OP and their combination for 24 h. Values were expressed as means of three independent experiments each in triplicate; for each value, SE is less than 8 μM.

Ultimately, the summary table of calculated IC_{50} (Table 2) highlighted that APs exhibited cytotoxicity differently according to cell type and that the combination of them did not always have synergic effects. So, we can conclude that cells of different origin showed different sensitivity to these environmental pollutants.

Table 2. Comparison between values of IC$_{50}$ (µM) for HepG2, Caco-2, MRC5 and HEK293 in the presence of 4-NP, 4-OP and their combination (OP+NP) for 24 h. Values were expressed as means of three independent experiments each in triplicate; for each value, SE is less than 8 µM.

IC$_{50}$	HepG2	Caco-2	MRC5	HEK293
OP	80.07	105.22	65.42	61.65
NP	78.84	93.26	75.79	62.64
OP+NP	81.85	53.91	37.38	63.8

5.2.2 4-OP reduces HepG2 cell proliferation

As in the case of 4-NP, given the cytotoxicity observed in MTT assays, we wondered whether 4-OP could affect cell cycle progression. Therefore, we performed a BrdU incorporation assay in HepG2 cells treated with 4-OP. We observed that 4-OP, already at a concentration of 25 µM, reduced the S-phase entry of cells and that at 50 µM there was a similar effect (Figure 30 A). Comparing the effect of 4-OP with 4-NP on the cell cycle progression of HepG2 we noted that 50 µM OP reduces cell cycle progression similarly to 4-NP at the concentration of 100 µM (Figure 11 A). Given the importance of p53 protein in controlling cell proliferation we evaluated its expression in the presence of 4-OP. Western blot analysis highlighted that p53 expression increased after treatments with 4-OP 25 µM and decreased with 4-OP 50 and 100 µM (Figure 30 B). This result agreed with the BrdU incorporation experiment where, with 4-OP 25 µM, there was a plateau of proliferation reduction. The result was also in line with what we observed with 4-NP (Figure 15).
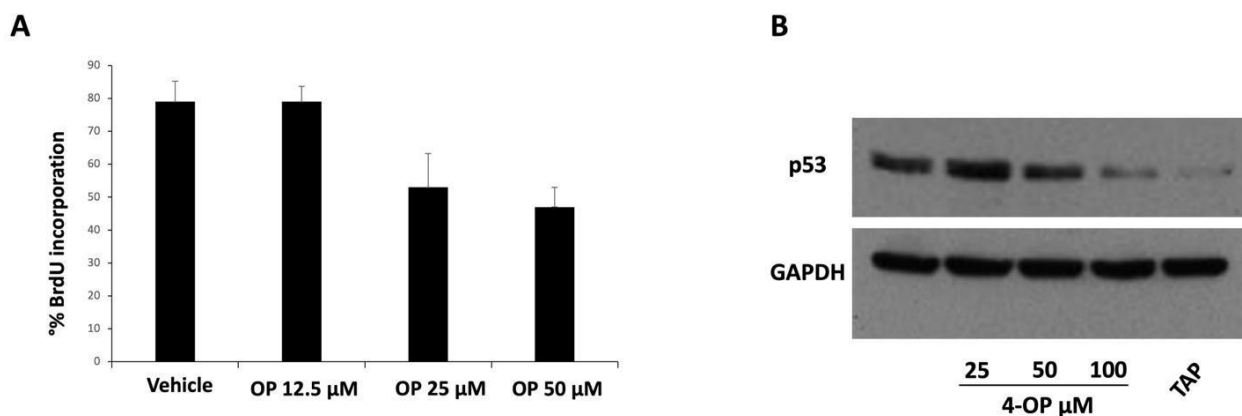
Figure 30. 4-OP affects cell cycle progression. (A) BrdU incorporation assay in HepG2 cells after 24 h of treatment with increasing concentrations of 4-OP. Results are expressed as means ± SE of counts obtained from several fields in the same coverslip. (B) Western blot of p53 in HepG2 cells in the presence of 4-OP. TAP was used as a positive control.

5.2.3 4-OP induces apoptosis in HepG2 cells

We hypothesized that cytotoxicity due to 4-OP could be also related to an increased apoptosis. Thus, we investigated whether 4-OP could trigger programmed cell death. By a TUNEL assay, we labelled apoptotic cells in green and total cells in blue (Hoechst staining). After 24 h of treatment we observed that already at the concentration of 12.5 μM and 25 μM, 4-OP caused the appearance of apoptotic cells (Figure 31).
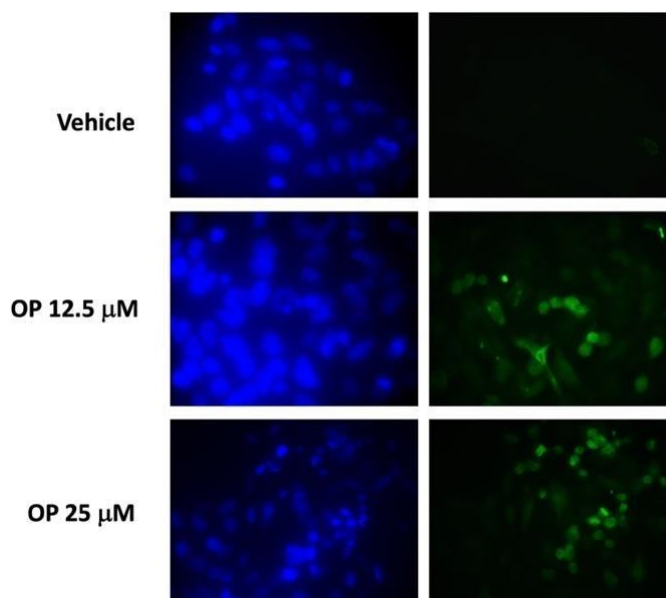
Figure 31. TUNEL assay. Microscopic visualization of apoptotic nuclei (green) and total nuclei (Hoechst staining) in HepG2 cells treated with different concentration of 4-OP for 24 h. (Magnification 40x, with oil).

We confirmed the occurrence of apoptosis by western blot analyses, evaluating the level of cleaved caspase 3 in the presence of increasing concentrations of 4-OP in HepG2 cells. We observed that there was an increase in active caspase 3 in cells treated with 4-OP 25, 50 and 75 μM for 7 h (Figure 32).
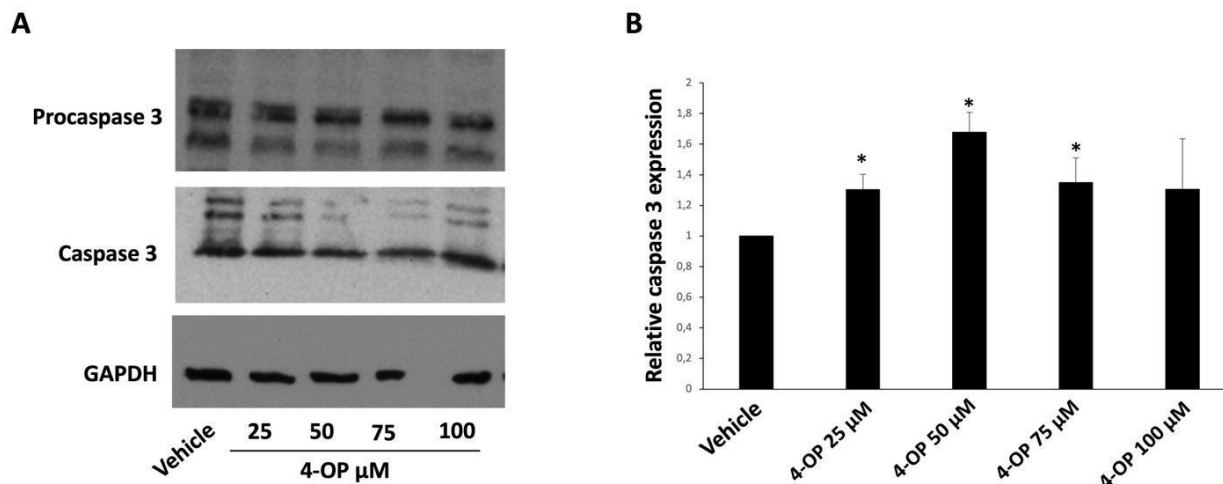
Figure 32. 4-OP induces apoptosis. (A) Representative western blot of caspase 3 in HepG2 cells treated with different concentration of 4-OP for 7 h. DMSO is vehicle. (B) Densitometric analysis of caspase 3 of three independent experiments. Protein levels are normalized with respect to GAPDH expression. Data are expressed as means ± SE of three experiment. Statistical analysis was performed using Student's t-test. * $p < 0.05$ vs. vehicle treated-cells.

In addition, we also investigated the effect of 4-OP on apoptosis in intestinal Caco-2 cell line. So far, we have only one experiment that highlighted that 4-OP at the concentration of 50 and 100 μM induced after 24 h a slight reduction in procaspase 3 (inactive form) and a slight increase in active caspase 3 (Figure 33). However, compared with HepG2, the increase in caspase 3 was less pronounced. This behaviour suggests again that the two cell lines exhibit different sensitivity to the pollutant.
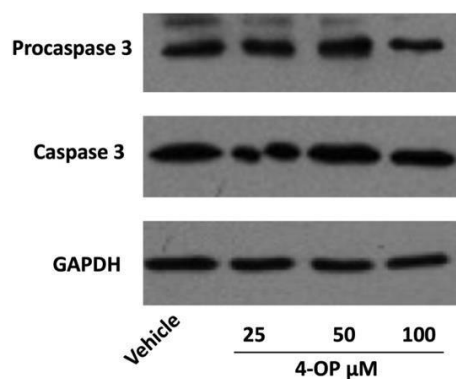
Figure 33. 4-OP triggers apoptosis in Caco-2 cells. Representative western blot of caspase-3 in Caco-2 cells in the presence of different concentrations of 4-OP.

5.2.4 4-OP triggers ER-stress in HepG2 cells

As mentioned earlier, apoptosis can be induced by a persistent ER stress condition. Therefore, we evaluated how 4-OP affected the expression of stress markers such as GRP78 and XBP1. First, we investigated by western blot the expression of the chaperone GRP78 in HepG2 cells treated with different concentrations of 4-OP for 24 h. As shown in figure 34, 4-OP at concentrations of 50, 75 and 100 μM caused an increased expression of GRP78 (Figure 34 A and B). By conventional PCR, then, we found that 4-OP, at a concentration of 100 μM, clearly induced the splicing of XBP1, an early marker of ER-stress (Figure 34 C). On the whole, these data confirmed the presence of an UPR typical of the ER-stress.
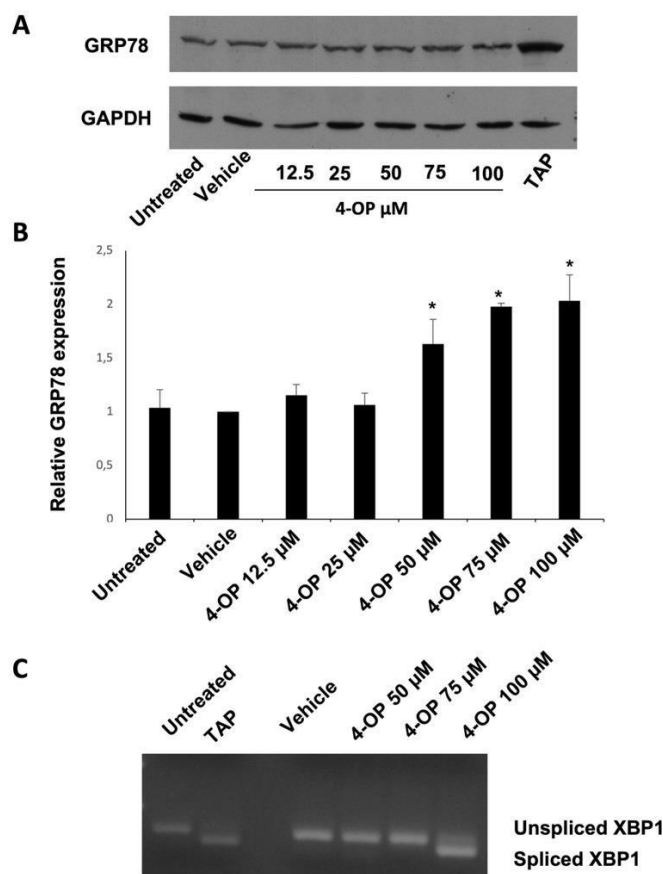
Figure 34. 4-OP triggers ER-stress in HepG2 cells. (A) Representative western blot of GRP78 in HepG2 cells treated with increasing concentrations of 4-OP for 24 h. (B) Densitometric analysis relative to three independent experiments. Protein levels are normalized with respect to GAPDH expression. Data are expressed as means ± SE of three experiment. Statistical analysis was performed using Student's t-test. * $p < 0.05$ vs. vehicle treated-cells. (C) Splicing of XBP1 analyzed by PCR in HepG2 cells in the presence of 4-OP for 4 h. In all experiments, TAP was used as a positive control.

With studies still ongoing, we are also investigating the effect of this environmental pollutant on ER-stress in other cell lines such as Caco-2 and MRC5. Precisely by western blot analysis we found a slight increase in the chaperone GRP78 in Caco-2 cells treated with 50 and 75 μM of 4-OP; with 4-OP 100 μM, however, there was a reduction in GRP78 expression (Figure 35 A and B).

In MRC5 cells, we observed that 4-OP induced a marked increase in GRP78 as early as concentrations of 25 and 50 μM (Figure 35 C).

In summary, we can conclude that 4-OP was able to induce ER-stress in different cell lines. However, these studies need to be confirmed and expanded with further experiments.
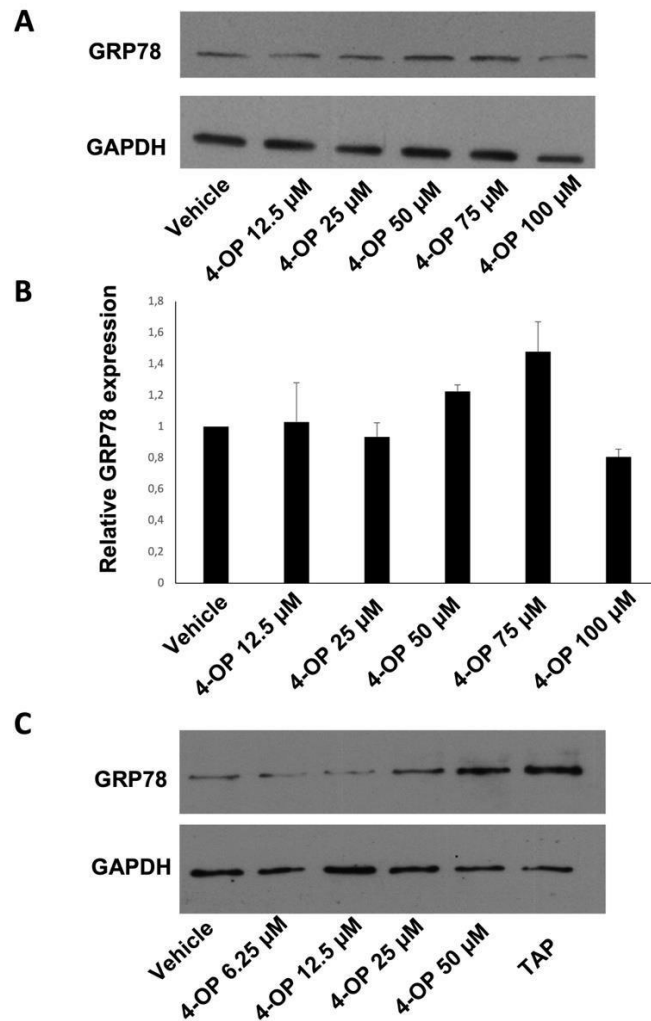
Figure 35. 4-OP affects ER-stress in other cell lines. (A) Representative western blot of GRP78 in Caco-2 cells treated with different concentration of 4-OP. (B) Densitometric analysis of GRP78 in Caco-2 cells. Protein levels are normalized with respect to GAPDH expression. Data are expressed as means ± SE. (C) Western blot of GRP78 in MRC5 cell line in the presence of 4-OP, vehicle (DMSO) and TAP used as control.

5.2.5 4-OP affects autophagic flux in HepG2 cells

We are also conducting studies on how APs may affect the autophagic process. During autophagy flux, the ribosome-free membrane of the ER detaches and elongates to form autophagosomes containing the organelles and substances to be degraded. Autophagosomes, then, fuse with lysosomes that provide hydrolases important for degradative processes, thus forming autophagolysosomes. In this stage of maturation, an important role is played by the LC3 protein, which binds to the polar head of phosphatidylethanolamine (PE) converting from LC3-I to LC3-II form. The ratio of LC3-II to LC3-I isoform is a gold standard marker of autophagy (Xi et al, 2022).

During the process of fusion with the lysosome, LC3-II-binding protein P62 is degraded; in fact, P62 is considered a negative marker of autophagy, since its level of expression is high when autophagy is inhibited. (Xi et al, 2022).

In the light of this scientific literature, we evaluated by western blot the expression of LC3-I, LC3-II and P62 in HepG2 cells in the presence of different concentrations of 4-OP. Specifically, for LC3, we performed treatments on HepG2 cells with lower concentrations of 4-OP for 24 h, whereas, for P62, treatments with higher concentrations of 4-OP for 4 h. We observed a decrease of LC3 with treatments of 4-OP at the concentrations of 25 and 50 μM, instead, there was an accumulation of LC3-I with lower doses of 4-OP (Figure 36 A). Both phenomenona were in line with an increased autophagy: first, an accumulation of LC3 and then, at higher doses of 4-OP, its degradation. In the case of P62, we found a progressive reduction of the protein at increasing concentrations of 4-OP, diagnostic of induction of the autophagic flux (Figure 36 B). TAP and starvation were used as positive controls of autophagic flux induction. So far, we have only one experiment, therefore, these are preliminary data which need to be confirmed. It will be also worthwhile to analyze the expression of LC3 at shorter treatment times to evaluate any further increase of LC3-II isoform which could confirm the early induction of the autophagic process. However, from these preliminary data we could conclude that 4-OP influences autophagic flux.
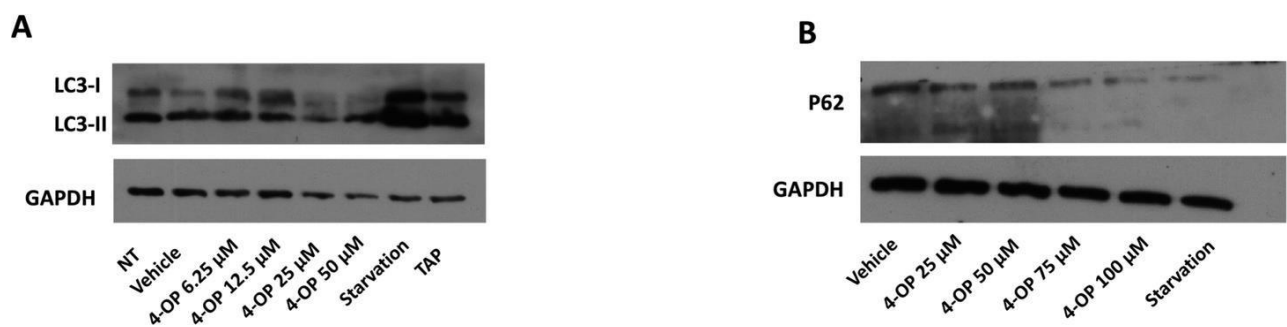
Figure 36. 4-OP affects autophagic flux. (A) Western blot of LC3 in HepG2 cells treated with different concentration of 4-OP for 24 h. (B) Western blot of P62 in HepG2 cells in the presence of increasing concentration of 4-OP for 4 h. Starvation and TAP are used as positive controls.

In addition, to confirm, with a different approach, that 4-OP influenced the formation of autophagosomes, we performed immunofluorescence staining for LC3 in HepG2 cells. In this assay, it is possible to monitor the accumulation or the disappearance of autophagosomes which appear as red perinuclear puncta in the cell. We found that 4-OP already at concentrations of 6.25 μM induced an accumulation of autophagosomes compared with cells treated with vehicle alone (DMSO). Instead, at 25 μM of 4-OP puncta clearly reduced, indicating that LC3 degradation occurred. Immunofluorescence data agreed with western blot results, where at 25 and 50 μM of 4-OP the level of LC3 was reduced (Figure 37).
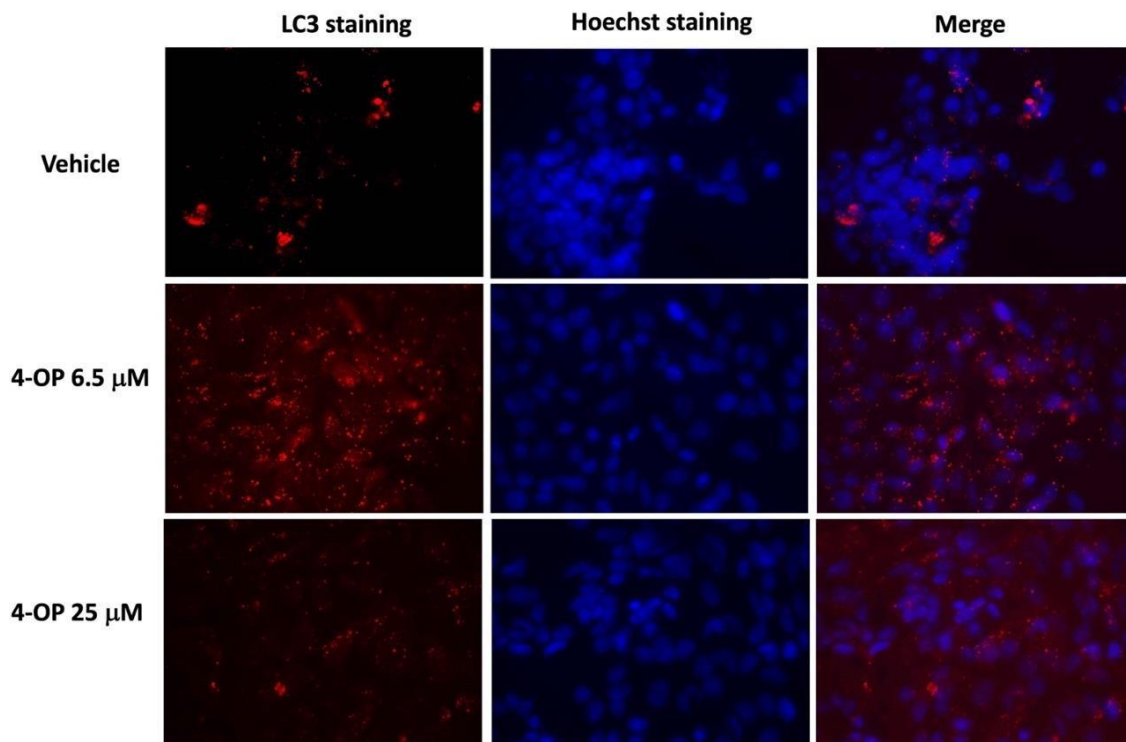
Figure 37. 4-OP influences autophagosomes formation. Immunofluorescence in which LC3-positive structures are marked in red while total nuclei in blue (Hoechst staining). (Magnification 40x, with oil).

5.2.6 4-OP and 4-NP modulate intracellular Ca²⁺ homeostasis

In human cells there is a close cross talk between ER-stress, calcium homeostasis imbalance, mitochondrial dysfunction, and apoptosis activation (Biagioli et al, 2008; Martucciello et al, 2020). Therefore, we investigated whether 4-OP and 4-NP could induce intracellular calcium mobilization by assaying the activity of TG2, a calcium-dependent enzyme expressed in Caco-2 cells. We found that 4-NP, at the concentration of 50 and 100 μM, and 4-OP, at the concentration of 100 μM, induced

a significant increase of TG2 activity. These findings suggested that APs could cause calcium mobilization from some cellular store or more generally that they could affect calcium homeostasis (Figure 38).
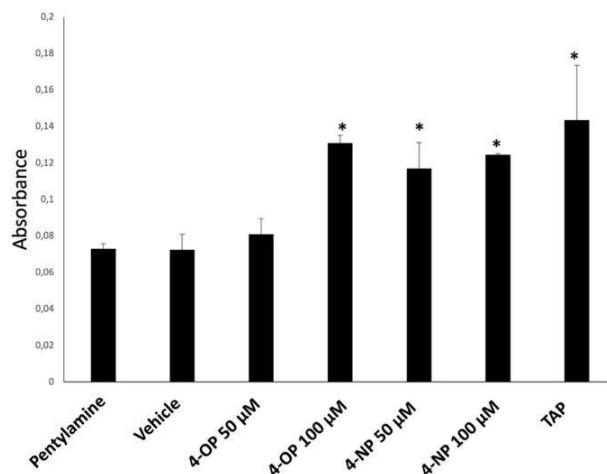
Figure 38. 4-OP and 4-NP affects calcium homeostasis. TG2 activity assay performed on Caco-2 cells treated with different concentrations of 4-NP or 4-OP for 1h. Basal TG2 activity was registered in the presence of pentylamine-biotin alone. TAP was used as a positive control. Data were expressed as means $\pm$ SE of values from three independent experiments. Statistical analysis was performed using Student's t-test. * $p < 0.05$ vs. vehicle treated-cells.

5.2.7 4-OP induces oxidative stress in HepG2 cells

I mentioned in the introduction that APs can induce cytotoxicity and organ and tissue damage by generating a large amount of ROS. SOD and CAT are part of the first line of antioxidant cellular defence. Thus, we investigated whether 4-OP affected the antioxidant system. We evaluated CAT activity in HepG2 cells treated with increasing concentrations of 4-OP. After 24 h of treatments, we observed that CAT activity increases in the presence of 4-OP. The increase was pronounced with 100 μM 4-OP treatments (Figure 39 A). By western blot we, then, evaluated the expression of SOD in HepG2 treated with 4-OP for 24 h. 4-OP 25 μM induced a reduction in SOD expression, whereas at 50 and 100 μM we observed a return to baseline (Figure 39 B and C). I will discuss in detail in the discussion of the possible significance of these changes in the antioxidant system induced by 4-OP.
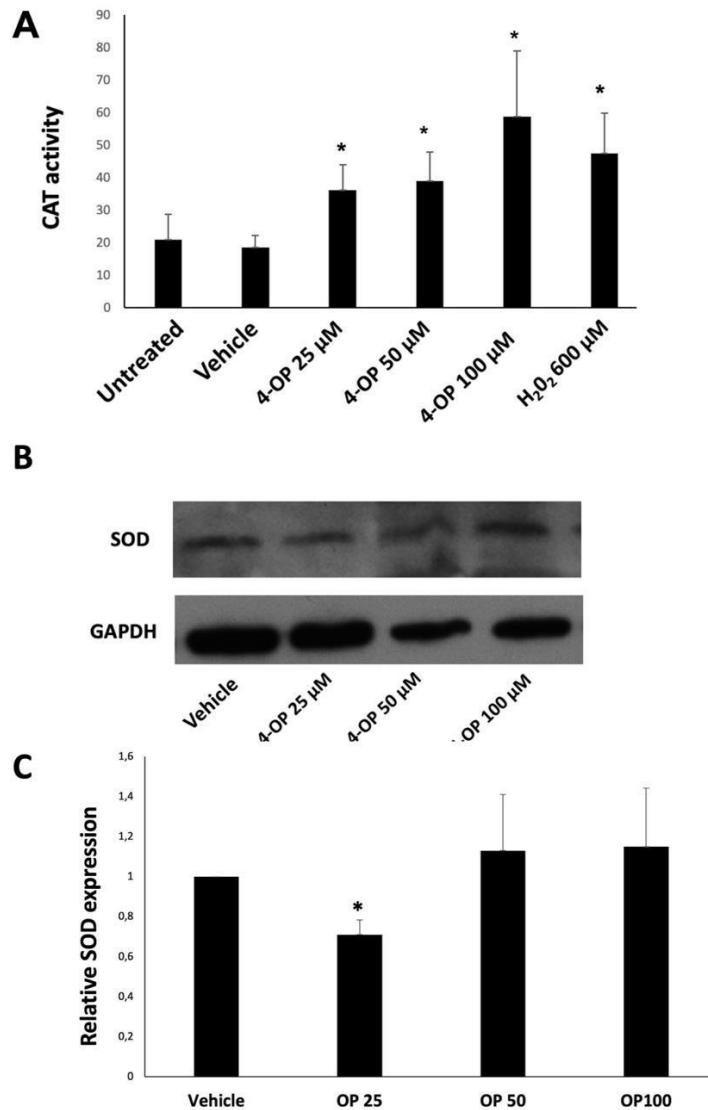
Figure 39. 4-OP affects antioxidant system in HepG2 cells. (A) Catalase activity evaluated in HepG2 cells treated with increasing concentrations of 4-OP for 24 h. H_2O_2 600 μM was used as a positive control. Data are expressed as means ± SE of three experiment. (B) Western blot of SOD in HepG2 cells cultured with different concentration of 4-OP for 24 h. (C) Densitometric analysis of SOD expression normalized respect to GAPDH. Data are expressed as means ± SE of three experiment. Statistical analysis was performed using Student's t-test. *p < 0.05 vs. vehicle treated-cells.

5.2.8 Characterization of HepG2 spheroids

In the attempt to confirm all our findings, previously obtained in 2D models, in a more complex 3D model of study, we first set up a protocol of liquid-overlay to obtain HepG2 spheroids. To asses differentiation of hepatic cells into spheroids, the analysis of the expression of two differentiation markers, albumin and CYP1A2, was done by real time PCR. We found that as early as day 5, the mRNA levels of albumin and CYP1A2 increased compared with cells at time zero. The phenomenon

became more pronounced after 12 days of incubation (Figure 40 A and B). These preliminary data suggested that hepatic differentiation was taking place.
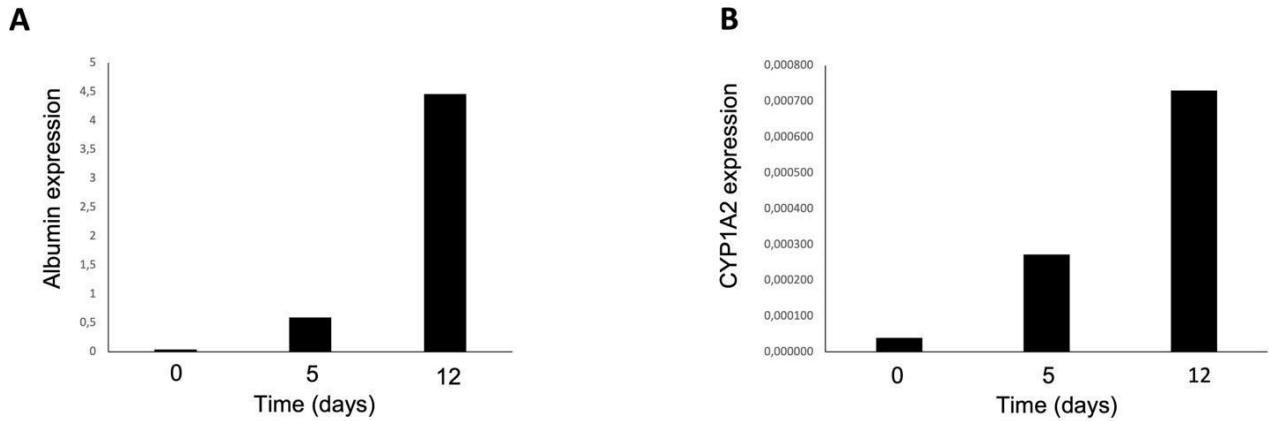
Figure 40. Evaluation of liver differentiation. Measurement of albumin and CYP1A2 expression by Real Time PCR at the beginning of spheroids formation (time zero) and after 5 (A) and 12 (B) days of incubation.

These studies are still in the early stages, but they encourage us to continue with the future prospective to evaluate possible biological effects of APs using an *in vitro* model that is closer to the real structure and function of the human organ.

5.3 Characterization of cardenolides anti-cancer activities

5.3.1 P. tomentosa compounds reduce cell viability in cancer cells

We focused our attention on compounds extracted and characterized for the first time from the aerial parts of *P. tomentosa* in the work of Hosseini et al. (2019). Precisely, these compounds were: 12β,6′-dihydroxycalotropin β ,6 -dihydroxycalotropin (1), 16α-hydroxycalotropin (2), 12 β -hydroxycalactin (3), calotropin (4), and calactin (5) (Figure 41).
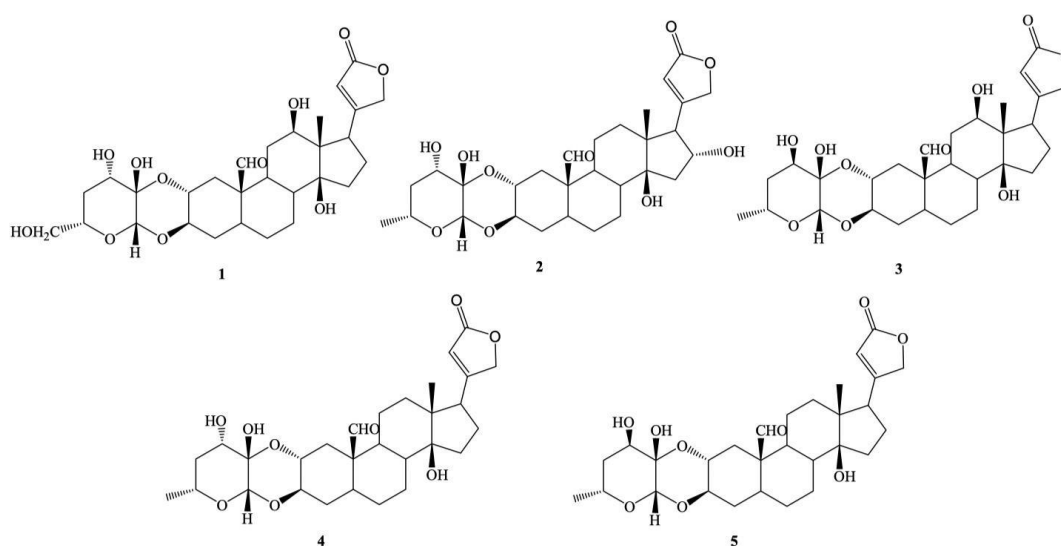
Figure 41. Structures of cardenolides extracted from *P. tomentosa.*

To investigate whether these compounds could exert cytotoxic action, we performed MTT assays on two cancer cell lines (HepG2 and Caco-2), on an immortalized noncancer cell line (MRC5) and on primary cells (HUVECs). After cells were treated with 1 μM of each compound for 24 h we observed that the most cytotoxic were compounds 4 and 5, the least cytotoxic was compound 3, while compound 1 and 2 showed intermediate cytotoxicity (Figure 42).
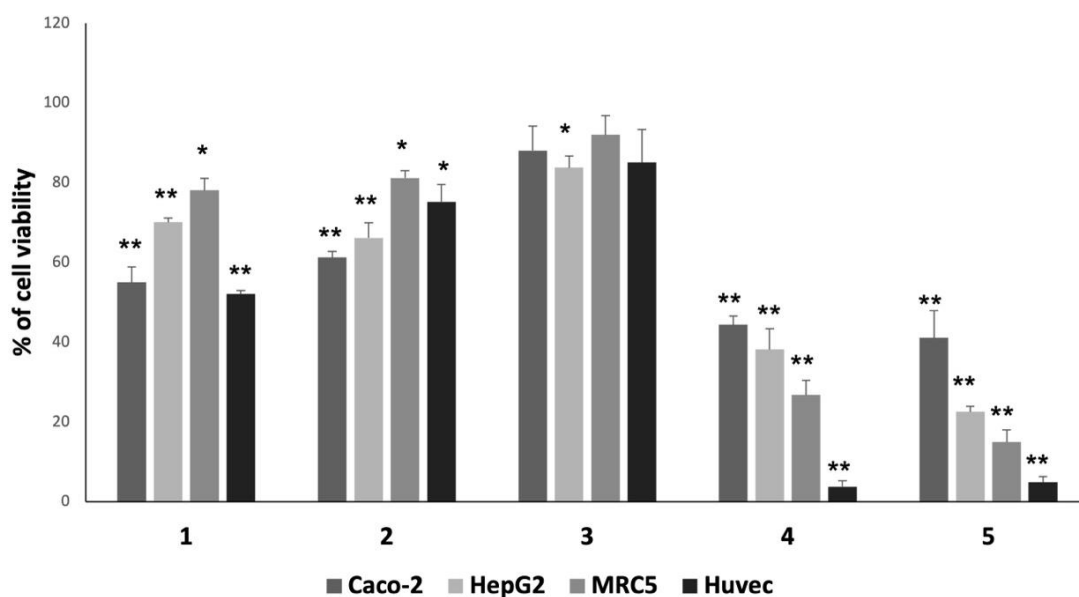
Figure 42. MTT assay on cancer cell line (Caco-2 and HepG2), on an immortalized cell line (MRC5) and normal cells (HUVEC) treated with 1 μM of *P. tomentosa* compounds for 24 h. Results were expressed as means and ± SE of three independent experiments performed three times. Statistical analysis was performed using Student's t-test. * $p < 0.05$ and ** $p < 0.01$ vs. cells treated with the vehicle (DMSO).

To understand whether these compounds differentially affected the viability of cancer and noncancer cells, we also calculated IC_{50} on HepG2, Caco-2 and MRC5 (Table 3). Comparison between HepG2 and Caco-2 showed that HepG2 were more sensitive to the cytotoxic action of compound 5 while they were similarly affected by the other compounds. We also found that noncancer cells were more sensitive to compounds 1 and 2 than cancer cells but equally or less affected by the other compounds.

Table 3. Values of IC_{50} (μM) for HepG2, Caco-2 and HepG2 treated with *P. tomentosa* compounds. Each SE value (not shown) is less than 10% of the calculated IC_{50}.

Compound	Caco-2	HepG2	MRC5
1	1.538	2.610	2.210
2	2.429	2.340	2.315
3	4.507	6.285	5.980
4	0.767	0.830	0.424
5	0.650	0.127	0.990

5.3.2 The cell cycle of HepG2 is affected by compounds of P. tomentosa

Given the very high sensitivity of HepG2 cells to compound 5, we performed next studies on this cell line. Considering the reduction in cell viability, we investigated the effect of *P. tomentosa* compounds on cell cycle progression. After treatments with 1 μM of each compound we evaluated the entry into S-phase by performing a BrdU incorporation assay. In this assay all nuclei are labelled blue (Hoechst staining) while proliferating ones are labelled red (BrdU staining). Compounds 2, 4, and 5 significantly affected cell cycle progression but compounds 1 and 3 slightly and not significantly reduced the BrdU incorporation. The most active was compound 5 (Figure 43).
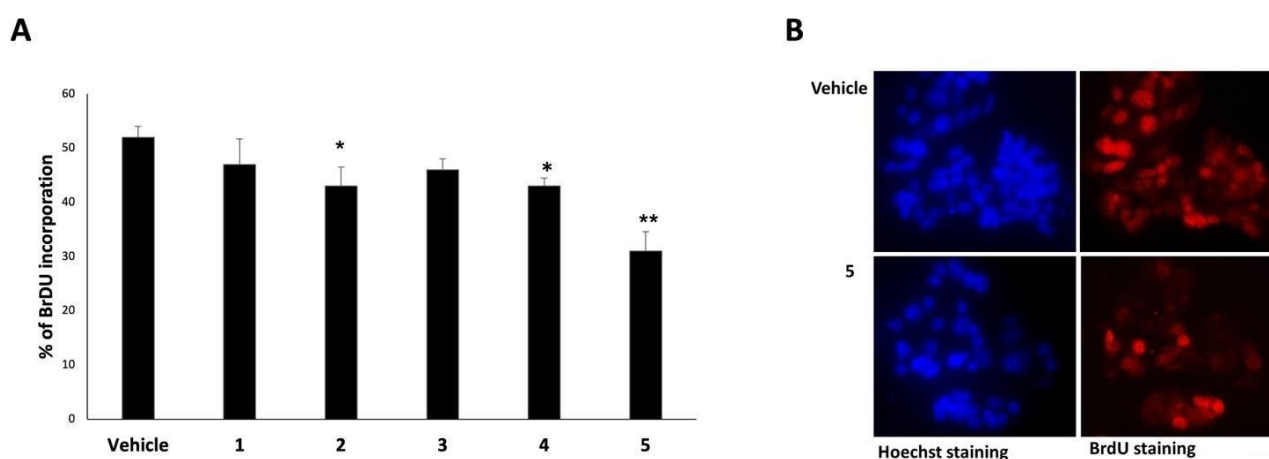
Figure 43. Effects on cell cycle progression in HepG2 cells in the presence of 1 μM of *P. tomentosa* compounds for 24 h. (A) Quantification of BrdU incorporation. Data are expressed as means ± SE of three experiment. Statistical analysis was performed using Student's t-test. * $p < 0.05$ and ** $p < 0.01$ vs. cells treated with the vehicle (DMSO). (B) Representative microscopic visualization of all Hoechst-labelled nuclei (blue) and only proliferating ones incorporating BrdU (red) in cells treated with compound 5 and vehicle (magnification 40x, with oil).

We next examined whether *P. tomentosa* compounds modulated the expression of p53, given the important role that this protein plays in controlling proliferation. HepG2 cells were cultured with 1 μM of *P. tomentosa* compounds for 24 h and we observed, by western blot, an increase of p53 level in all compounds, except compound 5, which decreased p53 amount (Figure 44).
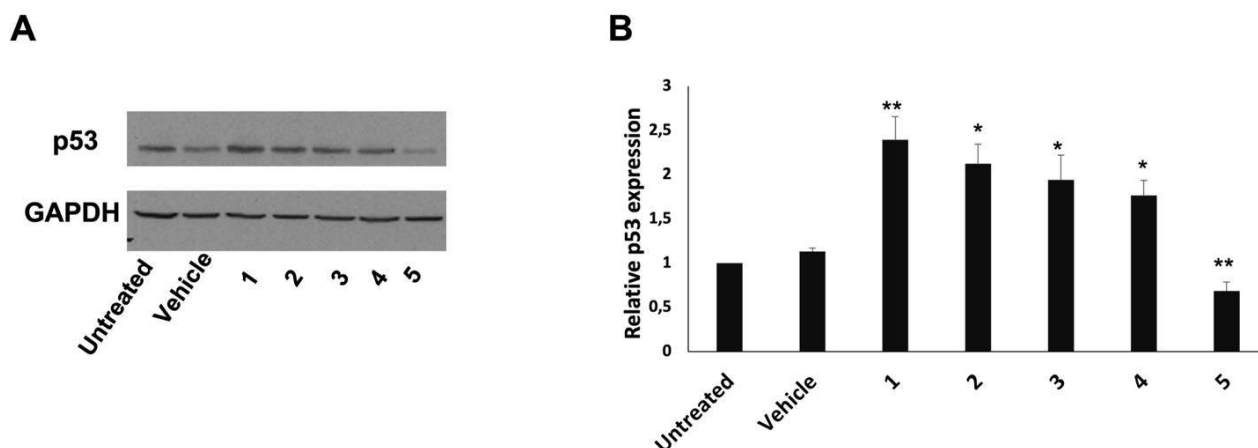
Figure 44. Expression of p53 analysed by western blot. (A) Representative Western blot of p53 level in HepG2 cells treated with 1 μM of *P. tomentosa* compounds for 24 h. (B) Densitometric analysis related to three independent experiments. Protein levels are normalized with respect to GAPDH housekeeping protein expression. Data are expressed as means ± SE of three experiment. Statistical analysis was performed using Student's t-test. * $p < 0.05$ and ** $p < 0.01$ vs. vehicle treated-cells.

We also evaluated p53 expression at 48 h by western blot. Densitometric analysis detected that compound 5 reduced p53 expression after 48 h of stimulation. The other treatments had no significant effect on p53 expression (Figure 45).
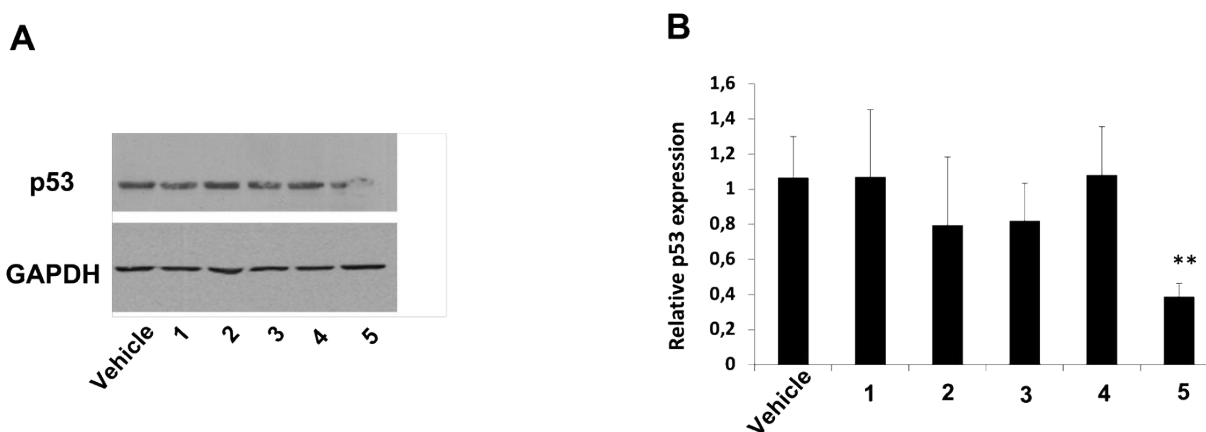
Figure 45. Expression of p53 in HepG2 cells treated with 1 μM of *P. tomentosa* compounds for 48 h. (A) Representative western blot. (B) Densitometric analysis related to three independent experiments. Protein levels are normalized with respect to GAPDH housekeeping protein expression. Data are expressed as means ± SE of three experiment. Statistical analysis was performed using Student's t-test. ** $p < 0.01$ vs. vehicle treated-cells.

Also, we assessed cytosol-nucleus translocation of p53 by effecting stimuli of shorter duration (4h) but higher concentration (5 μM). As we observed from the western blot, nuclear p53 levels were

higher than cytosolic p53 levels in the treated cells except for compound 5, which induces a reduction in nuclear p53 relative to vehicle (Figure 46). Nuclear p53 levels was normalized with respect to Lamin B protein, a protein constitutively expressed in the cell nucleus while cytosolic levels with respect to GAPDH. STS was used as a positive control.

Figure 46. Western blot of cytosolic and nuclear p53 in HepG2 cell treated with 5 μM di *P. tomentosa* compounds for 4 h.

5.3.3 Influence of P. tomentosa compounds on cell migration of HepG2 cells

One of the characteristics of cancer cells is migration, a phenomenon underlying secondary tumour implants and metastasis. With a view to studying anti-tumour effects of CGs, we evaluated whether cardenolides extracted from *P. tomentosa* influenced migration of HepG2 tumour cell line. First, we realized a scratch-wound-healing-assay on confluent cells and followed wound closure after 24, 48 and 72 h of treatments with 1 μM of each compound.

As seen in Figure 47, compounds 1 and 5 interfered with wound closure after 48 and 72 h, compound 3 had effect only at 48 h, compound 2 at 72 h while compound 4 had no effect at any time (Figure 47)
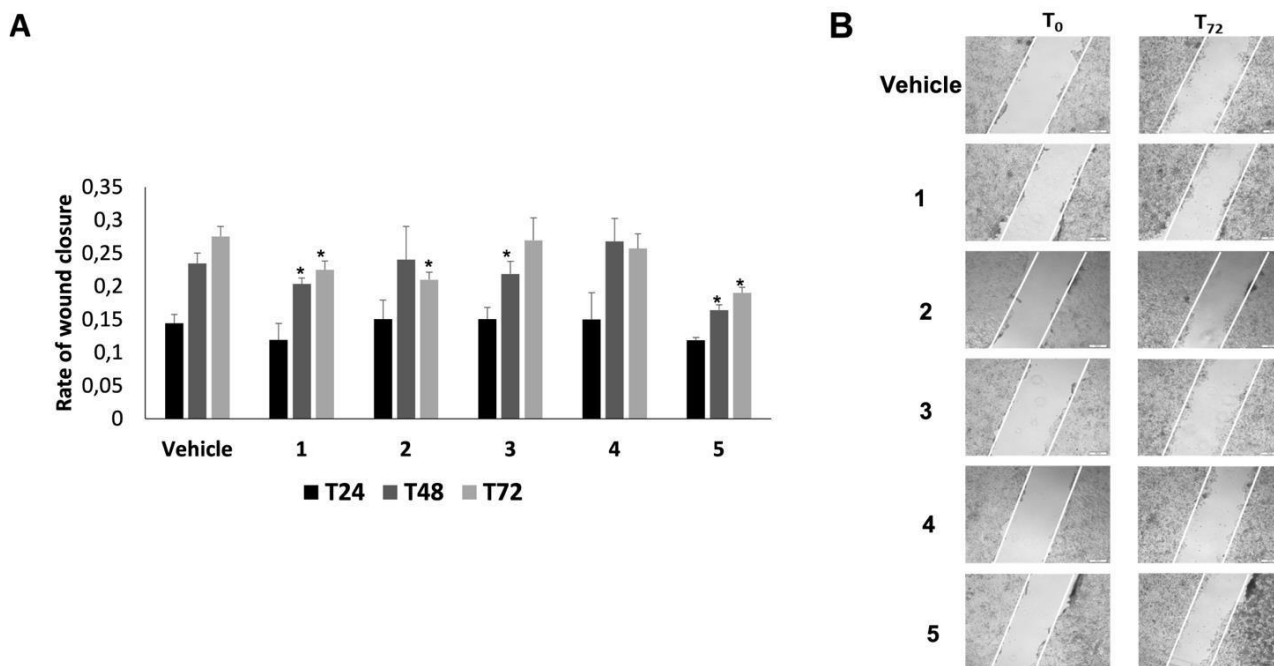
Figure 47. Scratch-wound-healing-assay. (A) Analysis of wound closure in the presence of 1 μM of *P. tomentosa* compounds for 24, 48 and 72 h. Data are reported as means ± SE of three experiment, each in duplicate. Statistical analysis was performed using Student's t-test. * $p < 0.05$ vs. vehicle treated-cells. (B) Microscopic visualization of representative areas of wound closure at the beginning of treatments (T_0) and after 72 h of treatments (T_{72}).

Since the effect of these compounds on cell migration was not very pronounced, we also performed a transwell migration assay, a more complex model very useful to assess the ability of cells to move across a permeable barrier. We treated HepG2 cells with compounds that had the greatest effect in counteracting wound closure (compounds 1,3,5) at a concentration of 1 μM for 18 h. As shown in Figure 48, all three compounds were able to reduce the migration of cells compared with those treated only with vehicle (DMSO). In particular, compound 5 was the most potent. Data from transwell migration assay agreed with those from scratch-wound-healing-assay.
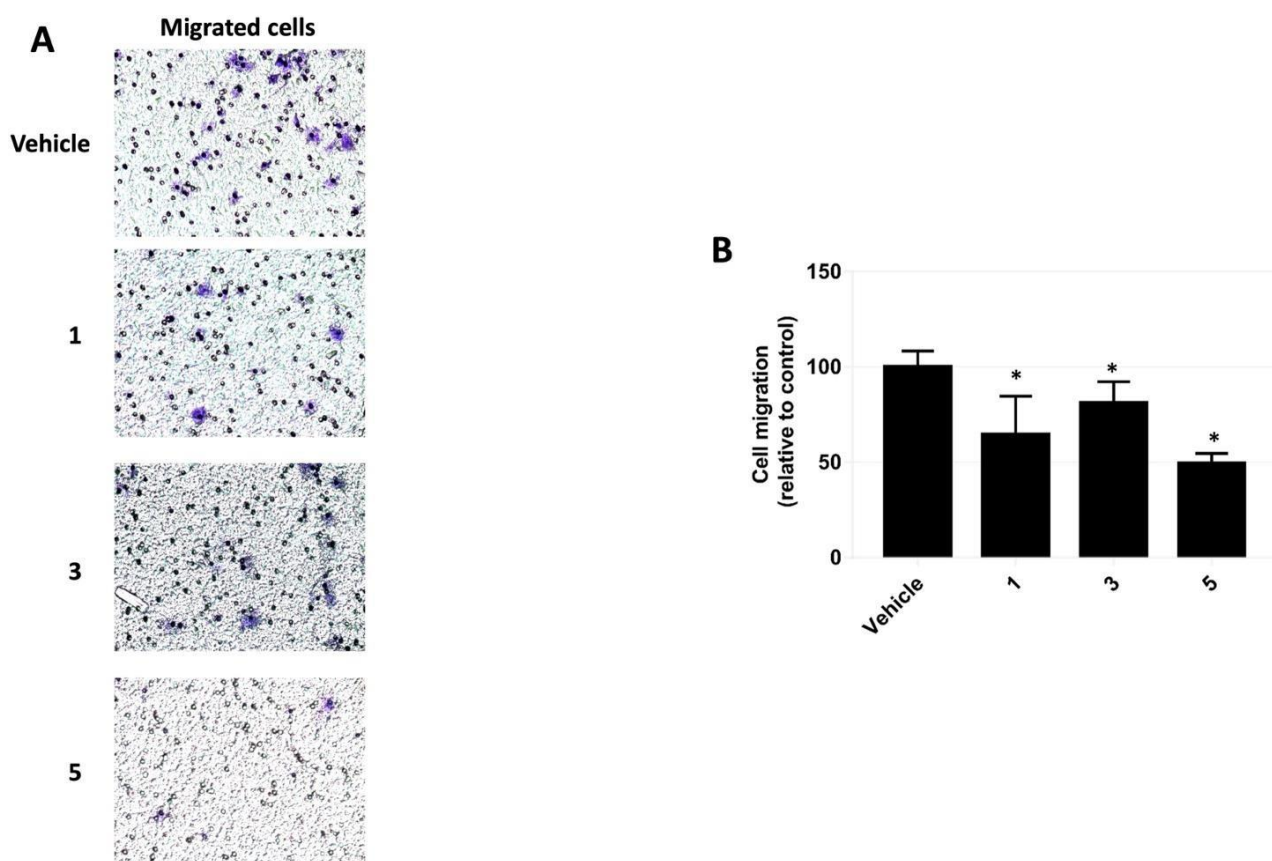
Figure 48. Transwell migration assay in HepG2 cells cultured with 1 μM of *P. tomentosa* compounds for 18 h. (A) Microscopic visualization of representative areas of migrated cells labelled with crystal violet. (B) Analysis of cell migration. Migration was estimated with respect to vehicle-treated cells. Data are reported as means and ± SE of three independent experiments, each in duplicate. Statistical analysis was performed using Student's t-test. * $p < 0.05$ vs. vehicle treated-cells.

5.3.4 Activation of apoptosis by P. tomentosa compounds

Then we investigated whether the cytotoxicity recorded in the MTT assay was also related to the activation of apoptosis. Therefore, by western blot, we evaluated the expression of caspase 3 after treating HepG2 cells with 2 μM of compounds for 7 h (Figure 49 A and B). As we noted from densitometric analysis, all compounds were able to activate caspase 3 and the most active were compounds 4 and 5. Next, we also evaluated the activity of caspase 3 enzyme by an ad hoc assay in HepG2 cells cultured for 24 h with 1 μM of compounds. Data analysis showed that all compounds caused caspase 3 activity increase except compound 3 (Figure 49 C). In all experiments STS, an inducer of apoptosis, was used as a positive control.
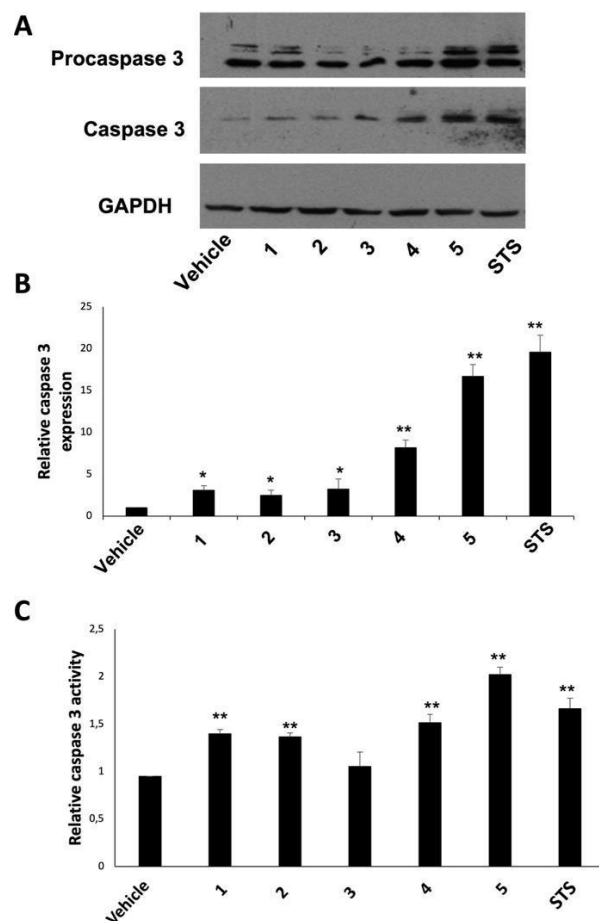
Figure 49. Activation of caspase 3 in HepG2 cells. (A) Representative western blot of caspase 3 in HepG2 treated for 7 h with 2 µM *of P. tomentosa* compounds, vehicle or STS. (B) Densitometric analysis of cleaved caspase 3 related to three independent experiments. Protein levels are normalized with respect to GAPDH housekeeping protein expression. Data are expressed as means ± SE of three experiment. Statistical analysis was performed using Student's t-test. $* p < 0.05$ and $** p < 0.01$ vs. vehicle treated-cells. (C) Relative caspase 3 activity normalized to the activity recorded in untreated cells. Data are expressed as means ± SE of three experiment. Statistical analysis was performed using Student's t-test. $** p < 0.01$ vs. vehicle treated-cells.

We also evaluated caspase activation in a nontumour MRC5 cell line in the presence of 4-OP. Western blot revealed that the compounds active on noncancer cells were different from those active on cancer cells. Specifically, on MRC5 cells, compounds 1, 2 and 3 were more active than compounds 4 and 5 in inducing caspase 3 activation. So, the activity of these compounds is strictly dependent on cell type (Figure 50).
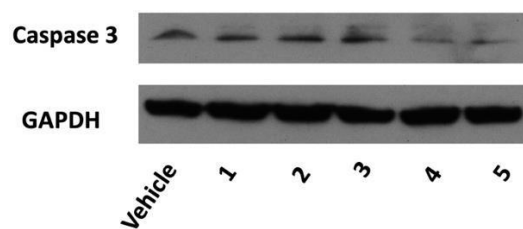
Figure 50. Representative western blot of caspase 3 in MRC5 cells treated with *P. tomentosa* compounds for 24 h.

Finally, to confirm biochemical data on apoptosis, we identified cells that had activated programmed cell death by the TUNEL assay. With this assay, apoptotic nuclei were labelled in green and can be compared with all nuclei labelled in blue with Hoechst. By microscopic analysis of HepG2 treated with 1 μM of the compounds for 24 h, we observed that compounds 4 and 5 caused apoptotic nuclei to be clear; while the others produced an effect less appreciable (Figure 51). These data agreed with caspase 3 activation being more pronounced precisely in treatments with compounds 4 and 5.
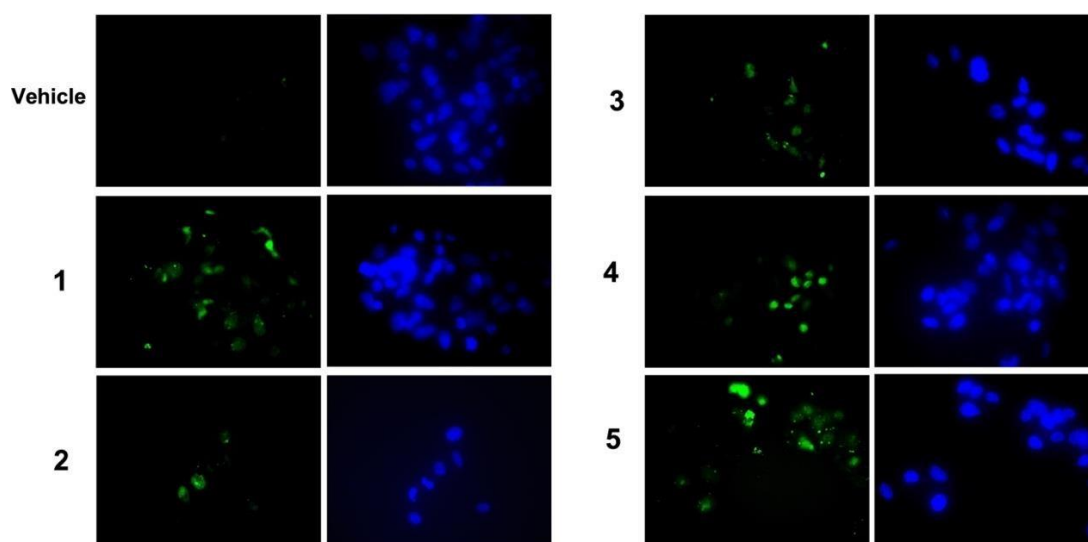
Figure 51. TUNEL assay. Microscopic visualization of apoptotic nuclei (green) and total Hoechst-labelled nuclei (blue) of HepG2 cells treated with 1 μM of *P. tomentosa* compounds for 24 h. (Magnification 40x, with oil).

5.3.5 Effects of P. tomentosa compounds on ER stress

As reported in a study by Limonta et al. (2019), natural compounds can trigger cancer cell apoptosis by activating ER-stress (Limonta et al, 2019). Therefore, we wanted to evaluate ER-stress in HepG2 in the presence of *P. tomentosa* compounds. By PCR, we analysed the occurrence of splicing of XBP1 since the spliced form of this transcript is an early marker of ER-stress. None of the treatments caused

splicing of XBP1; it was observed only in treatments with TAP, an inducer of ER-stress (Figure 52 A). By western blot, we evaluated the expression of another ER-stress marker, GRP78 protein after treating HepG2 with 1 µM of the compounds for 24 h. As shown in Figure 52 B and C, there was no increase in GRP78 in the presence of the compounds; rather we detected a decrease in its expression. Again, TAP was used as a positive control of ER-stress.
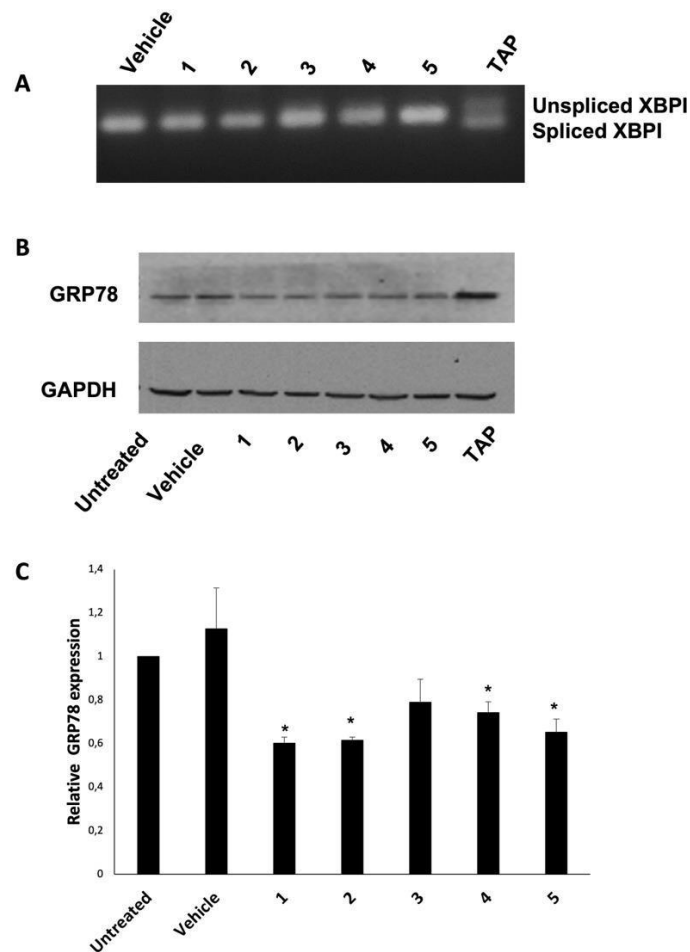
Figure 52. ER-stress in presence of *P. tomentosa* compounds in HepG2 cells. (A) Agarose gel showing unspliced form and spliced form di XBP1, amplified by conventional PCR. (B) Representative western blot of GRP78 in HepG2 cells treated with 1 µM of each compound for 24 h. (C) Densitometric analysis of three independent experiments. Protein levels are normalized with respect to GAPDH housekeeping protein expression. Data are expressed as means ± SE of three experiment. Statistical analysis was performed using Student's t-test. * $p < 0.05$ vs. vehicle treated-cells.

5.3.6 Modulation of autophagy by P. tomentosa compounds

As mentioned in the introduction, a desirable feature of anti-cancer compounds is the modulation of autophagy. It is a process that, at the basal level, promotes cellular homeostasis, but under stressful conditions it can trigger pro-death pathways. First, we evaluated by western blot in HepG2 cells treated with 1 μM of *P. tomentosa* compounds for 24 h the expression of the two forms of LC3 (Figures 53). As shown by densitometric analysis all compounds led to an increase in form II of LC3. In particular, compound 5 caused both a marked increase in form II of LC3 and a pronounced decrease in form I of LC3 (Figures 53). TAP was used as a positive control of autophagy induction.
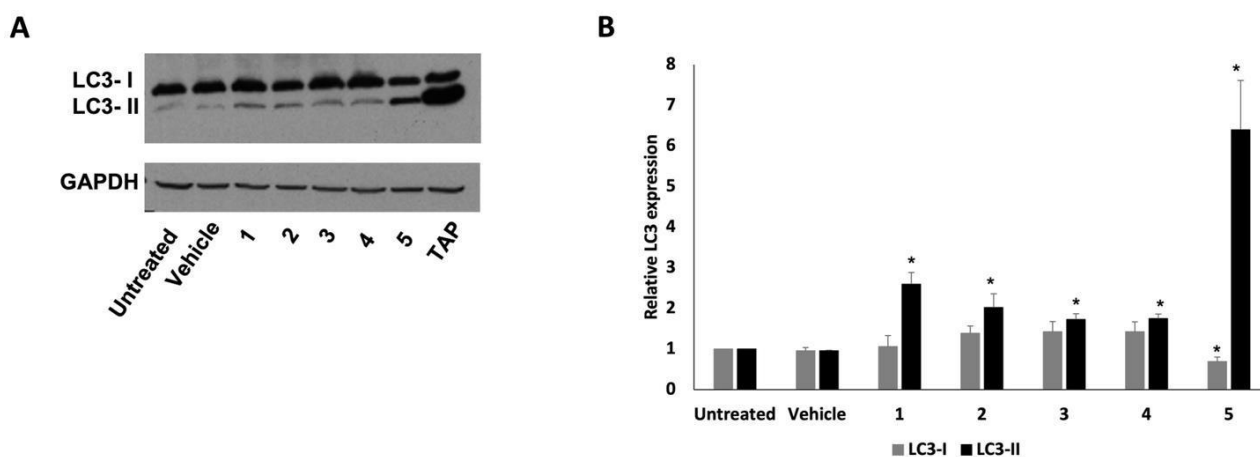
Figure 53. LC3 expression in HepG2 cells cultured with *P. tomentosa* compounds. (A) Representative western blot of LC3 I and II for in HepG2 cells treated with 1 μM of each compound for 24 h. (B) Densitometric analysis of three independent experiments. Protein levels are normalized with respect to GAPDH housekeeping protein expression. Data are expressed as means ± SE of three experiment. Statistical analysis was performed using Student's t-test. * $p < 0.05$ vs. vehicle treated-cells

To assess autophagic flux, we studied another marker, the P62 protein. HepG2 cells were treated with 2 μM of the compounds for 4 h. By western blot, we observed that all compounds induced a reduction in P62 expression levels. In this case, 2 h of starvation was used as a positive control of autophagy induction (Figure 54)
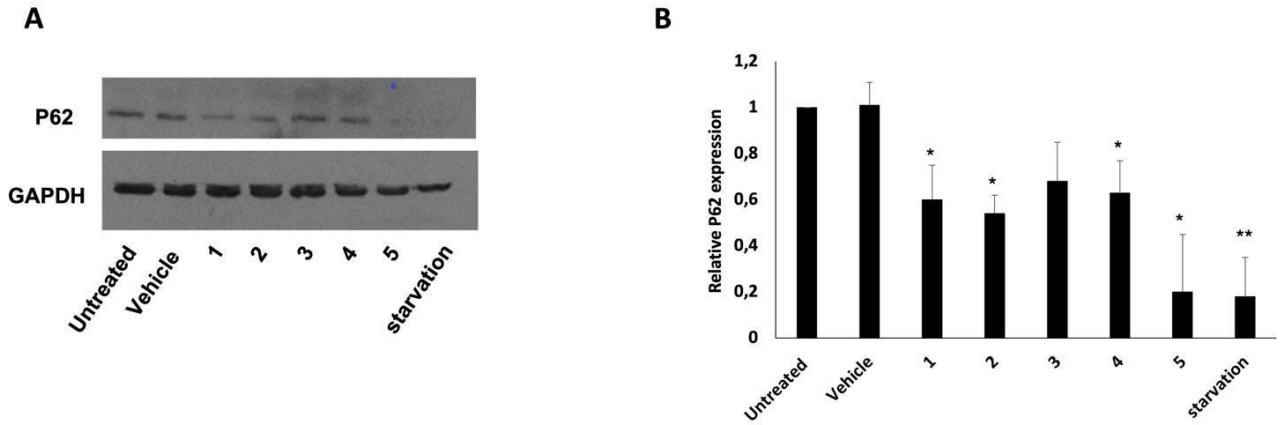
Figure 54. P62 expression in HepG2 cells cultured with *P. tomentosa* compounds. (A) Representative western blot of P62 in HepG2 treated for 4 h with 2 μM *of P. tomentosa* compounds. (B) Densitometric analysis of three independent experiments. Protein levels are normalized with respect to GAPDH housekeeping protein expression. Data are expressed as means ± SE of three experiment. Statistical analysis was performed using Student's t-test. * p < 0.05 vs. vehicle treated-cells.

Chapter 6. Discussion and conclusions

In this chapter I will discuss findings obtained during my PhD thesis in the light of the relevant and recent literature. Discussion are presented divided into two sections regarding the two main topic of my research, the characterization of biological and toxicological effects of APs and the characterization of anti-cancer features of cardenolides from *P. tomentosa.*

6.1 Discussion regarding alkylphenols results

APs are part of the class of nonionic surfactants and for their chemical characteristics they are often used in multiple industrial applications (Chowke et al, 2017). Once released into the environment, they undergo degradative processes generating shorter-chain APs namely 4-NP and 4-OP (Acir and Guether, 2018). Over time, they have been found accumulated in different environmental compartments such as groundwater, sediment, surface water, soils and air (Graca et al, 2015; Vikelesoe et al, 2002, Olaniyan et al, 2018). Thus, they have become part of the food chain and have been detected in fish, clams, shrimps, milk, fruits, and vegetables (Diao et al, 2017; Maggioni et al, 2013; Dodgen et al,2013; Ademollo et al, 2008). As a consequence, humans are constantly exposed to these environmental pollutants through mainly ingestion of contaminated water and food but also inhalation and dermal absorption. Many population studies have detected amounts of APs in human tissues and fluids such as adipose tissue, liver, maternal plasma, amniotic fluid, breast milk, and urine (Espinosa et al, 2009, Shekar et al, 2016, Ademollo et al, 2008, Park et al, 2017). These compounds act as endocrine disruptors as they mimic the structure of β-estradiol and interact with the endogenous receptor (Soares et al, 2008, Acir and Guenther, 2018). As we mentioned in the introduction, they can have many toxic effects on different tissues and organs through the trigger of different cellular processes. Precisely, the scientific literature report that they exert toxic action on reproductive, nervous, immune, and gastrointestinal systems by inducing cell death, oxidative stress, mitochondrial and endoplasmic reticulum damage, injury, and tissue disorganization (Albaladejo et al, 2014; Gong et al, 2006; Bian et al, 2006; Aydogan et al, 2008; Lepretti et al, 2015; Magnifico et al, 2018). The main route of exposure is ingestion of contaminated water and food therefore the gastrointestinal system could be particularly compromised by APs. In addition, the liver is the main organ involved in detoxifying substances foreign to our bodies (Grant D.M., 1991). It has been shown that APs

accumulate in the liver, which difficulty eliminates them (Kourouma et al, 2015; Nomura et al, 2008). Therefore, our attention has been focused on studying the toxic effects and molecular mechanisms underlying APs toxicity on a human liver cell line (HepG2), which is considered a good *in vitro* model for toxicological studies (Gomez-Lechon et al, 2014). The results of this study have been partially published in 2021 (Paolella et al., 2021). However, we will also present data on other cell lines that represent other possible target organs (manuscript in preparation).

In the first instance, by a MTT assay, we observed that 4-NP and 4-OP induced reduction in cell viability of HepG2 in a dose-dependent manner and that the effect was very evident in both cases when we used the compounds at the concentration of 100 μM. With 4-NP, we also found that stressed (starved) cells were much more sensitive to cytotoxicity induced by the compound. In fact, already with treatments of 4-NP 25 μM the mortality was about 80%. In the work of Lepretti et al (2015) it has been shown that 4-NP induced dose-dependent mortality on Caco-2. Therefore, we evaluated the effect of 4-OP on Caco-2 by showing that it presented similar effect to 4-NP. The low-dose effect was slightly more pronounced in Caco-2 although overall HepG2 cells were more sensitive to treatments. The combination of the two pollutants, moreover, on HepG2, did not give synergistic effects, which were visible, on the other hand, on Caco-2 cells. However, at the 100 μM concentration of the mixture no additional mortality of the mixture was observed compared to single APs at 25 and 50 μM in Caco-2. The calculation of IC_{50} highlighted that: 4-NP and 4-OP had similar toxic effects on HepG2, Caco-2 were slightly more sensitive to 4-NP than 4-OP, and the mixture of compounds had synergistic effect on Caco-2. Considering the difference in action of the compounds according to cell type we evaluated the behaviour of these pollutants on the non-tumour cell line MRC5 representing a lung model, being the lung another potential target organ. 4-NP and 4-OP similarly reduced the viability of MRC5 cells with marked effects at concentrations of 75 and 100 μM. In addition, the combination of the compounds presented synergistic effect. On HEK293, a kidney cell model, on the other hand, the synergistic effect of the mixture was not observable; however, the single substances similarly reduced renal cell viability. The synergistic effect of the endocrine disruptors agrees with studies in the literature. Gan et al (2015) demonstrated that 4-NP and Bisphenol A, when combined, had synergistic action in reducing the viability of the Human Prostate Epithelial Cell Line RWPE-1 (Gan et al, 2015). This behaviour was also observed in *in vivo* models. The combination of xenoestrogens accentuated pathological abnormalities of mice female reproductive tract such as increased corpora lutea, endometrial hypertrophy, and changes in the size and morphology of the uterus (Vo et al, 2015).

To understand how these substances reduced cell viability, we investigated whether they acted on the cell cycle. Data in the literature demonstrated the ability of APs to block the cell cycle (Qui et al, 2013; Can et al, 2005). We found that in HepG2 cells 4-NP significantly reduced entry into the S phase of the cell cycle at 100 μM and that 4-OP had similar effect at 50 μM. 4-NP at low doses counteracted the pro-proliferative action of EGF. Considering that cell proliferation requires phosphorylation events and subsequent translocation into the nucleus of ERK (Shevzov et al, 2015), we evaluated the action of 4-NP on its phosphorylation level and found that the pollutant reduced the phosphorylation of ERK induced by the pro-proliferative stimulus of EGF. P53, the guardian of the genome, is a protein involved in both cell cycle management and apoptosis. Precisely, it interacts with p21, which inhibits cyclin-dependent kinase D/CDK4 and E/CDK2 complexes by blocking phosphorylation of protein substrates essential for S-phase initiation. In addition, p53 can trigger apoptosis by inducing transcription of pro-apoptotic genes such as bcl-2 or by activating Apafl (Apoptotic peptidase activating factor 1) and cytochrome c (Feroz et al, 2020). We observed an increased expression of p53 in HepG2 treated with 25 and 50 μM of 4-NP; p53 returned to basal state at the concentration of 100 μM. In contrast, 4-OP induced increase in p53 expression only at 25 μM and a reduction at higher concentrations. Duan et al (2017) demonstrated that 4-NP in rats caused damage to spermatogenesis by inducing apoptosis dependent on increased p53 expression. The reduction could be compatible with treatments at high concentrations and with the theory that cells would no longer be able to recover from the damage and therefore the turnover of p53 expression is accelerated (Feroz et al, 2020). As seen in the introduction, these environmental pollutants can trigger programmed cell death in both *in vivo* and *in vitro* models. Therefore, we investigated the expression and activity of caspase 3, a cysteine protease effector of the apoptotic process (Porter and Janicke, 1999), in the presence of APs. Caspase 3 was particularly active in HepG2 cells treated with 4-NP 50 and 100 μM. Western blot revealed that both 4-NP and 4-OP induced increased expression of caspase 3 in HepG2. By the TUNEL assay, we confirmed that 4-OP, already at low doses (12.5 μM) was responsible for apoptotic body formation. With experiments still in progress, we observed that on intestinal Caco-2 cells, 4-OP at concentrations of 50 and 100 μM carried a slight reduction of procaspase 3 and a slight increase of its cleaved and active form. The increase in the active form of caspase 3 is less evident on Caco-2 than on HepG2. So, the different cell lines showed different sensitivity to the compounds.

From the literature, we learn that endocrine disruptors can cause apoptosis induced by an ER-stress process. For example, Kusonoki et al (2008) and Sasaya et al (2012) demonstrated that in PC12 prostate cells, apoptosis was induced by ER stress following exposure to APs. Lepretti et al (2015) also highlighted that 4-NP triggered programmed cell death in intestinal cells via ER stress. Indeed,

when reticulum stress is prolonged the UPR fails and apoptosis is triggered. Precisely, when there are aggregates of misfolded proteins, the chaperone GRP78 dissociates from the ER and PERK, ATF6 and IRE1 are activated. PERK blocks general protein synthesis with phosphorylation of eIF2α factor. The PERK pathway leads to activation of ATF4, which, in turn, induces transcription of genes required to restore ER homeostasis. Proteolytic activation of ATF leads to the expression of XBP1, which must undergo splicing by IRE1 to be active. The spliced form of XBP1 migrates into the nucleus and controls transcription of genes encoding molecules to restore reticulum homeostasis. However, a prolonged stress condition induces the expression of CHOP (C/EBP homologous protein) which induces pro-apoptotic factors (Szegezdi et al, 2006). On these bases, we evaluated the expression of some ER-stress markers in the presence of APs. With 4-NP we found increased expression of GRP78 and splicing of XBP1 at concentrations of 50 and 100 μM; in contrast, CHOP expression appeared only with treatments of 100 μM. We can say that there was an initial attempt to restore reticulum homeostasis in HepG2 that failed especially at high stimulus concentrations, where CHOP appeared. 4-OP increased GRP78 expression and induced XBP1 splicing at concentration of 100 μM in HepG2 cells. With studies still in progress, we are evaluating ER stress induced by 4-OP on other cell lines. From western blots we understood that this pollutant caused a slight increase of GRP78 in Caco-2 in all treatments except at 100 μM where a decrease was observed. In MRC5, in contrast, GRP78 overexpression dose dependently increased at all concentrations tested. All these data need to be confirmed with further experiments. To understand whether apoptosis was related to ER stress, we used salubrinal, a selective inhibitor of eIF2α dephosphorylation that blocks reticulum stress (Boyce et al, 2005). Indeed, in its presence, GRP78 expression was reduced in HepG2 cells cultured with 4-NP compared to those treated with 4-NP alone. By western blot, we also observed that cells treated with salubrinal and 4-NP exhibited reduced activation of caspase 3. From these data we deduced that in HepG2 the apoptosis induced by this AP is closely related to the condition of prolonged ER stress.

For a long time, it was thought that the distance between ER and mitochondria was about 100 nm, now, thanks to electron tomography and digital microscopy, it has been seen that, at repose, the distance between the two organelles is between 10 and 25 nm. So, a tethering between cellular organelles is conceivable. Under stress conditions, moreover, the distance also becomes below 10 nm (Giacomello and Pellegrini, 2016). So, the two organelles are physically and functionally connected through specialized areas known as mitochondria-associated ER membranes (MAMs). The connection is particularly important for maintaining calcium homeostasis and to regulate cellular processes such as apoptosis (Kumar and Maity, 2021). One of the proteins involved in tethering between these two organelles is mitofusin 2 (MFN2) involved in mitochondrial fusion (Kumar and

Maity, 2021). To investigate the influence of ER stress on mitochondrial dynamics, we evaluated the expression of MFN2 and DRP1 (dynamin related protein 1), a cytosolic GTPase recruited to the mitochondrial membrane during mitochondrial damage to induce mitochondrial fragmentation (Smirnova et al, 2001). Western blots highlighted that 4-NP induced significant increase in MFN2 from concentrations of 25 μM. Only 100 μM of 4-NP, on the other hand, significantly increased DRP1 expression. This behaviour is compatible with the role of these proteins. MFN2 may decrease mitochondrial membrane stability by encouraging pore formation making it easier for subsequent fragmentation by DRP1 leading to cytochrome c release and initiation of apoptosis. So, the overexpression of MFN2 at low doses of 4-NP can be interpreted as an adaptive phase of the cell trying to restore homeostasis. At high doses of pollutant, on the other hand, the increased expression of DRP1 indicates irreparable mitochondrial damage. Our results agree with studies showing that both MFN2 and DRP1 proteins are overexpressed under conditions of ER stress-induced apoptosis (Wang et al, 2012; Frank et al, 2001). In addition, treatments with salubrinal, reduced the expression of MFN2 and DRP1 in the presence of 4-NP. This finding is particularly important as it gives us insight into the complex crosstalk between ER and mitochondria during cellular stress on which cell fate depends. Given that in human cells there is a close correlation between ER stress, mitochondrial dynamics, activation of apoptosis, and calcium homeostasis (Biagioli et al, 2008; Martucciello et al, 2020), we investigated whether APs were able to mobilize calcium. By assaying the activity of TG2, a calcium-dependent enzyme expressed in Caco-2 cells, we indirectly demonstrated that 4-OP 100 μM and 4-NP 50 and 100 μM induced an increase in intracellular calcium levels. From this result, we can conclude that these environmental pollutants could lead to mobilization of calcium from intracellular stores or more generally affect calcium homeostasis. These data were consistent with work by Michelangeli et al (2008), in which APs were shown to cause abnormal elevation of intracellular calcium in TM4 Sertoli cells, and with research by Liu et al (2008) in which 4-NP induced calcium increase in bovine adrenal chromaffin cells.

It has been observed that 4-NP could simultaneously induce autophagy and apoptosis in Sertoli cells (Duan et al, 2016). Furthermore, it is known that autophagy and apoptosis are closely related. Autophagy is a cellular process in which cells degrade and recycle organelles and macromolecules to derive energy when under stress. In accordance with cellular, tissue and microenvironment conditions, autophagy can act as a pro-death or a pro-survival mechanism. There is a complex crosstalk between autophagy and apoptosis in which one influences the other and vice versa (Bata and Cosford, 2021). With studies still in progress, we are investigating the influence of 4-OP on the autophagic process. Considering the crucial role in autophagosome maturation played by the conversion of LC3-I to LC3-II (Xi et al, 2022), we evaluated the expression of these two forms in

HepG2 in the presence of 4-OP. We found that low-dose treatments induced a slight increase in LC3-II while with 25 and 50 μM of 4-OP there was a reduction in LC3-II isoform. A very interesting article entitled "How to interpret LC3 immunoblotting" explains how LC3-II, being degraded by lysosomal proteases in the last stages of autophagy, can disappear under prolonged or too intense stress (Mizushima and Yoshimori, 2007). By a microscopic immunofluorescence detection of LC3, we revealed that 4-OP 6.25 μM (low dose) produced more autophagosomes than 4-OP 25 μM. This finding agreed with western blot. In parallel, we studied the expression of another marker of autophagy, the P62 protein. Precisely, this molecule, after maturation and elongation of the autophagosome, can bind LC3-II (to the N-terminus) and to ubiquitinated proteins (to the C-terminus) and is considered a suppressor of autophagy (Xi et al, 2022). 4-OP induced a dose-dependent decrease in P62 expression thus evidencing an increase in autophagic flux. Even if these results should be confirmed by further experiments, altogether they indicate a role of 4-OP in autophagy induction. It will be important, as the study by Mizushima and Yoshimori (2007) suggests, to investigate the expression of LC3-II in the presence of inhibitors of lysosomal proteases or autophagosome-lysosome fusion such as bafilomycin A1. It would also be useful to evaluate the expression of this protein at shorter times with 4-OP high-dose treatments.

One of the main mechanisms by which APs induce toxicity is the generation of reactive oxygen species (ROS) (Magnifico et al, 2018; Saggu et al, 2014; Aydogan et al, 2008; Gong et al, 2006). The first line of defence against oxidants is composed of two enzymes: superoxide dismutase (SOD) and catalase (CAT). Precisely, SOD converts superoxide radical and singlet oxygen to H_2O_2 and CAT degrades H_2O_2 to H_2O and O_2. Several studies in the literature report that CAT and SOD decrease their expression or activity in the presence of APs (Mao et al, 2010; Kourouma et al, 2015) while others report that they increase (Almeida et al, 2023; Derakhshesh et al, 2017; Yeltekin et al., 2018). So, we can conclude that the activity and expression of antioxidant enzymes following exposure to 4-NP and 4-OP is variable and dependent on biological models and cell types.

In our case, we found that 4-OP induced dose-dependent increase in catalase activity after 24 h of treatments in HepG2 cells. SOD expression was decreased with OP 25 μM and returned to basal level with OP 50 and 100 μM. In the interpretation of these data, we must take into consideration the cell model used, since it is reported in the literature that the HepG2 cell line is particularly resistant to the action of ROS because it has high baseline catalase activity (Zhao et al, 2019). However, considering the function of the enzyme, and on the bases of our preliminary data, we might think that the cells are responding to an increase in ROS by increasing the activity of CAT trying to restore homeostasis.

Finally, we can conclude that APs alter the functionality of enzymes constituting the antioxidant defence system of cells.

The majority of the studies presented in my thesis were performed on two dimensional (2D) monolayer cell cultures. However, 2D monolayer cell cultures have limitations: loss of numerous functions such as cell-cell and cell-matrix contacts, which results in reduced differentiation, flattened morphology with altered cytoskeleton, altered signaling pathways, and dysregulated liver enzyme involved in pollutant metabolism (Stamper at al, 2019). On the other hand, three dimensional (3D) cultures better represent cellular functions by mimicking the structure and architecture of tissues and organs (Guenness et al, 2013). Therefore, we are developing a protocol to obtain 3D liver cultures with HepG2, called spheroids. Preliminary data on the evaluation of spheroids differentiation markers are encouraging, thus we are planning experiments aimed to mainly analyze the metabolomic profile of spheroids in the presence and in the absence of APs.

6.2 Discussions regarding *Pergularia tomentosa* compounds results

One of the aims of my Ph.D. program was to understand the possible cytotoxicity induced by cardenolides extracted for the first time from the aerial parts of the plant *Pergularia tomentosa*. In particular, we wanted to understand the potential anti-tumour effect and whether these compounds exerted selective cytotoxic action on cancer cells. The results of this study have been published in 2022 (Martucciello et al., 2022). As I described in the introduction, over time, an extensive literature has developed around the anti-tumour effects of CGs. They constitute a family of secondary compounds with a similar structure found in animals and plants (Botelho et al, 2019). They can act on several human cancer cell lines by triggering cellular and molecular mechanisms such as apoptosis, blocking proliferation, and autophagy (McKonkey et al, 2000; Yeh et al, 2003; Daniel et al, 2003; Meng et al, 2016; Trenti et al 2014). In addition, it has been shown that they can also be used as adjuvants in radiotherapy and chemotherapy (Verheye and Bohm, 1998; Lawrence 1988; Nasu et al, 2002). The semi-erect perennial herb *P. tomentosa* is a rich source of CGs (Hamed et al, 2006; Hosseini et al, 2019). These compounds, usually, have a typical structure with steroid rings A/B and C/D fused in *cis* and those B/C fused in *trans*. However, the cardenolides extracted from *P. tomentosa* have peculiar structural features: the A/B rings are *trans*-fused and the glycosidic portion is represented, often, by a single sugar that is bonded to the steroid core through two bonds with hemiacetalic and acetalic functions, respectively, generating a characteristic chemical attachment called dioxanoid attachment (Piacente et al, 2009). Works by Hamed et al (2006) Piacente et al

(2009), and Hosseini et al (2019) highlighted that these compounds exerted a potent cytotoxic action on different human cancer cell lines. Therefore, we focused our attention on cardenolides extracted, for the first time, from the leaves of this plant. Precisely, compound 5 is calactin, compound 4 is calotropin, whereas compound 3 is a derivative of calactin and 1 and 2 are derivatives of calotropin. First, by MTT assays, we evaluated cytotoxicity on two cancer cell lines (HepG2 and Caco-2), on one immortalized noncancer cell line (MRC5), and on normal cells (HUVEC). We observed that compounds 1 and 2 affected cancer cell viability similarly; compound 3 was the least effective, whereas the most potent compounds were 4 and 5. These compounds also significantly reduced the viability of noncancer cells, so we can conclude that they do not have a specific action on cancer cells. This behaviour agrees with what has been reported in other scientific works. For example, Clifford and Kaplan (2013) observed that healthy mammalian cells were more sensitive to bufalin than cancer cells (Clifford and Kaplan, 2013). However, in the review by Calderon-Montano et al (2014) it has been inferred that the cytotoxic action depended strictly on the cell type, on which of the CGs was tested, and from their concentration (Calderon-Montano et al, 2014). By calculating IC_{50} we understood that each cell type has a different sensitivity to the compounds and that human liver cancer cells (HepG2) were particularly sensitive to calactin. Therefore, we focused most of our attention on understanding the action of compounds on this cell line. Given the observed toxicity and considering that other cardenolides blocked the cell cycle, we evaluated, by BrdU incorporation assay, the effect of *P. tomentosa* compounds on cell cycle progression of HepG2. All compounds induced, with varying strength, the reduction of entry into the S phase of cells; the most potent was compound 5. This result agreed with the MTT assay. Knowing that p53 is a transcription factor highly inducible by numerous stress signals we investigated its expression. Precisely p53 involves activation of p21/WAF1. p21 binds cyclin E2/CdK2 and D/Cdk4 complexes and arrests the cell cycle in G1 phase (Chen et al, 2016). By western blot analysis, we found that compounds induced increased expression of p53 except compound 5, which, on the other hand, reduced p53 expression. P53 is a transcriptional factor and must migrate into the nucleus to perform its functions. An increase in nuclear p53 is, often, associated with cell cycle arrest and apoptosis (Mesaeli and Phillipson, 2004). By western blot we found that cardenolides 1, 2, 3, 4 induced increased expression of nuclear p53. Calactin, on the other hand, reduced the expression of nuclear p53. So, we can think that compound 5 was acting on cancer cells by different mechanisms from the others.

To better characterize the anti-tumour potential of *P. tomentosa* cardenolides, we evaluated the action of these compounds on cell migration, as one of the main features of tumours is the migration of malignant cells to give rise to metastasis and secondary tumour implants. We observed that all compounds were able to counteract the migration of HepG2 cells and that the most potent was

compound 5. The result is in line with a study by Schneider et al (2016) in which several CGs were shown to inhibit migration and invasion of lung cancer cells. Next, we investigated whether the reduction in viability was related to the induction of apoptosis. Western blot revealed that all compounds were able to activate cleavage of caspase 3 making it active. Moreover, the activity assay for this cysteine protease was in complete agreement with the western blot. Finally, microscopic analysis following the TUNEL assay confirmed the two previous data. So, *P. tomentosa* compounds activated apoptosis in HepG2 and compounds 4 and 5 were found to be the most active. By western blot, we noted that on MRC5 noncancer cells compounds 1, 2 and 3 were more potent than compounds 4 and 5 in inducing caspase 3 activation. Once again, the theory that the activity of CGs is closely related to the cell type on which they are tested is confirmed.

A study by Limonta et al (2015) showed that natural compounds could trigger programmed cell death through a prolonged ER-stress condition. However, it has also been found that cancer cells need increased protein synthesis to proliferate rapidly by bringing the endoplasmic reticulum under stress conditions. Usually, this situation leads to upregulation of the chaperone GRP78 in cancer cells, as it prevents the accumulation of misfolded proteins and consequent cell death. So, GRP78 has become a real target of some cancer therapies (Luo and Lee, 2013). By PCR analyses, we found that none of the *P. tomentosa* compounds were able to activate alternative splicing of XBP1, diagnostic of ER-stress (Luo et al, 2022). By western blot we observed that the expression of GRP78 in the presence of these cardenolides slightly reduced. This finding is in agreement with the activation of caspase 3. Indeed, reduced expression of GRP78 may prevent UPR and promotes the initiation of tumour cell death (Luo and Lee, 2013). Other CGs also exhibited this behaviour on GRP78 expression. For example, Lanthanoside C occurred as an inhibitor of GRP78 expression, triggering this pathway in pancreatic cancer cells (Ha et al, 2021).

An interesting review by Skubnik et al (2021) analyzed how different CGs can be modulators of autophagy. Also of recent interest is the study of the interaction between autophagy and apoptosis in cancer cells and noncancer cells. Precisely, there is a balance between autophagy flux and apoptosis that is strictly dependent on the context in which the cell is located. Many scientists argue that when autophagy is inhibited, apoptosis also decreases; others believe that they inhibit each other. Furthermore, in the tumour environment, autophagy plays a dual role by providing energy and material to the cancer cell on the one hand, and on the other hand, if it persists, it can trigger apoptosis (Xi et al, 2022). So, interesting for developing new anti-cancer drugs, is to evaluate how they affect the autophagy-apoptosis relationship. Therefore, in the presence of *P. tomentosa* compounds we evaluated the expression of LC3-II and P62, proteins involved in the autophagy process. We found

that these cardenolides induced increased expression of LC3-II and decreased expression of P62. This phenomenon is particularly evident for compound 5. This behaviour is in perfect agreement with that described in work by Miao et al (2013) performed on HepG2. Precisely, the researchers showed that bufalin (another CG) induced strong expression of LC3-II and other pro-autophagy molecules (Miao et al, 2014). As the review by Xi et al (2022) highlighted, the p53 protein could be the balance needle in determining the relationship between apoptosis and autophagy. Indeed, this protein interacts with apoptotic (Bcl2) and autophagic (beclin-1) family of molecules. In addition, the strong induction of autophagy may be related to reduced expression of p53 (Xi et al, 2022), observed when HepG2 were treated with calactin (compound 5). It is also found that other CG such as digitoxin could block p53 expression by inducing mitotic catastrophe (Elbaz et al, 2012).

6.3 Conclusions

In conclusion, during my Ph.D. course, I studied both APs induced cytotoxicity and the anti-tumour properties of cardenolides extracted from the aerial parts of *P. tomentosa* using human cell cultures in both cases. Regarding APs, I demonstrated that 4-NP and 4-OP exert cytotoxicity by reducing the viability of different cell lines representing possible target organs. I revealed that the main mechanism underlying this phenomenon involves the arrest of cell cycle progression and apoptosis. The triggering of programmed cell death is deeply linked to APs-induced cellular stress conditions such as ER-stress, mitochondrial dysfunction, oxidative stress, altered calcium homeostasis and induction of autophagic flux. Thus, I have shown that these widespread environmental pollutants are a potent insult to cellular homeostasis, representing a serious danger to human health. On the other hand, I realized that *P. tomentosa* compounds can reduce the viability of HepG2 tumour cells and other cell lines. In addition, I observed that the action of these compounds is cell-dependent and that they seem to not selectively act on cancer cells. However, these cardenolides, particularly calactin, exert anti-tumour action on HepG2 by blocking proliferation, migration and triggering autophagy and apoptosis. In light of these results, they may represent excellent starting structures to develop future anti-cancer drugs or more efficient adjuvants to current therapies.

With this research, I have shown how using similar approaches and experimental models, we can understand the effects of synthetic and natural compounds on cellular physiology and molecular mechanisms. Cell cultures are still very useful laboratory models in the biomedical field to test *in vitro* toxicity of substances, to extract nucleic acids and proteins and performing subsequent biochemical analyses, and to carry out functional and regulatory studies. There are numerous advantages of using cell cultures. They represent simpler systems than whole organs, allow experiments to be easily reproduced and environmental and physicochemical conditions to be

controlled. They are useful for understanding molecular mechanisms such as signaling underlying a given cellular response. They are easier to manage than *in vivo* models, reducing costs and ethical issues. However, the other side of the coin is that cell cultures represent a simplified model of study compared to the whole organism and there is often a difficult correlation between culture conditions and what happens *in vivo*, losing organ specific activities. To overcome this limit, the classic two-dimensional cell cultures have been joined by three-dimensional cultures, which make the *in vitro* conditions more like those *in vivo* by mimicking the structure and architecture of whole organs. Indeed, our future goal is to realize spheroids to perform biochemical and metabolomic analyses after treatments with the interest compounds and to evaluate the agreement between 2D and 3D cellular systems. Therefore, I can conclude that the use of human cell cultures and the methodological approach is the point of union between our research themes focused on understanding both the cytotoxic effects induced by environmental pollutants such as alkylphenols and the anti-cancer properties of natural compounds candidates to become possible anti-cancer drugs.

ABBREVIATIONS

(2D) Two dimensional

(3D) Three dimensional

(4-NP) 4-Nonylphenol

(4-OP) 4-Octylphenol

(4-tOP) 4-tert-Octylphenol

(Ab) Antibody

(ALP) Alkaline Phosphatase

(ALT) Alanine Transaminase

(AP-1) Activator Protein 1

(Apaf-1) Apoptotic protease activating factor-1

(APEOs) Alkylphenol ethoxylates

(APs) Alkylphenols

(AST) Aspartate Aminotransferase

(ATF6) Activating Transcription Factor 6

(ATP) Adenosine Triphosphate

(BBS) Borate Buffered Saline

(BrdU) Bromodeoxyuridine

(BSA) Bovine Serum Albumin

(CaBP-9K) Calbidin-D9K

(CAT) Catalase

(cDNA) complementary DNA

(CER) Cytoplasmatic extraction reagent

(CGs) Cardiac Glycosides

(CHOP) C/EBP homologous protein

(COX-2) Cyclooxygenase-2

(CYP1A2) Cytochrome P450 1A2

(d.w.) Dry weight

(DMEM) Dulbecco's modified eagle medium

(DMSO) Dimethyl sulfoxide

(DRP1) Dynamin-related protein 1

(DTT) Dithiothreitol

(dUTP) 2´-Deoxyuridine-5´-Triphosphate

(EDCs) Endocrine chemical destroyers

(EDTA) Ethylenediaminetetraacetic acid

(EGF) Epithelial Growth Factor

(EGFR) Epithelial Growth Factor- Receptor

(eIF2α) Eukaryotic Initiation Factor 2

(eNOS) Endothelial Nitric Oxide Synthase

(ER) Endoplasmatic reticulum

(ERK) Extracellular signal-Regulated Kinase

(FBS) Fetal Bovine Serum

(FDA) Food and Drug Administration

(GAPDH) Glyceraldehyde-3-Phosphate Dehydrogenase

(GFP) Green Fluorescent Protein

(GRB2) Growth factor receptor-bound protein 2

(GRP78) Glucose-Regulated Protein 78

(GSH) Reduced Glutathione

(HRP) Horseradish Peroxidase

(IFN- γ) Interferon gamma

(IGFBP1) Insulin-like growth factor-binding protein-1

(IgG1) Immunoglobulin G1

(IL-17) Interleukin-17

(IL-22) Interleukin-22

(IL-4) Interleukin-4

(IL-6) Interleukin-6

(IL-8) Interleukin-8

(iNOS) Inducible Nitric Oxide Synthase

(IP₃) Inositol 1,4,5-trisphosphate

(IRE1) Inositol-requiring enzyme type 1

(LC3) Microtubule-associated proteins 1A/1B light chain 3B

(LEFTY2) Left-Right Determination Factor 2

(LV) Left ventricular

(LVEF) Left ventricular ejection fraction

(MAMs) Mitochondria-associated ER membranes

(MAPK) Mitogen-activated protein kinase

(MDA) Malondialdehyde

(MEM) Eagle's Minimum Essential Medium

(MFN2) Mitofusin 2

(MTT) 3-(4,5-dimethylthiazol-2-yl)-2,5-diphenyltetrazolium bromide

(NER) Nuclear Extraction Reagent

(NF-kB) Nuclear factor kappa-light-chain-enhancer of activated B cells

(OD) Optical Density

(ODC) Ornithine Decarboxylase

(PARP) Poly (ADP-ribose) polymerase

(PBS) Phosphate Buffered Saline

(PCR) Polymerase Chain Reaction

(PFA) Paraformaldehyde

(PLC) Phospholipase C

(pNA) p-Nitroaniline

(PRL) Prolactin

(PVDF) Polyvinylidene Fluoride

(RORγt) Retinoic acid receptor-related orphan receptor γ thymus

(ROS) Reactive Oxygen Species

(SAL) Salubrinal

(SDS-PAGE) Sodium Dodecyl Sulphate - PolyAcrylamide Gel Electrophoresis

(SDS) Sodium Dodecyl Sulphate

(SE) Standard Error

(SOD) Superoxide Dismutase

(SOS) Son of sevenless

(SQTM1) Sequestosome 1

(STS) Staurosporin

(T-BBS) Borate Buffered Saline-Tween

(T-TBS) Tris Buffered Saline-Tween

(TAP) Thapsigargin

(TBS) Tris Buffered Saline

(TdT) Terminal deoxynucleotidyl Transferase

(TEM) Electron Microscopy

(TG2) Type 2 Transglutaminase

(Th1) T-helper-1

(Th2) T-helper-2

(TMB) 3,3',5,5'-Tetramethylbenzidine

(TPA) 12-O-tetradecanoylphorbol-13-acetate

(TRITC) 5/6-Tetramethyl-Rhodamine Isothiocyanate

(TRPV6) Transient receptor potential cation channel subfamily 6

(TSLP) Thymic Stromal Lymphopoietin

(TUNEL) Terminal deoxynucleotidyl transferase dUTP Nick End Labeling

(UPR) Unfolded Protein Response

(XBP1) X-Box Binding Protein 1

REFERENCES

Acir I.H., Guenther K. (2018). Endocrine-disrupting metabolites of alkylphenol ethoxylates - A critical review of analytical methods, environmental occurrences, toxicity, and regulation. *Sci.Total Environ*. 635:1530-1546. DOI: 10.1016/j.scitotenv.2018.04.079

Ademollo N., Ferrara F., Delise M., Fabietti F., Funari E. (2008). Nonylphenol and octylphenol in human breast milk. *Environ. Int.* 34 (7):984–987. DOI: 10.1016/j.envint.2008.03.001

Afaq F., Saleem M., Aziz M.H., Mukhtar H. (2004). Inhibition of 12-Otetradecanoylphorbol-13-acetate-induced tumor promotion markers in CD-1 mouse skin by oleandrin. *Toxicol. Appl. Pharmacol*. 195:361–369. DOI: 10.1016/j.taap.2003.09.027

Ahmed A., Pitt B., Rahimtoola S.H., Waagstein F., White M., Love T.E., Braunwald E. (2008). Effects of digoxin at low serum concentrations on mortality and hospitalization in heart failure: A propensity-matched study of the DIG trial. *Int. J. Cardiol.* 123(2):138-46. DOI: 10.1016/j.ijcard.2006.12.001

Albaladejo E.P., Fernandes D., Lacorte S., Porte C. (2017). Comparative toxicity, oxidative stress and endocrine disruption potential of plasticizers in JEG-3 human placental cells. *Toxicol. In Vitro.* 38:41-48. DOI: 10.1016/j.tiv.2016.11.003

Aydoğan M., Korkmaz A., Barlas N., Kolankaya, D. (2008). The effect of vitamin C on bisphenol A, nonylphenol and octylphenol induced brain damages of male rats. *Toxicology* 249 (1):35–39. DOI: 10.1016/j.tox.2008.04.002

Ayogu J.I., Odoh A.S. (2020) Prospects and Therapeutic Applications of Cardiac Glycosides in Cancer Remediation. *ACS Comb. Sci*. 22(11):543-553. DOI: 10.1021/acscombsci.0c00082

Balakrishnan B., Thorstensen E., Ponnampalam A., Mitchell M.D. (2011). Passage of 4-nonylphenol across the human placenta. *Placenta*. 32(10):788-92. DOI: 10.1016/j.placenta.2011.07.014

Bata N., Cosford N.D.P. (2021). Cell Survival and Cell Death at the Intersection of Autophagy and Apoptosis: Implications for Current and Future Cancer Therapeutics. *ACS Pharmacol. Transl. Sci.* 4(6):1728–1746. DOI: 10.1021/acsptsci.1c00130

Biagioli M., Pifferi S., Ragghianti M., Bucci S., Rizzuto R., Pinton P. (2008). Endoplasmic reticulum stress and alteration in calcium homeostasis are involved in cadmium-induced apoptosis. *Cell Calcium.* 43(2):184-95. DOI: 10.1016/j.ceca.2007.05.003

Bian Q., Qian J., Xu L., Chen J., Song L., Wang X. (2006). The toxic effects of 4-tert-octylphenol on the reproductive system of male rats. *Food Chem. Toxicol*. 44(8):1355-61. DOI: 10.1016/j.fct.2006.02.014

Bianco M., Mita L., Portaccio M., Diano N., Sica V., De Luca B., Mita D.G., Romano Carratelli C., Viggiano E. (2011). Differential accumulation levels in the brain of rats exposed to the endocrine disruptor 4-tert-octylphenol (OP). *Environ. Toxicol. Pharmacol.* 31(1):198-204.

Bielawski K., Winnicka K., Bielawska A. (2006). Inhibition of DNA topoisomerases I and II, and growth inhibition of breast cancer MCF-7 cells by ouabain, digoxin and proscillaridin A. *Biol. Pharm. Bull.* 29(7):1493-7. DOI: 10.1248/bpb.29.1493

Botelho A.F.M., Pierezan F., Soto-Blanco B., Melo M.M. (2019). A review of cardiac glycosides: Structure, toxicokinetics, clinical signs, diagnosis and antineoplastic potential. *Toxicon.*158:63-68. DOI: 10.1016/j.toxicon.2018.11.429

Boyce M., Bryant K.F., Jousse C., Long K., Harding H.P., Scheuner D., Kaufman R.J., Ma D., Coen D.M., Ron D., Yuan J. (2005). A selective inhibitor of eIF2alpha dephosphorylation protects cells from ER stress. *Science*. 307(5711):935-9. DOI: 10.1126/science.1101902

Bradford M.M. (1976). A rapid and sensitive method for the quantitation of microgram quantities of protein utilizing the principle of protein-dye binding. *Anal. Biochem*. 72:248-54. DOI: 10.1006/abio.1976.9999

Calderón-Montaño J.S., Burgos-Morón E., Orta M.L., Maldonado-Navas D., García-Domínguez I., López-Lázaro M. (2014). Evaluating the cancer therapeutic potential of cardiac glycosides. *Biomed. Res. Int.* 794-930. DOI: 10.1155/2014/794930

Campbell P. (2002). Alternatives to nonylphenol ethoxylates. Review of toxicity, biodegradation & technical-economic aspects. *ToxEcology Environmental Consulting*, Vancouver, B.C., Canada. Report for Environment Canada.

Can A., Semiz O., Cinar O. (2005). Bisphenol-A induces cell cycle delay and alters centrosome and spindle microtubular organization in oocytes during meiosis. *Mol. Hum. Reprod.* 11(6):389-96. DOI: 10.1093/molehr/gah179

Chen J. (2016). The Cell-Cycle Arrest and Apoptotic Functions of p53 in Tumor Initiation and Progression. *Cold Spring Harb. Perspect. Med.* 6(3). DOI: 10.1101/cshperspect.a026104

Chokwe T.B., Okonkwo J.O., Sibali L.L. (2017). Distribution, exposure pathways, sources and toxicity of nonylphenol and nonylphenol ethoxylates in the environment. *Water SA.* Vol. 43 No. 4. DOI: 10.4314/wsa.v43i4.01

Clifford R. J., Kaplan J.H. (2013). Human breast tumor cells are more resistant to cardiac glycoside toxicity than non-tumorigenic breast cells. *PLoS One.* 8(12). DOI: 10.1371/journal.pone.0084306

Daniel D., Süsal C., Kopp B., Opelz G., Terness, P. (2003). Apoptosis-mediated selective killing of malignant cells by cardiac steroids: maintenance of cytotoxicity and loss of cardiac activity of chemically modified derivatives. *Int. Immunopharmacol.* 3(13-14):1791-1801. DOI: 10.1016/j.intimp.2003.08.004

De Almeida W., Matei J.C., Kitamura R.S.A, Gomes M.P., Leme D.M., De Assis H.C.S, Vicari T., Cestari M.M. (2023). Alkylphenols cause cytotoxicity and genotoxicity induced by oxidative stress in RTG-2 cell line. *Chemosphere*. 313:1373-87. DOI: 10.1016/j.chemosphere.2022.137387

Derakhshesh N., Movahedinia A., Salamat N., Hashemitabar M., Bayati V. (2017). Using a liver cell culture from Epinephelus coioides as a model to evaluate the nonylphenol-induced oxidative stress. *Mar. Pollut. Bull.* 122(1-2):243-252. DOI: 10.1016/j.marpolbul.2017.06.049

Diao P., Chen Q., Wang R., Sun D., Cai Z., Wu H., Duan S. (2017). Phenolic endocrine-disrupting compounds in the Pearl River Estuary: occurrence, bioaccumulation and risk assessment. *Sci. Total Environ*. 584-585:1100–1107. DOI: 10.1016/j.scitotenv.2017.01.169.

Dodgen L.K., Li J., Parker D., Gan J.J. (2013). Uptake and accumulation of four PPCP/ EDCs in two leafy vegetables. *Environ. Pollut.* 182:150–156. DOI: 10.1016/j.envpol.2013.06.038

Duan P., Hu C., Quan C., Yu T., Huang W., Chen W., Tang S., Shi Y., Martin F.L., Yang K. (2017). 4-Nonylphenol induces autophagy and attenuates mTOR-p70S6K/4EBP1 signaling by modulating AMPK activation in Sertoli cells. *Toxicol. Lett.* 267:21-31. DOI: 10.1016/j.toxlet.2016.12.015

Duan P., Hu C., Quan C., Yu T., Zhou W., Yuan M., Shi Y., Yang K. (2016). 4-Nonylphenol induces apoptosis, autophagy and necrosis in Sertoli cells: Involvement of ROS-mediated AMPK/AKT-mTOR and JNK pathways. *Toxicology.* 341-343:28-40. DOI: 10.1016/j.tox.2016.01.004

Elbaz H.A., Stueckle T.A., Tse W., Rojanasakul Y., Dinu C.Z. (2012). Digitoxin and its analogs as novel cancer therapeutics. *Exp. Hematol. Oncol.* 1(1):4. DOI: 10.1186/2162-3619-1-4

Feroz W., Sheikh A.M.A.S. (2020). Exploring the multiple roles of guardian of the genome: P53. *Egyptian Journal of Medical Human Genetics.* 21:49 DOI:10.1186/s43042-020-00089-x

Frank S., Gaume B., Bergmann-Leitner E.M., Leitner W.W., Robert E.G., Catez F., Smith C.L., Youle R.J. (2001). The Role of Dynamin-Related Protein 1, a Mediator of Mitochondrial Fission, in Apoptosis. *Dev. Cell.* 1(4):515-25. DOI: 10.1016/S1534-5807(01)00055-7

Gan W., Zhou M., Xiang Z., Han X., Li D. (2015). Combined effects of nonylphenol and bisphenol a on the human prostate epithelial cell line RWPE-1. *Int. J. Environ. Res. Public Health* 12(4):4141-55. DOI: 10.3390/ijerph120404141

Giacomello M., Pellegrini L. (2016). The coming of age of the mitochondria-ER contact: a matter of thickness. *Cell Death Differ*. 23(9):1417-27. DOI: 10.1038/cdd.2016.52

Giamogante F., Poggio E., Barazzuol L., Covallero A., Calì T. (2021). Apoptotic signals at the endoplasmic reticulum-mitochondria interface. *Adv. Protein Chem. Struct. Biol*. 126:307-343. DOI: 10.1016/bs.apcsb.2021.02.007

Gómez-Lechón M.J., Tolosa L., Donato M.T. (2014). Cell-based models to predict human hepatotoxicity of drugs. *Rev. Toxicol.* 31:149-156.

Gong Y., Han X.D. (2006). Effect of nonylphenol on steroidogenesis of rat Leydig cells. J. Environ. Sci. Health B. 41(5):705-15. DOI: 10.1080/03601230600701866

Graca B., Staniszewska M., Zakrzewska D., Zalewska T. (2016). Reconstruction of the pollution history of alkylphenols (4-tert-octylphenol, 4-nonylphenol) in the Baltic Sea. *Environ. Sci. Pollut. Res. Int.* 23(12):11598-610. DOI: 10.1007/s11356-016-6262-8

Grada A., Otero-Vinas M., Prieto-Castrillo F., Obagi Z., Falanga, V. (2017). Research techniques made simple: analysis of collective cell migration using the wound healing assay. *J. Invest. Dermatol.*137(2):e11-e16. DOI: 10.1016/j.jid.2016.11.020

Grant D. M. (1991). Detoxification pathways in the liver. *J. Inherit. Metab. Dis.* 14(4):421-30. DOI: 10.1007/BF01797915

Guenther K., Heinke V., Thiele B., Kleist E., Prast H., Raecker T. Endocrine disrupting nonylphenols are ubiquitous in food. (2002). *Environ. Sci. Technol.* 36:1676–80. DOI: 10.1021/es010199v

Gunness P., Mueller D., Shevchenko V. Heinzle E., Ingelman-Sundberg M., Noor F. (2013). 3D organotypic cultures of human HepaRG cells: a tool for in vitro toxicity studies *Toxicol. Sci.* 133(1):67–78. DOI: 10.1093/toxsci/kft021

Ha P.D., Tsai Y.L., Lee A.S. (2021). Suppression of ER-stress induction of GRP78 as an anti-neoplastic mechanism of the cardiac glycoside Lanatoside C in pancreatic cancer: Lanatoside C suppresses GRP78 stress induction. *Neoplasia.* 23(12):1213-1226. DOI: 10.1016/j.neo.2021.10.004

Hamed A.I., Plaza A., Balestrieri M.L., Mahalel U.A., Springuel I.V., Oleszek W., Pizza C., Piacente, S. (2006). Cardenolide glycosides from Pergularia tomentosa and their proapoptotic activity in Kaposi's sarcoma cells. *J. Nat. Prod.* 69(9):1319-22. DOI: 10.1021/np0602228l

Han K.Q., Huang G., Gu W., Su Y.H., X.Q., Ling C.Q. (2007). Anti-tumor activities and apoptosis-regulated mechanisms of bufalin on the orthotopic transplantation tumor model of human hepatocellular carcinoma in nude mice. *World J. Gastroenterol.* 13(24):3374-9. DOI: 10.3748/wjg.v13.i24.3374

Hassan S.W., Umar R.A., Ladan M.J., Nyemike P., Wasagu R.S.U, Lawal M, Ebbo A.A. (2007). Nutritive Value, Phytochemical and Antifungal Properties of Pergularia tomentosa L. (Asclepiadaceae). *Inter. J. Pharmacol.* 3(4):334-40. DOI: 10.3923/ijp.2007.334.340

Hosseini M., Ayyari M., Meyfour A., Piacente S., Cerulli A., Crawford A., Pahlavan S. (2020). Cardenolide-rich fraction of Pergularia tomentosa as a novel antiangiogenic agent mainly targeting endothelial cell migration. *Daru J. Pharm. Sci.* 28(2):533-543. DOI: 10.1007/s40199-020-00356-7

Hosseini S.H., Masullo M., Cerulli A., Martucciello S., Ayyari M., Pizza C., Piacente S. (2019). Antiproliferative cardenolides from the aerial parts of pergularia tomentosa. *J. Nat. Prod.* 82(1):74-79. DOI: 10.1021/acs.jnatprod.8b00630

Iwata M., Eshima Y., Kagechika H., Miyaura H. (2004). The endocrine disruptors nonylphenol and octylphenol exert direct effects on T cells to suppress Th1 development and enhance Th2 development. *Immunol. Lett.* 94 (1–2):135–139. DOI: 10.1016/j.imlet.2004.04.013

Jambor T., Tvrdá E., Bistáková J., Forgács Z., Lukáč N. (2016). The potential impact of 4-octylphenol on the basal and stimulated testosterone formation by isolated mice Leydig cells. *J. Cent. Eur. Agric.* 17(4):1274–1286. DOI:10.5513/JCEA01/17.4.1844

Jiang L., Yang Y., Zhang Y., Liu Y., Pan B., Wang B., Lin Y. (2019). Accumulation and toxicological effects of nonylphenol in tomato (Solanum lycopersicum L) plants. *Sci. Rep.* 9(1):7022. DOI: 10.1038/s41598-019-43550-7

Jin Z., Li Y., Pitti R., Lawrence D., Pham V.C., Lill R.J., Ashkenazi A. (2009). Cullin3-based polyubiquitination and p62-dependent aggregation of caspase-8 mediate extrinsic apoptosis signaling. *Cell.* 137(4):721-35. DOI: 10.1016/j.cell.2009.03.015

Jonkers N., Knepper T.P., De Voogt P. (2001). Aerobic biodegradation studies of nonylphenol ethoxylates in river water using liquid chromatography electrospray tandem mass spectrometry. *Environ. Sci Technol.* 35:335–40. DOI: 10.1021/es000127o

Kazemi S., Khalili-Fomeshi M., Akbari A., Kani S.N.M., Ahmadian S.R., Ghasemi-Kasman M., (2018). The correlation between nonylphenol concentration in brain regions and resulting behavioral impairments. *Brain Res. Bull.* 139:190–196. DOI: 10.1016/j.brainresbull.2018.03.003

Kim S., An B.S., Yang H., Jeung E.B. (2013). Effects of octylphenol and bisphenol A on the expression of calcium transport genes in the mouse duodenum and kidney during pregnancy. *Toxicology.* 303:99-106. DOI: 10.1016/j.tox.2012.10.023

Ko D.K., Lee D.R., Song H., Kim J.H., Lim C.K. (2019). Octylphenol and nonylphenol affect decidualization of human endometrial stromal cells. *Reprod. Toxicol.* 89:13-20. DOI: 10.1016/j.reprotox.2019.06.003

Kourouma A., Keita H., Duan P., Quan C., Bilivogui K.K., Qi S., Christiane N.A., Osamuyimen A., Yang K. (2015). Effects of 4-nonylphenol on oxidant/antioxidant balance system inducing hepatic steatosis in male rat. *Toxicol. Rep.* 2:1423-1433. DOI: 10.1016/j.toxrep.2015.10.006

Kumar V., Maity S. (2021). ER Stress-Sensor Proteins and ER-Mitochondrial Crosstalk-Signaling Beyond (ER) Stress Response. *Biomolecules.*11(2):173. DOI: 10.3390/biom11020173

Kusunoki T., Shimoke K., Komatsubara S., Kishi S., Ikeuchi T. (2008). p-Nonylphenol induces endoplasmic reticulum stress-mediated apoptosis in neuronally differentiated PC12 cells. *Neurosci. Lett.* 431(3):256-61. DOI: 10.1016/j.neulet.2007.11.058

Langenhan J.M., Peters N.R., Guzei I.A, Hoffmann F.M., Thorson J.S. (2015). Enhancing the anticancer properties of cardiac glycosides by neoglycorandomization, *Proc. Natl. Acad. Sci. U. S. A.* 102(35):12305-10. DOI: 10.1073/pnas.0503270102

Lawrence T.S. Ouabain sensitizes tumor cells but not normal cells to radiation. (1988). *Int. J. Radiat. Oncol. Biol. Phys.* 15(4):953-8. DOI: 10.1016/0360-3016(88)90132-0.

Lepretti M., Paolella G., Giordano D., Marabotti A., Gay F., Capaldo A., Esposito C., Caputo I. (2015). 4-Nonylphenol reduces cell viability and induces apoptosis and ER-stress in a human epithelial intestinal cell line. *Toxicol. In Vitro*. 29(7):1436-44. DOI: 10.1016/j.tiv.2015.04.022

Lichtstein D., Steinitz M., Gati I., Samuelov S., Deutsch J., Orly J. (1998). Biosynthesis of digitalis-like compounds in rat adrenal cells: hydroxycholesterol as possible precursor. *Life Sci.* 62:2109–2126. DOI: 10.1016/s0024-3205(98)00186-6

Limonta P., Moretti R.M., Marzagalli M., Fontana F., Raimondi M., Marelli M.M. (2019). Role of endoplasmic reticulum stress in the anticancer activity of natural compounds. *Int. J. Mol. Sci.* 20(4):961. DOI: 10.3390/ijms20040961

Liu P.S., Liu G.H., Chao W.L. (2008). Effects of nonylphenol on the calcium signal and catecholamine secretion coupled with nicotinic acetylcholine receptors in bovine adrenal chromaffin cells. *Toxicology.* 244(1):77-85. DOI: 10.1016/j.tox.2007.11.005

Lopez-Espinosa M.J., Freire C., Arrebola J.P., Navea N., Taoufiki J., Fernandez M.F., Ballesteros O., Prada R., Olea N. (2009). Nonylphenol and octylphenol in adipose tissue of women in Southern Spain. *Chemosphere*.76(6):847-52. DOI: 10.1016/j.chemosphere.2009.03.063

Luo B., Lee A.S. (2013). The critical roles of endoplasmic reticulum chaperones and unfolded protein response in tumorigenesis and anticancer therapies. *Oncogene.* 32(7):805-18.

Luo X., Alfason L., Wei M., Wu S., Kasim V. (2022). Spliced or Unspliced, That Is the Question: The Biological Roles of XBP1 Isoforms in Pathophysiology. *Int. J. Mol. Sci.* 23(5):2746. DOI: 10.3390/ijms23052746

Maggioni S., Balaguer P., Chiozzotto C., Benfenati E. (2013). Screening of endocrine disrupting phenols, herbicides, steroid estrogens, and estrogenicity in drinking water from the waterworks of 35 Italian cities and from PET-bottled mineral water. *Environ. Sci. Pollut. Res.* 20 (3):1649–1660. DOI: 10.1007/s11356-012-1075-x

Magnifico M.C., Xhani M., Popov M., Saso L., Sarti P., Arese M. (2018). Nonylphenol and Octylphenol Differently Affect Cell Redox Balance by Modulating the Nitric Oxide Signaling. Oxid *Med. Cell Longev.* 2018:1684827. DOI: 10.1155/2018/1684827

Mao Z., Zheng Y.L., Zhang Y.Q. (2010). Behavioral impairment and oxidative damage induced by chronic application of nonylphenol. *Int. J. Mol. Sci.* 12(1):114-27. DOI: 10.3390/ijms12010114

Martucciello S., Masullo M., Cerulli A., Piacente S. (2020). Natural Products Targeting ER Stress, and the Functional Link to Mitochondria. *Int. J. Mol. Sci.* 21(6):1905. DOI: 10.3390/ijms21061905

Martucciello S., Paolella G., Romanelli A.M., Sposito S., Meola L., Cerulli A., Masullo M., Piacente S., Caputo I. (2022). Pro-Apoptotic and Pro-Autophagic Properties of Cardenolides from Aerial Parts of Pergularia tomentosa. *Molecules.* 27(15):4874. DOI: 10.3390/molecules27154874

McConkey D.J., Lin Y., Nutt, L.K., Ozel, H.Z., Newman, R.A. (2000). Cardiac glycosides stimulate Ca^{2+} increases and apoptosis in androgen-independent, metastatic human prostate adenocarcinoma cells. *Cancer Res*. 60(14):3807-12.

Mekhail T., Kaur H., Ganapathi R., Budd G.T., Elson P., Bukowski R.M. (2006). Phase 1 trial of Anvirzel in patients with refractory solid tumors. *Invest. New. Drugs.* 24(5):423-7. DOI: 10.1007/s10637-006-7772-x

Meng L., Wen Y., Zhou M., Li J., Wang T., Xu P., Ouyang, J. (2016). Ouabain induces apoptosis and autophagy in Burkitt's lymphoma Raji cells. *Biomed. Pharmacother*. 84:1841-1848. DOI: 10.1016/j.biopha.2016.10.114

Mesaeli N., Phillipson C. (2004). Impaired p53 expression, function, and nuclear localization in calreticulin-deficient cells. *Mol. Biol. Cell.* 15(4):1862-70. DOI: 10.1091/mbc.e03-04-0251

Miao Q., L Bi L.L., Li X., Miao S., Zhang J., Zhang S., Yang Q., Xie Y.H., Zhang J., Wang S.W. (2013). Anticancer effects of bufalin on human hepatocellular carcinoma HepG2 cells: roles of apoptosis and autophagy. *Int. J. Mol. Sci.* 14(1):1370-82. DOI: 10.3390/ijms14011370

Michelangeli F., Ogunbayo O.A., Wootton L.L., Lai P.F., Al-Mousa F., Harris R.M., Waring R.H., Kirk C.J. (2008). Endocrine disrupting alkylphenols: structural requirements for their adverse effects on Ca2+ pumps, Ca2+ homeostasis & Sertoli TM4 cell viability. *Chem. Biol. Interact.*176(2-3):220-6. DOI: 10.1016/j.cbi.2008.08.005

Mijatovic T., Van Quaquebeke E., Delest B., Debeir O., Darro F., Kiss R. (2007). Cardiotonic steroids on the road to anti-cancer therapy. *Biochim. Biophys. Acta -Reviews on Cancer.* 1776(1):32-57. DOI: 10.1016/j.bbcan.2007.06.002

Mizushima N., Yoshimori T. (2007). How to interpret LC3 immunoblotting. *Autophagy.* 3(6):542-5. DOI: 10.4161/auto.4600

Nasu S., Milas L., Kawabe S., Raju, U., Newman R.A. (2002). Enhancement of radiotherapy by oleandrin is a caspase-3 dependent process. *Cancer Lett*. 185(2):145-51. DOI: 10.1016/s0304-3835(02)00263-x

Newman R.A., Kondo Y., Yokoyama T., Dixon S., Cartwright C., Chan D., Johansen M., Yang P. (2007). Autophagic cell death of human pancreatic tumor cells mediated by oleandrin, a lipid-soluble cardiac glycoside. *Integr. Cancer. Ther.* 26(4):354-64. DOI: 10.1177/1534735407309623

Newman R.A., Yang P., Pawlus A.D., Block K.I. (2008). Cardiac glycosides as novel cancer therapeutic agents. *Mol Interv*. 8(1):36-49. DOI: 10.1124/mi.8.1.8

Nomura S., Daidoji T., Inoue H., Yokota H. (2008). Differential metabolism of 4-n- and 4-tert-octylphenols in perfused rat liver. *Life Sci.* 83(5-6):223-8. DOI: 10.1016/j.lfs.2008.06.009

Olaniyan L.W.B., Omobola O.O., Noxolo T.M., Anthony I.O. (2018). Environmental Water Pollution, Endocrine Interference and Ecotoxicity of 4-tert-Octylphenol: A Review. *Rev. Environ. Contam. Toxicol.* 248:81-109. DOI: 10.1007/398_2018_20

Oyadomari S., Mori M. (2004). Roles of CHOP/GADD153 in endoplasmic reticulum stress. *Cell Death Differ.* 11(4):381-9. DOI: 10.1038/sj.cdd.4401373

Paolella G., Romanelli A.M., Martucciello S., Sposito S., Lepretti M., Esposito C., Capaldo A., Caputo I. (2021). The mechanism of cytotoxicity of 4-nonylphenol in a human hepatic cell line involves ER-stress, apoptosis, and mitochondrial dysfunction. *J. Biochem. Mol. Toxicol.* 35(7):e22780. DOI: 10.1002/jbt.22780

Park H., Kim K. (2017). Urinary Levels of 4-Nonylphenol and 4-t-Octylphenol in a Representative Sample of the Korean Adult Population. *Int. J. Environ. Res. Public Health*. 14(8):932. DOI: 10.3390/ijerph14080932

Piacente S., Masullo M., De Nève N., Dewelle J., Hamed A., Kiss R., Mijatovic, T. (2009). Cardenolides from Pergularia tomentosa display cytotoxic activity resulting from their potent inhibition of Na+/K+-ATPase. *J. Nat. Prod.* 72(6):1087–91. DOI: 10.1021/np800810f

Piccioni F., Roman B.R., Fischbeck K.H., Taylor J.P. (2004). A screen for drugs that protect against the cytotoxicity of polyglutamine-expanded androgen receptor. *Hum. Mol. Genet.* 13(4):437–46. DOI: 10.1093/hmg/ddh045

Porter A.G., Jänicke R.U. (1999). Emerging roles of caspase-3 in apoptosis. *Cell Death Differ* 6(2):99-104. DOI: 10.1038/sj.cdd.4400476

Prassas I., Diamandis E. P. (2008). Novel therapeutic applications of cardiac glycosides. *Nat. Rev. Drug Discov*. 7(11):926. DOI: 10.1038/nrd2682

Qi Y., Zhang Y., Liu Y., Zhang W., (2013). Nonylphenol decreases viability and arrests cell cycle via reactive oxygen species in Raji cells. *Exp. Toxicol. Pathol*. 65(1–2):69–72. DOI: 10.1016/j.etp.2011.06.002.

Rahimtoola S.H. (2004). Digitalis therapy for patients in clinical heart failure. *Circulation*. 109(24):2942–2946. DOI: 10.1161/01.CIR.0000132477.32438.03

Sadakane K., Ichinose T., Takano H., Yanagisawa R., Koike E., Inoue K. (2014). The alkylphenols 4-nonylphenol, 4-tert-octylphenol and 4-tert-butylphenol aggravate atopic dermatitis-like skin lesions in NC/Nga mice: alkylphenols aggravate atopic dermatitis in NC/Nga mice. *J. Appl. Toxicol.* 34 (8), 893–902. DOI: 10.1002/jat.2911

Saggu S., I Sakeran M.I., Zidan N., Tousson E., Mohan A., Rehman H. (2014). Ameliorating effect of chicory (Chichorium intybus L.) fruit extract against 4-tert-octylphenol induced liver injury and oxidative stress in male rats. *Food Chem. Toxicol.* 72:138-46. DOI: 10.1016/j.fct.2014.06.029

Sasaya H., Yasuzumi K., Maruoka H., Fujita A., Kato Y., Waki T., Shimoke K., Ikeuchi T. (2012). Apoptosis inducing activity of endocrine-disrupting chemicals in cultured PC12 cells. *Adv. Biol. Chem.* 02(02):92–105. DOI: 10.4236/abc.2012.22012

Schevzov G., Kee A.J., Wang B., Sequeira V.B., Hook J., Coombes J.D., Lucas C.A., Stehn J.R., Musgrove E.A., Cretu A., Assoian R., Fath T., Hanoch T., Seger R., Pleines I., Kile B.T., Hardeman E.C., Gunning P.W. (2015). Regulation of cell proliferation by ERK and signal-dependent nuclear translocation of ERK is dependent on Tm5NM1-containing actin filaments. *Mol. Biol. Cell.* 26(13):2475-90. DOI: 10.1091/mbc.E14-10-1453

Schneider N.F.Z., Geller F.C., Persich L., Marostica L.L., Pádua M.R., Kreis W., Braga F.C., Cláudia Simões C.M.O. (2016). Inhibition of cell proliferation, invasion and migration by the cardenolides digitoxigenin monodigitoxoside and convallatoxin in human lung cancer cell line. Nat. Prod. Res. 30(11):1327-31. DOI: 10.1080/14786419.2015.1055265

Shatat A., Sweidan N., Zarga M.A. (2022). Two new compounds from Pergularia tomentosa growing wildly in Jordan. *J. Asian Nat. Prod. Res.*1-8. DOI: 10.1080/10286020.2022.2131548

Shekhar S., Sood S., Showkat S., Lite C., Chandrasekhar A., Vairamani M., Barathi S., Santosh W. (2017). Detection of phenolic endocrine disrupting chemicals (EDCs) from maternal blood plasma and amniotic fluid in Indian population. *Gen. Comp. Endocrinol*. 241:100-107.

Shen Y., White E. (2001). p53-dependent apoptosis pathways. *Adv. Cancer Res.* 82:55-84. DOI: 10.1016/s0065-230x(01)82002-9

Shikimi H., Sakamoto H., Mezaki Y., Ukena K., Tsutsui K. (2004). Dendritic growth in response to environmental estrogens in the developing Purkinje cell in rats. *Neurosci. Lett*. 364 (2):114–118. DOI: 10.1016/j.neulet.2004.04.023

Škubník J., Pavlíčková V.S., Psotová J., Rimpelová S. (2021). Cardiac Glycosides as Autophagy Modulators. *Cells.* 10(12):3341. DOI: 10.3390/cells10123341

Smirnova E., Griparic L., Shurland D.L., Van der Bliek A.M. (2001). Dynamin-related protein Drp1 is required for mitochondrial division in mammalian cells. *Mol. Biol. Cell.* 12(8):2245-56. DOI: 10.1091/mbc.12.8.2245

Snykers S., De Kock J., Rogiers V., Vanhaecke T. (2009). In vitro differentiation of embryonic and adult stem cells into hepatocytes: state of the art. Stem Cells 27:577–605. *Stem Cells*. 27(3):577-605. DOI: 10.1634/stemcells.2008-0963

Soares A., Guieysse B., Jefferson B., Cartmell E., Lester E.N. (2008). Nonylphenol in the environment: a critical review on occurrence, fate, toxicity and treatment in wastewaters. *Environ. Int.* 34(7):1033-49. DOI: 10.1016/j.envint.2008.01.004

Soto A.M., Justicia H., Wray J.W., Sonnenschein C. (1991). P-Nonylphenol: an estrogenic xenobiotic released from "modified" polystyrene. Environ. Health Perspect. 92:167–73. DOI: 10.1289/ehp.9192167

Srivastava M., Eidelman O., Zhang J., Paweletz C., Caohuy H., Yang Q., Jacobson K.A., Heldman H., Huang W., Jozwik C., S Pollard B.S., Pollard H.B. (2004). Digitoxin mimics gene therapy with CFTR and suppresses hypersecretion of IL-8 from cystic fibrosis lung epithelial cells. *Proc. Natl. Acad. Sci. U S A.* 101(20):7693-8. DOI: 10.1073/pnas.0402030101

Štampar M., Tomc J., Filipič M., Žegura B. (2019). Development of in vitro 3D cell model from hepatocellular carcinoma (HepG2) cell line and its application for genotoxicity testing. *Arch. Toxicol.* 93(11):3321-3333. DOI: 10.1007/s00204-019-02576-6

Suen J.L., Hung C.H., Y H.S., Huang S.K. (2012). Alkylphenols—potential modulators of the allergic response. *Kaohsiung J. Med. Sci*. 28 (7): S43–8. DOI: 10.1016/j.kjms.2012.05.009

Szegezdi E., Logue S.E., Gorman A.M., Samali A. (2006). Mediators of endoplasmic reticulum stress-induced apoptosis. *EMBO Rep.* 7(9):880-5. DOI: 10.1038/sj.embor.7400779

Thiele B., Heinke V., Kleist E., Guenther K. (2004). Contribution to the structural elucidation of 10 isomers of technical p-nonylphenol. *Environ. Sci. Technol*. 38(12):3405–11. DOI: 10.1021/es040026g

Trenti A., Grumati P., Cusinato F., Orso G., Bonaldo P., Trevisi L. (2014). Cardiac glycoside ouabain induces autophagic cell death in non-small cell lung cancer cells via a JNK-dependent decrease of Bcl-2. *Biochem. Pharmacol.*, 89(2):197-209. DOI: 10.1016/j.bcp.2014.02.021

Verheye-Dua F.A., Böhm, L. (2000). Influence of Apoptosis on the Enhancement of Radiotoxocity by Ouabain. *Strahlentherapie Onkol.* 176(4):186-191. DOI: 10.1007/s000660050055

Verheye-Dua F.A., Böhm, L. (1998). Na+, K+-ATPase inhibitor, ouabain accentuates irradiation damage in human tumour cell lines. *Radiat. Oncol. Investig.* 6(3):109-19. DOI: 10.1002/(SICI)1520-6823(1998)6:3<109::AID-ROI1>3.0.CO;2-1

Vikelsoe J., Thomsen M., Carlsen L. (2002). Phthalates and nonylphenols in profiles of differently dressed soils. *Sci. Total. Environ*. 296:105–16. DOI: 10.1016/s0048-9697(02)00063-3

Vo T.T.B., Nguyen P.V., Duong H.T.T, Nguyen T.D., Huynh H.T.H, Van Nong H. (2015). Potential effect of combined xenoestrogens during gestation stages on mouse offspring. *J. Environ. Biol.* 36(2):337-44.

Wang F., Chen Y., Ouyang H. (2011). Regulation of unfolded protein response modulator XBP1s by acetylation and deacetylation. *Biochem. J.* 433(1):245-52. DOI: 10.1042/BJ20101293

Winnicka K., Bielawski K., Bielawska, A. (2006). Cardiac glycosides in cancer research and cancer therapy. *Acta Pol. Pharm.* 63(2): 109-15.

Xi H., Wang S., Wang B., Hong X., Liu X., Li M., Shen R., Dong Q. (2022). The role of interaction between autophagy and apoptosis in tumorigenesis (Review). *Oncol. Rep.* 48(6):208. DOI: 10.3892/or.2022.8423

Yang Z.J., Chee C.E., Huang S., Sinicrope F.A. (2011). The role of autophagy in cancer: therapeutic implications. *Mol. Cancer. Ther.* 10(9):1533-41. DOI: 10.1158/1535-7163.MCT-11-0047

Yapa N.M.B., Lisnyak V., Reljic B., Ryan M.T. (2021). Mitochondrial dynamics in health and disease. *FEBS Lett.* 595(8):1184-1204. DOI: 10.1002/1873-3468.14077

Yeh J.Y., Huang W.J., Kan S.F., Wang P.S. (2003). Effects of bufalin and cinobufagin on the proliferation of androgen dependent and independent prostate cancer cells. *Prostate*. 54(2):112-24. DOI: 10.1002/pros.10172

Yeltekin A.C., Oğuz A.R. (2018). Antioxidant responses and DNA damage in primary hepatocytes of Van fish (Alburnus tarichi, Güldenstadt 1814) exposed to nonylphenol or octylphenol. *Drug Chem. Toxicol.* 41(4):415-423. DOI: 10.1080/01480545.2018.1461899

Ying G.G., Williams B., Kookana R. (2002). Environmental fate of alkylphenols and alkylphenol ethoxylates--a review. *Environ. Int.* 28(3):215-26. DOI: 10.1016/s0160-4120(02)00017-x

Yu J., Yang X., Luo Y., Yang X., Yang M., Yang J., Zhou J., Gao F., He L., Xu J. (2017). Adverse effects of chronic exposure to nonylphenol on non-alcoholic fatty liver disease in male rats. *PLoS One*.12(7):e0180218. DOI: 10.1371/journal.pone.0180218

Zhang Z., Wu Z., He L. (2008). The accumulation of alkylphenols in submersed plants in spring in urban lake, China. *Chemosphere*. 73(5):859-63. DOI: 10.1016/j.chemosphere.2008.05.016

Zhao M.X., Wen J.L., Wang L., Wang X.P., Chen T.S. (2019). Intracellular catalase activity instead of glutathione level dominates the resistance of cells to reactive oxygen species. *Cell Stress Chaperones*. 24(3):609-619. DOI: 10.1007/s12192-019-00993-1

Zumbado M., Boada L.D., Torres S., Monterde J.G., Dıaz-Chico B.N., Afonso J.L., Cabrera J.J., Blanco A. (2002). Evaluation of acute hepatotoxic effects exerted by environmental estrogens nonylphenol and 4-octylphenol in immature male rats. *Toxicology*. 175(1-3):49-62. DOI: 10.1016/s0300-483x(02)00046-x